Universidad de Oviedo

Departamento de Biología de Organismos y Sistemas
Programa de Doctorado en Recursos Biológicos y Biodiversidad

Combining model simulations and empirical data to disentangle the factors driving the growth and distribution of marine phytoplankton

Combinando modelos y datos empíricos para esclarecer los factores que controlan el crecimiento y la distribución del fitoplancton marino

TESIS DOCTORAL

Sofía Sal Bregua

Oviedo, Junio 2014

variable en el tiempo y que acopla tanto las condiciones biogeoquímicas como físicas del océano. Inicializando aleatoriamente un conjunto de especies caracterizadas según distintos grupos funcionales, somos capaces de reproducir dicho patrón y observamos que éste se debe a no uno, sino a diversos factores como son: la exclusión competitiva entre especies especialistas y oportunistas, la coexistencia de especies con similares requerimientos en zonas de estabilidad ambiental, la dispersión oceánica, o la temperatura a través de un *thermal mid-domain effect* (TMDE).

El capítulo 4 de esta tesis se centró en la recopilación y estandarización de datos de abundancia microplanctónica, creando una base de datos única en estudios de diversidad de fitoplancton marino. Dicha compilación cubre un amplio rango de ecosistemas marinos y consta de medidas de abundancia, biomasa y biovolumen para cada especie en cada estación y profundidad. Las identificaciones de las especies fueron realizados por el mismo taxónomo, lo que proporciona una mayor consistencia a la colección y asegura que las estimaciones de la diversidad de especies sean fidedignas. Además, para cada estación se recoge información ambiental mediante una compilación de parámetros oceanográficos, lo que aporta una caracterización de la zona de estudio y por tanto la idoneidad de la base de datos para el estudio de los controles medioambientales y biológicos de la diversidad marina.

Por último, en el capítulo 5 hacemos uso de la compilación anterior para demostrar empíricamente la existencia de un gradiente latitudinal de diversidad en el fitoplancton marino, donde el máximo número de especies aparece nuevamente en los trópicos. En este capítulo tratamos de explicar la emergencia de dicho patrón a partir de la temperatura, cuyo efecto parece ser clave según predicen varias teorías. A partir de datos empíricos (capítulo 4), modelamos las curvas de tolerancia térmica de las especies para entender la relación entre temperatura y diversidad y proponemos una nueva hipótesis denominada como *thermal niche effect* (TNE). Ésta resulta de la combinación entre la superposición que tiene lugar entre los nichos fisiológicos de las especies, como predice el TMDE, y el aumento exponencial de la tasa de crecimiento con la temperatura que predicen las teorías metabólicas. Éste parece verse reflejado en los nichos realizados de las especies, donde se observa un incremento de la máxima probabilidad de ocurrencia de las especies con la temperatura. El patrón resultante de dicha hipótesis es muy similar a la relación entre diversidad y temperatura observada en datos empíricos. Esto permite predecir con mayor certeza cuál será la distribución futura de las especies en el océano bajo las predicciones de calentamiento global.

RESUMEN (en Inglés)

Marine phytoplankton are the largest primary producers of the ocean, being responsible for most of the exchange of CO_2 with the atmosphere. These unicellular organisms are the base of the marine food chain and control the biogeochemical functioning of the ecosystem. Under the prediction of climate warming, models forecast from a decline in the overall biomass to changes in their distribution. This has consequences for the rest of the food chain, affecting the total production, biogeochemical cycles and the global carbon cycle. Understanding what factors and how influence growth and distribution of marine phytoplankton is therefore essential to predict with certainty the future of the ecosystem and supposes the main objective of this study .

Recent studies have found a unimodal relationship between mass-specific growth rate and cell size of marine phytoplankton when the size range under study includes picophytoplanton. The first part of this manuscript (Chapters 1 and 2), focuses on assessing the factors that influence the emergence of such curvature. Using different compilations of growth rates and size data for a large number of species, we evaluated the influence of both temperature and phylogeny, which has been little considered explicitly in allometric studies of marine phytoplankton. Our results reveal that the unimodal relationship is due to the lower growth rates of picophytoplankton, being this the result of an evolutionary adaptation to warm oligotrophic

environments rather than a size effect. Also as consequence of this adaptation, we observed that such curvature depends on the temperature at which the growth rates are measured. We also found a strong correlation between cell size and temperature, which implies an additional bias to the temperature correction on growth rate, and thus may lead to erroneous conclusions in the size-scaling of marine phytoplankton growth rate.

In Chapter 3 we focus on assessing the factors that control the emergence of a latitudinal gradient of diversity for marine phytoplankton (LDG). This pattern explains an increase in the number of species from the poles to the equator, showing the highest diversity at the tropical areas. Here we used a time-varying 3D ecosystem model where biogeochemical and physical ocean conditions are coupled. Using a set of species randomly initialized and characterized according to several functional groups, we were able to reproduce the LDG. We also found that it emerges as result of not one but several factors including: competitive exclusion between opportunists and gleaner species, the coexistence of species with similar fitness in areas of environmental stability, dispersion by oceanic currents or temperature through a *mid-domain thermal effect* (TMDE).

Chapter 4 has focused on the compilation and standardization of microplankton data abundance, being an unique database for marine phytoplankton diversity studies. This database covers a wide range of marine ecosystems and provides measures of abundance (cells/ml), biovolume and biomass for each species at each station and depth. One of the major strengths of this database is that species identification was performed by the same taxonomist, what provides greater strength to the collection and ensures that estimates of species diversity are reliable. Furthermore, environmental information is attached for each station through the compilation of different oceanographic parameters. This allows the characterization of the study area and therefore the suitability of the database for the study of environmental and biological controls of marine diversity.

Finally, in Chapter 5 we used the previous compilation to show with empirical data that a latitudinal gradient of diversity emerges for the whole community of marine phytoplankton, where the maximum number of species is observed, as expected, at the tropics. In this chapter we focus on the role of temperature as driver of the LDG, whose relevance has been suggested by many theories. Using empirical data (Chapter 4), we fit the thermal tolerance curve of species to study the relationship between temperature and diversity and propose a new hypothesis to explain the emergence of LDG, the *thermal niche effect* (TNE). This results from the combination of both the overlapping of the species physiological niches, as predicted by the TMDE, and the exponential increase of growth rate with temperature predicted by metabolic theories. The latter seems to be reflected in the realized niches of species, where an increase in the maximum probability of occurrence of species with increasing temperature is observed. The resulting pattern of this hypothesis is closer to the relationship between diversity and temperature observed in empirical data. This allows to forecast with higher accuracy the future distribution of species over the ocean under the predictions of global warming.

A mis abuelos Paonga, Teté y Hernán.

Contents

General Introduction **1**

Functional traits and environmental limitations 1

Global patterns of species richness 3

Phytoplankton predictions under climate warming 4

Global models versus empirical data 4

Objectives 6

1 Temperature, nutrients, and the size-scaling of phytoplankton growth in the sea **9**

1.1 Introduction 10

1.2 Methods, Results and Discussion 10

1.3 Acknowledgements 16

2 Thermal adaptation, phylogeny and the unimodal size scaling of marine phytoplankton growth **17**

2.1 Introduction 18

2.2 Material and Methods 20

2.2.1 Phylogenetic analyses 21

2.2.2 Size-scaling of growth rate and species thermal tolerance curves 22

2.2.3 Temperature normalization 22

2.3 Results 23

2.4 Discussion 28

2.5 Supplementary table and figures 33

3 Multiple drivers of the latitudinal diversity gradient in marine phytoplankton 39
3.1 Introduction . . . 40
3.2 Material and Methods . . . 41
3.2.1 Model simulations . . . 43
3.2.1.1 Simulation 1: DIN + SST + PAR niches (full model) . . . 43
3.2.1.2 Simulation 2: DIN niches only . . . 43
3.2.1.3 Simulation 3: SST niches only . . . 45
3.3 Results . . . 45
3.3.1 Simulation 1:DIN + SST + PAR niches (full model) . . . 45
3.3.2 Simulation 2: DIN niches only . . . 45
3.3.3 Simulation 3: SST niches only . . . 47
3.4 Discussion . . . 49

4 Marine microplankton diversity database 55
4.1 Introduction . . . 56
4.2 Dataset Descriptors . . . 58
4.3 Material and Methods . . . 59
4.3.1 Study region . . . 59
4.3.2 Experimental or sampling design. . . . 59
4.3.3 Sampling methods . . . 59
4.3.4 Analysis . . . 61
4.3.5 Taxonomy and systematics . . . 66
4.4 Dataset status and accessibility . . . 66
4.5 Data Structural Descriptors . . . 67
4.5.1 Dataset File . . . 67
4.5.2 Variable definitions: . . . 67

5 The combined effects of thermal mid-domain and growth-temperature response curves on the latitudinal diversity gradient in marine phytoplankton 71
5.1 Introduction . . . 72
5.2 Material and Methods . . . 74

5.2.1 Empirical data 74
5.2.2 Niche modelling 75
5.3 Results 76
5.4 Discussion 82
5.5 Supplementary figure 86

General Discussion **89**
The trade-off between intrinsic maximum growth and half-saturation constant 89
The relevance of the *thermal niche effect* 90

Conclusiones **93**

Agradecimientos **97**

References **103**

General Introduction

The ocean covers more than 70% of the Earth' surface and is the life support system for our planet providing roughly half of its primary production (Field et al., 1998). The main primary producers are phytoplankton, unicellular organisms that form the base of the marine food chain and drive marine ecosystem function. Phytoplankton are key participants in the *biological pump* (Figure 1). Through the process of photosynthesis, they fix more than a hundred million tons of carbon in the form of CO_2 (Behrenfeld et al., 2006). Therefore, even small changes in their growth may affect atmospheric CO_2, having potential implications for the global ecosystem.

Functional traits and environmental limitations

Phytoplankton growth rate is limited by the availability of resources such as light and nutrients and by temperature. **Light** is essential for the photosynthetic processes and growth rate describes an unimodal response to irradiance levels. Whereas at high irradiance levels photoinhibition occurs, low levels result in too little energy to sustain growth. In the ocean, light decreases exponentially with increasing depth. In contrast, the deep ocean is rich in **nutrients** while these are usually depleted in surface waters, mostly due to uptake by phytoplankton during the photosynthesis. Phytoplankton is generally limited by inorganic nutrients such as nitrate, phosphate and silicate. Nutrient limitation can vary over time, by location and by species and is usually described by a Monod equation (Monod, 1949).

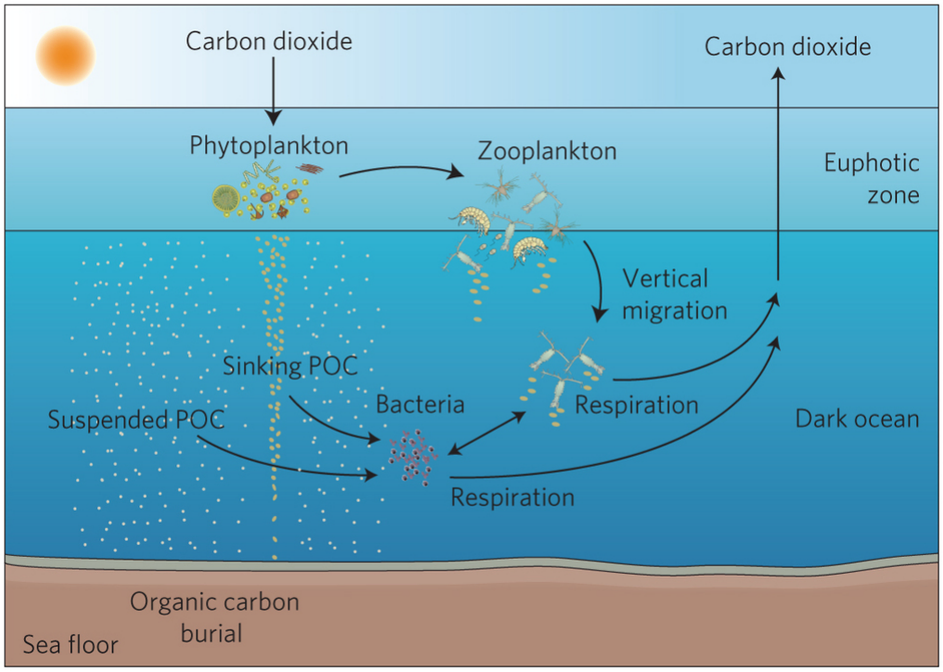

Figure 1: The Biological Pump. (Adapted from Herndl and Reinthaler (2013))

Metabolic rates are also linked to **temperature**. Phytoplankton growth rate shows an unimodal response to temperature where each species has an optimum temperature at which its growth is maximum (Eppley, 1972). Below this optimum, growth rate increases at a rate defined by a specific value of Q_{10}. This value depends on the species and is often parametrized by the Arrhenius function (Arrhenius, 1915). Above the optimum temperature, growth decreases due to different factors such as inactivation or denaturation of proteins (Ratkowsky et al., 1983). This decline is sharper than the increase below the optimum and hence, thermal tolerance curves are usually negative skewed. In addition, across species, maximum growth rates increase exponentially with increasing temperature (Eppley, 1972).

In addition to growth rate, phytoplankton **cell size** is an essential ecological trait. It is also correlated to temperature and resource availability, influencing nutrient acquisition (Kiørboe, 1993; Tilman, 1982) and metabolic rates (Brown et al., 2004; Gillooly et al., 2001; Moisan et al., 2002). Cell size plays a key role in determining the abundance and distribution of phytoplankton species. Indeed, size classes are

not equally distributed over the ocean but its distribution is linked to contrasting environmental regimes (Finkel et al., 2010; Li, 2002; Margalef, 1978; Reynolds, 1984). For instance, small picophytoplankton species dominate oligotrophic areas whereas larger phytoplankton such as diatoms predominate in nutrient-rich waters (Falkowski et al., 1998).

Growth rates, temperature, nutrients and cell size are all interrelated. Disentangling this puzzle is essential to understand ecosystem functioning and thus to help predict its future, but it is complicated when also considering biological interactions or physical processes that occur in nature. The use of ecosystem models is essential to be able to perform controlled simulation experiments and understand the relative importance of the different functional traits and environmental limitations.

Global patterns of species richness

The distribution of species over the ocean is heterogeneous. Some areas, such as upwelling regions, are the most productive on the planet whereas others are almost devoid of life. The latitudinal diversity gradient (LDG) is probably the most striking pattern at a global scale. This pattern is common to terrestrial and marine systems and for many different taxonomic groups. The LDG explains an increase of diversity from the poles to the equator, where a peak on the number of species is found at the tropical areas (Bates, 1862; Colwell and Hurtt, 1994; Humboldt and Bonpland, 1807; Pianka, 1966; Rohde, 1992; Stevens, 1989; Wallace, 1854).

Many different hypotheses have been developed to explain the mechanisms responsible for the LDG. Some relate the number of species in a region to resource availability (Arrhenius, 1921; Currie, 1991; Gaston, 2000; Rosenzweig, 1995; Wright, 1983), through effects on productivity (Gaston, 2000; Irigoien et al., 2004; Mittelbach et al., 2001; Tilman, 1982) or to temperature through its influence on metabolic rates (Allen et al., 2002; Rohde, 1992; Turner, 2004). In addition, hypotheses based on null models have been developed to explain the emergence of the LDG (Brayard et al., 2005; Colwell and Lees, 2000).

Despite several patterns in the distribution of phytoplankton have been detected, most refer to specific taxonomic groups (Cermeño and Falkowski, 2009; Fuhrman et al., 2008; Passy, 2008; Rombouts et al., 2009; Wang et al., 2011). However few studies have studied the LDG for entire communities (Irigoien et al., 2004; Ptacnik et al., 2010).

Phytoplankton predictions under climate warming

The prediction of the response of Earth's ecosystems to global climate change is a major scientific challenge. Recent studies have shown that an increase in temperature could reduce the global phytoplankton biomass (Boyce et al., 2010). Current climate models also predict an expansion of oligotrophic regions during the next century (Sarmiento et al., 2004) and a gradual shift toward smaller primary producers reducing the energy flow to higher trophic levels (Morán et al., 2010). Warmer oceans could reduce up to 20% CO_2 uptake by pelagic communities (López-Urrutia et al., 2006). However, the effect of temperature is often masked by other effects such as the availability of resources. This strong interaction between resource availability and temperature has been evidenced by direct measurements of carbon fluxes in terrestrial and aquatic ecosystems (Enquist et al., 2003; Sobek et al., 2005). For the planktonic community unpredictable changes in diversity can be expected (Gitay et al., Gitay2002; Hays et al., 2005). Warming temperatures could also lead to changes on the geographical ranges of marine species. As phytoplankton growth is directly related to temperature, if the change in temperature is so abrupt as to not allow adaptation to warming, it will bring a sharp decline in the diversity of phytoplankton in tropical waters and a poleward shift in species' thermal niches (Thomas et al., 2012).

Global models versus empirical data

Understanding the relative importance of diversity theories in natural systems is hindered by the difficulty to perform experimental work at such broad scales and by the fact that the driving variables (i.e. temperature, nutrients and PAR) are correlated latitudinally. Although large datasets with sufficient gradients in

the proposed explanatory variables exist for terrestrial plants (Gentry, 1988), for marine phytoplankton data are either inconsistent or lack some key variables (Buitenhuis et al., 2012; Leblanc et al., 2012). For this reason, computer models provide one of the most useful tools in order to simulate the real ocean conditions and experimentally understand its behaviour through *in silico* simulations. But, ultimately, results retrieved from model simulations must be tested with empirical observations or even satellite data in order to make predictions more credible.

Objectives

The main objective of this thesis is to delimit the major factors driving the growth and the latitudinal distribution of marine phytoplankton. Our aim is also to deal with the controversy between the different diversity hypotheses, caused by the scarcity of empirical diversity data of marine phytoplankton and the limitations of previous models. Therefore, we will use a combination of both empirical compilations and model simulations to achieve this goal. The specific objectives of each chapter are:

Chapter1

- To assess the unimodal relationship between weight-specific growth rate and cell size for marine phytoplankton in a compilation of field measurements.
- To test the validity of the temperature corrections on phytoplankton growth rate measurements, such as that proposed by the Metabolic Theory of Ecology (MTE), to evaluate the size scaling of marine phytoplankton.

Chapter 2

- To test the recently observed unimodal relationship between growth rate and cell size using different compilations of lab measurements.
- To assess the influence of temperature and the shared evolutionary history of species on the allometric scaling of growth rate.
- To show that the curvature is the result of the specialization of picophytoplankton across evolution to the warm conditions usually encountered in oligotrophic environments.

Chapter 3

- To reproduce the latitudinal diversity gradient (LDG) of marine phytoplankton using a time-varying 3D global ecosystem model where biogeochemical

and physical ocean conditions are coupled. In addition, phytoplankton types with stochastically assigned traits are randomly initialized and community structure and diversity are emergent properties.

- To elucidate what are the main mechanisms that drive the distribution of oceanic phytoplankton diversity. In particular, we will study the effects of resource competition and temperature, either combined or individually.
- To evaluate the extent of the thermal mid-domain (TMDE) theory on the LDG.

Chapter 4

- To compile a dataset of marine microplankton species abundance which allows to provide a reliable measure of microplankton species diversity and contribute to a better understanding of the processes of diversification in the ocean. To this end, the dataset must meet the next requirements:
  - A standardized taxonomic identification.
  - To provide environmental data in order to characterize the study area.
  - To cover a wide range of environmental ecosystems

Chapter 5

- To test the emergence of the LDG for the ″whole″ community of marine phytoplankton using the compilation in the Chapter 4.
- To evaluate the temperature-diversity relationship in order to test the theories which suggest temperature as the main driver of the LDG for marine phytoplankton: metabolic theory of ecology (MTE) and thermal mid-domain effect (TMDE).
- To explore whether the different probability of survival of the species within its thermal range, i.e. the shape of the physiological niche, may further explain the observed LDG.

- To analyse the relationship between the breadth of the niche and temperature.
- To evaluate the differences between the fundamental and realized niche of the species and how this affects the resulting LDG.

CHAPTER

1

Temperature, nutrients, and the size-scaling of phytoplankton growth in the sea

Sofía Sal & Ángel Lopez-Urrutia

Published in Limnology & Oceanography, Vol. 56(5), pp.1952–1955, (2011) as a Comment to: Chen and Liu (2011)

1.1 Introduction

Chen and Liu (2010) investigated the effects of cell size on phytoplankton mass-specific growth rate using a compilation of field measurements from surface waters around the world. After correcting for the effects of temperature, their analysis indicates that there is a modal size around 2.8-5.8 μm where mass-specific growth is maximal.

As Chen and Liu (2010) acknowledge, their analysis contrasts with allometric scaling theories that predict a continuous decrease of mass-specific growth rate with increasing size (Brown et al., 2004; López-Urrutia et al., 2006). In contrast, Chen and Liu's (2010) analysis shows that bellow the modal size, that is in the pico- to nano-phytoplankton size range, growth rate increases with cell size.

They argue that the unimodal pattern stems from picoplankton having evolved to have inherently low growth rates, independently of nutrient availability. Here we argue that the unimodal pattern they obtain might be due to an incorrect temperature correction and to an internal inconsistency in their database because a large portion of their picoplankton data contain a correction for photoacclimation effects, while the rest of their data do not.

1.2 Methods, Results and Discussion

To carry out their study, Chen and Liu (2010) used two data sets, one from ^{14}C incorporation and a second from dilution experiments. In both data sets, a unimodal pattern between mass-specific growth rate and cell size emerges. In these two data sets, however, cell size is correlated with nutrient availability, so it could be argued that, rather than a direct effect of cell size, the lower growth rates of smaller phytoplankton could be due to these organisms living under resource limitation (Raven, 1998), (*see* Fig.1C in Chen and Liu 2010). Chen and Liu (2010) tried to resolve these confounding effects due to correlation between nutrient availability and cell size by using a data set of phytoplankton growth rates measured under nutrient enrichment. The unimodal pattern still apparent in this nutrient-saturated dilution data set is probably the most striking result in their analysis. Chen and Liu

(2010) concluded that the lower growth rates in the picoplankton size range are an adaptive feature rather than a direct consequence of nutrient limitation.

We consider whether this pattern is due to a bias in the data compilation. In an effort to get the best data available, Chen and Liu (2010) used phytoplankton growth rates with a correction for photoacclimation for the two data sources that had this information available, while the rest of their nutrient-enriched dilution data are uncorrected. These corrected data happen to correspond to most of the low values in the picoplankton size range (Figure 1.1A). If we take this nutrient-enriched dilution data set and replace these photoacclimation-corrected data by the uncorrected values comparable to the rest of the data set, the unimodal pattern is

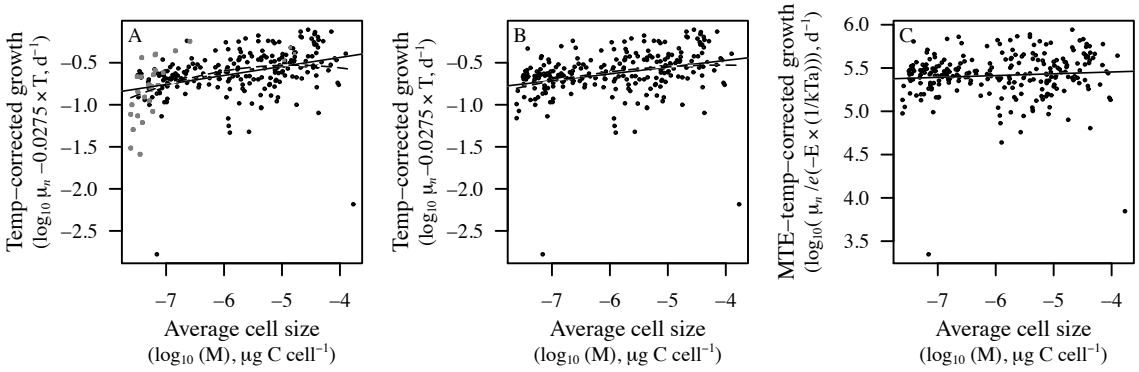

Figure 1.1: Relationship between temperature-corrected growth rate and average cell size (M) for the nutrient-enriched dilution data set. **(A)** Chen and Liu (2010) data. Grey filled symbols correspond to photoacclimation-corrected data. The solid line correspond to a linear fit ($\log_{10}(\mu_n) = 0.11\log_{10}(M) - 0.01$; ANOVA: r^2 = 0.14, n = 261, p-value < 0.001). The dashed line correspond to a quadratic fit ($\log_{10}(\mu_n) = -0.05[\log_{10}(M)]^2 - 0.48\log_{10}(M) - 1.67$; ANOVA: r^2 = 0.17, n = 261, p-value < 0.001). **(B)** Same as (A) but with all data uncorrected for photoacclimation. The solid line correspond to a linear fit ($\log_{10}(\mu_n) = 0.08\log_{10}(M) - 0.15$; ANOVA: r^2 = 0.09, n = 258, p-value < 0.001). The dashed line correspond to a quadratic fit ($\log_{10}(\mu_n) = -0.02[\log_{10}(M)]^2 - 0.18\log_{10}(M) - 0.91$; ANOVA: r^2 = 0.10, n = 258, p-value < 0.001). **(C)** Same as (B) but using the temperature correction based on MTE. In this panel, just a linear fit is shown ($\log_{10}(\mu_n) = 0.02\ \log_{10}(M) + 5.54$; ANOVA: r^2 = 0.01, n = 258, p-value = 0.203).

no longer evident (Figure 1.1B). The quadratic term in the unimodal fit is no longer significant (t-test, t = -1.255, df = 255, p = 0.211). Although now a linear fit is more appropriate, the linear relationship obtained is not what the metabolic theory of ecology (MTE) predicts. MTE predicts that metabolic rates and organism biovolume (BV) should scale as rate $\propto BV^{3/4}$ (West et al. 1999; López-Urrutia et al., 2006). Hence, size-specific metabolic rates (rate $\times BV^{-1}$), such as individual growth rate, should scale as $BV^{3/4} \times BV^{-1} = BV^{-1/4}$. Chen and Liu (2010) defines cell size as the carbon content. López-Urrutia et al. (2006) have shown that, when phytoplankton cell size is expressed in units of carbon instead of biovolume, phytoplankton growth rate scales isometrically with cell size (rate $\propto$ carbon^1), so carbon-specific growth rate (rate $\times$ carbon^{-1}) should be independent of cell carbon. This is due to phytoplankton carbon content and biovolume scaling as BV $\propto$ carbon$^{4/3}$ (Strathmann, 1967), so rate $\propto BV^{3/4} \propto$ (carbon$^{4/3}$)$^{3/4} \propto$ carbon.

Hence, following MTE, a plot of carbon-specific growth rate should yield no significant relationship with cell-carbon, whereas Figure 1.1B shows a positive relationship. We think that this trend could be due to the temperature correction used. Chen and Liu (2010) used a Q_{10} of 1.88 (Eppley 1972; Bissinger et al. 2008) so that $\log_{10}(\mu)$-0.0275×T is the temperature-corrected phytoplankton specific growth rate, where T is the temperature in Celsius. On the other hand, MTE uses the Van't Hoff - Arrhenius equation (Arrhenius, 1915) to describe the effects of temperature on metabolic rates:

$$\text{Rate} \propto e^{-E/kTa} \tag{1.1}$$

where k is Boltzmann's constant (8.62×10^{-5}eVK^{-1}), T_a is the absolute temperature (in Kelvin) and E is the average activation energy for the metabolic process under study. For autotrophs the effective activation energy for photosynthetic reactions should be close to 0.32 eV Allen et al. (2005). In the case of photosynthesis, the Van't Hoff-Arrhenius equation is just an approximation to a more complex process (Farquhar et al., 1980). The activation energy of 0.32 predicted by MTE is based on data from the effects of temperature on several photosynthetic processes (*see* appendix in Allen et al. 2005). López-Urrutia et al.

(2006) obtained effective activation energies for phytoplankton growth rates of 0.29 eV, not significantly different from the predicted value of 0.32 eV.

The Q_{10} in turn is an approximation to Van't Hoff - Arrhenius equation, so both temperature coefficients, E and Q_{10}, are interrelated by equation $Q_{10}=e^{(-E/(kTo^2))\times 10}$ where T_o is 273.15 K (*see* box 1 in Gillooly et al. 2002). Hence, the Q_{10} of 1.88 from Eppley (1972) is equivalent to an activation energy of approximately 0.405 eV, which is slightly higher than the activation energy predicted for autotrophs and the empirical value obtained by López-Urrutia et al. (2006). If growth rates from the nutrient-enriched dilution data set are plotted against temperature, the resultant activation energy is 0.36 eV (Figure 1.2), which is not significantly different from the value predicted by MTE (t-test, t = 2.08, df = 256, p = 0.15) but significantly lower than the value used by Chen and Liu (2010) (t-test, t = 12.522, df = 256, $p < 0.001$).

This subtle difference between the two temperature corrections might be responsible for the pattern obtained in Figure 1.1B. If instead of the temperature correction used by Chen and Liu (2010) based on Eppley's (1972) Q_{10} , we use the temperature correction based on MTE and the theoretical activation energy of 0.32 eV (equivalent to a Q_{10} of 1.64), we obtain no significant relationship between carbon-specific growth rate and average cell carbon (Figure 1.1C), in agreement with MTE. The Q_{10} used by Chen and Liu (2010), is based on the studies of Eppley (1972) and Bissinger et al. (2008) that analyze the temperature dependence of phytoplankton maximal growth rates. It should be noted that the temperature dependence of this maximally attainable mean growth rate might be different from the temperature dependence of growth rate under optimal conditions. For example, in Figure 1.2 we fit a line to the growth rates under nutrient- and light-saturated conditions, while Eppley (1972) and Bissinger et al. (2008) fits would represent the upper limit of the recorded growth rates. Our fit therefore attempts to predict the average growth rate of a population of phytoplankton living at optimum nutrient and light conditions, while Eppley (1972) and Bissinger et al. (2008) predict the maximum growth rate of the same population. Maximal and average metabolisms might have different temperature dependencies but it is the latter, as the one shown

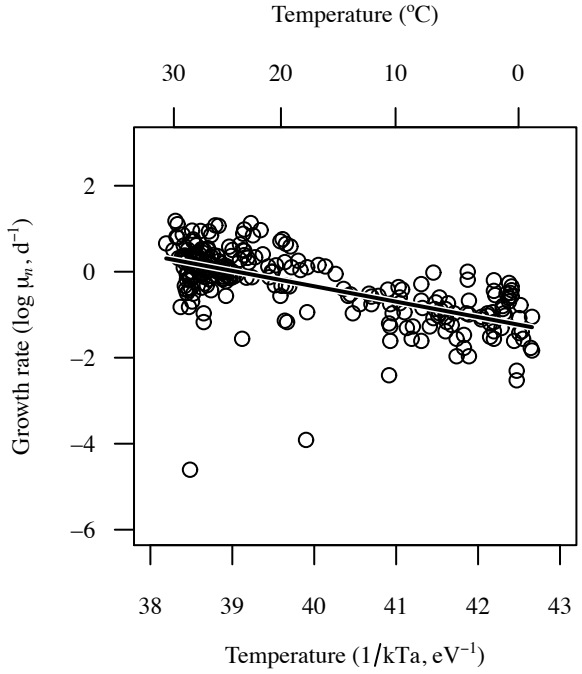

Figure 1.2: Effect of the temperature function ($1/kT_a$, lower axis) on log-transformed nutrient-saturated growth rate ($\log_{10}(\mu_n) = -0.36(1/kT_a) + 14$; ANOVA: $r^2 = 0.41$, $n = 258$). The corresponding temperatures in degrees Celsius are presented in the upper axis for reference.

in Figure 1.2, that needs to be used to obtain growth rates corrected for the effects of temperature.

When inferring the effect on metabolic processes of variables that might be correlated with temperature, like body size or nutrients, it should be borne in mind that the value used for the temperature correction might introduce some bias. We believe that the value used for the temperature correction should be derived theoretically, as the one used in Figure 1.1C, and not empirically, because solely based on a field data set like the one under analysis, it is impossible to discern the magnitude of the effects of temperature and of variables correlated with it. For example, it could be argued that the temperature coefficient we obtain in Figure 1.2 is dependent on the assumption that weight-specific growth rate is independent of

cell size, and that if we had corrected growth rate by the cell-size effects obtained in Figure 1.1B, we would have obtained a temperature coefficient closer to Eppley's (1972). To avoid this caveat, the temperature coefficient used should be based on some theory, like the one we used based on MTE, or corroborated by experimental work where the effect of the other variables can be controlled.

Such a criticism can be applied also, for example, to the activation energy of 0.29 eV for cell-size corrected phytoplankton growth rate obtained by López-Urrutia et al. (2006). This value is to some extent dependent on the assumption that growth rate scales with cell size to the 3/4 power. As cell size and temperature are correlated, taking a theoretical value for the effects of cell size to evaluate the effects of temperature, conditions in some way the activation energy obtained. A similar criticism can be made of field studies of the effects of cell size that do not take into account the effects of temperature or nutrient availability. For example, the results of Marañón (2008), who obtains an almost isometric scaling between phytoplankton production rates and cell volume, are dependent on the unlikely assumption that rates measured for the smallest cells do not coincide with the lowest nutrient levels.

Theory and experiments should have a major say in elucidating whether phytoplankton growth rates scale according to models of resource distribution networks as proposed by MTE or are constrained by surface diffusion. As explained above, MTE predicts that rate $\propto BV^{3/4}$, while nutrient uptake area considerations suggest that the scaling between primary production and BV should be rate $\propto BV^{2/3}$ (Aksnes and Egge, 1991). In terms of surface area, assuming $S \propto BV^{2/3}$, MTE predicts that rate $\propto S^{9/8} = S^{1.12}$, while surface diffusion theories predict that rate $\propto S^{1}$.

Paradoxically, a recent comprehensive study measuring metabolic rates of protists (Johnson et al., 2009) obtained a size scaling exponent of $S^{1.057}$, at the midpoint between resource distribution and surface-area theories. Johnson et al. (2009) incorrectly argued that, although they obtained a scaling between cell volume and metabolic rate of 0.72 with a 95% confidence interval of 0.65-0.79 (*see* their fig. S2), cell volume is not the appropriate metric for metabolic scaling

and cell carbon should be used instead. And because rate scales as carbon[1] they argue that metabolic scaling theories can't be applied to protists. This last argument by Johnson et al. (2009) is not correct; metabolic scaling theories derive the 3/4 scaling exponent on biovolume (West et al., 1999). MTE theories then assume that mass and biovolume scale isometrically (*see* assumption 6 in Banavar et al. 2010 and equation 8 in West et al. 1999) to derive the mass scaling exponent. Since metabolic rates scales as $BV^{3/4}$, the experimental data in Johnson et al. (2009) are also agree with MTE. In summary, data to allow a clear decision on which theory is correct are still lacking. In fact, the two theories might not be independent (Mei et al., 2009). Maybe organisms have to deal with both constraints, limitations on diffusion across surfaces and limitations on resource distribution networks, and that is why the measured scaling exponent is at the midpoint (Banavar et al., 2010).

1.3 Acknowledgements

This work was partially supported by projects CONSOLIDER Malaspina 2010 and METabolic OCean Analysis (METOCA) funded by Spanish National Investigation+Development+Innovation (I+D+I) Plan and by Theme 6 of the EU Seventh Framework Program through the Marine Ecosystem Evolution in a Changing Environment (MEECE 212085). S.S. was funded by a Formación de Personal Universitario (FPU) grant from the Spanish Ministry of Education.

CHAPTER

2

Thermal adaptation, phylogeny and the unimodal size scaling of marine phytoplankton growth

2.1 Introduction

Metabolism is the basis of the energetic exchange between organisms and the environment. According to the metabolic theory of ecology (MTE) (Brown et al., 2004), metabolic rates (M) scale with cell volume (BV) following a power-law of the form $M \propto aBV^b$, where *a* is a taxon-related constant and *b* is the size-scaling exponent, which commonly takes a value of approximately 3/4 (Kleiber, 1947). Hence, mass-specific metabolic rates, such as individual growth rate, should scale as -1/4 of the organism biovolume (Hemmingsen, 1960; López-Urrutia et al., 2006). In marine phytoplankton, some studies have supported this theoretical scaling (Banse, 1976; Blasco et al., 1982; Edwards et al., 2012; Niklas and Enquist, 2001), albeit they are usually based on the study of one or two size classes (Banse, 1976; Blasco et al., 1982). Indeed, the inclusion of a wider range of phytoplankton cell size, covering from picophytoplankton to large diatoms, leads to a weaker (Banse, 1982; Chisholm, 1992; Sommer, 1989) or almost inexistent relationship between mass-specific growth rate and cell volume (Huete-Ortega et al., 2012; Litchman et al., 2007; Marañón, 2008; Marañón et al., 2007). The controversy around the allometric scaling value has increased recently with the report of an unimodal (in a log-log scale) relationship between mass-specific growth rate and size (Chen and Liu, 2011, 2010; Marañón et al., 2013).

According to Chen and Liu (2011), the unimodality in the phytoplankton allometry can be mainly attributed to the lower growth rates by the smallest phytoplankton, specially the unicellular *Prochlorococcus* and *Synechococcus* (Chisholm, 1992). These lower growth rates have been related to an increase in the proportion of essential, non-scalable cellular components (membranes, nucleic acids) as cell and genome size is reduced, what leads to a reduction in the fraction of cytoplasm available for other scalable, catalytic components involved in growth rate (Raven, 1998; Raven et al., 2013). Reduction in genome and cell size minimizes the resources necessary for live and seems to be the result of picophytoplankton evolutionary adaptation to oligotrophic regions (Partensky and Garczarek, 2010). Raven (1998) suggested that the unimodal relationship between growth rate and cell size might be more a consequence of phylogenetic variations

in the taxon-related constant a in the allometric equation rather than to changes in b.

The shared evolutionary history of related species establishes a correlation between data in allometric scaling studies that, if not accounted for, can result in biased scaling exponents (Capellini et al., 2010; Ehnes et al., 2011; Kolokotrones et al., 2010). Phylogenetic approaches are commonly used to deal with intra- and interspecific trait variability combining evolutionary relationships between species and correlations between traits (Connolly et al., 2008; Felsenstein, 1985, 2008; Housworth, 2004; Ives et al., 2007). But the inclusion of such phylogenetic approaches in studies of metabolic scaling has been controversial, with authors questioning their validity or utility (Björklund, 1994; McNab, 2008; Ricklefs and Starck, 1996) arguing that phylogenetic correction does not significantly change the value of the estimated slope (reviewed in Glazier 2005) and others claiming the necessity to provide these analyses (Blackburn and Gaston, 1998; Garland et al., 1999). For terrestrial invertebrates, Ehnes et al. (2011) have shown that the inclusion of phylogeny removes the curvatures in allometric scaling models. In contrast, very few studies have applied phylogenetic approaches to the study of phytoplankton allometry (Bruggeman, 2011; Bruggeman et al., 2009; Connolly et al., 2008).

Failures to detect unimodal allometric scaling have also been attributed to the lack of homogeneity in the data used. Marañón et al. (2013), in an effort to avoid the uncertainties associated with the analysis of data measured under different growth conditions, maintained a series of phytoplankton cultures at the same temperature (18±0.5°C) and obtained a unimodal size scaling of phytoplankton growth rates. But each phytoplankton species has an optimum temperature at which its growth is maximum (Eppley, 1972; Thomas et al., 2012). The selection of the temperature at which to perform the size scaling experiments might be non-trivial if optimum temperature and phytoplankton cell size are correlated.

In this work we will assess whether a relationship between cell size and thermal optimum exists for marine phytoplankton. We will test the influence of temperature and the shared evolutionary history of species on the allometric scaling of growth

rate. Our final aim is to show that the curvature is the result of the specialization of picophytoplankton across evolution to the warm conditions usually encountered in oligotrophic environments.

2.2 Material and Methods

We used an extensive dataset of phytoplankton growth responses to temperature compiled by Thomas et al. (2012) for a total of 194 isolates/strains from estuarine and marine waters. These traits were estimated from >5000 growth rate measurements, synthesized from 81 studies between 1935 and 2011. This dataset only includes experiments were resources, such as light or nutrients, were not limited (details are provided in the supplementary information in Thomas et al. (2012).

To explore the relationship between cell size, maximum growth rate and temperature, we compiled cell volumes for each of the phytoplankton species in Thomas et al. (2012) dataset. Cell volumes were collected from the literature (Table S2.1). Cell sizes in the dataset ranged from 0.11 to 251184.82 μm^3 (0.59 to 78.28 Equivalent Spherical Diameter).

A phylogenetic tree is needed to evaluate whether the shared evolutionary history of species might influence the emergence of the unimodal pattern in the size scaling of growth rate. Branch lengths in the tree are essential to estimate the similarity between species. To build the phylogenetic tree, 18S and 16S (for cyanobacteria) rRNA sequences were retrieved from the GenBank database. We restricted the dataset to those phytoplankton species which have been sequenced, what resulted in a total of 121 isolates/strains. When the compilation in Thomas et al. (2012) included a species strain that was not sequenced we selected the sequence of another strain of the same species, assuming that the branch length between strains of a same species should be similar. When a species had several thermal growth response curves recorded but the phylogenetic information was restricted to only one strain we calculated an average thermal response for that species.

In addition to Thomas et al. (2012), we used a dataset compiled by López-Urrutia et al. (2006) (and used by Chen and Liu (2011) to demonstrate the existence of unimodal scaling). Here several measurements of growth rate at different temperatures are provided for each species together with cell volume. The difference between Thomas et al. (2012) and López-Urrutia et al. (2006) is that the latter only considers the exponential part of the growth response to temperature and includes also the effects of irradiance. Following the same procedure as for Thomas et al. (2012), we restricted the dataset to only those species that have been sequenced so the dataset was reduced from 1063 to 49 data points.

2.2.1 Phylogenetic analyses

Alignment of RNA sequences to build the phylogenetic tree was done with MUSCLE (using default settings) through the *muscle* package (Edgar, 2004) in *R* (R Development Core Team, 2008). The ends of the alignment were manually trimmed. The tree was calculated using maximum-likelihood (ML) analysis carried out using PhyML v.3.1 (Guindon and Gascuel, 2003), with the GTR+gamma+I model selected as the best tree using the Akaike information criterion (AIC) (Akaike, 1974). Package *ape* (Paradis et al., 2004) was used to call these external applications from *R*, where all analyses were carried out.

To introduce the information provided by the phylogenetic tree into the allometric scaling analysis, a Phylogenetic General Least Square (PGLS) regression (Felsenstein, 1985) was applied. Unlike standard linear regression, this accounts for the fact that data points might be correlated as result of shared evolutionary history. Following the methodology described in Kolokotrones et al. (2010), we used Pagel's covariance structure (Pagel, 1999) for the PGLS. This structure includes an extra parameter, λ, which assumes a Brownian motion to model the variance and allows to test for phylogenetic signal in the data. This value is optimized during the fitting process and takes values from 0 (phylogenetic independence between data) to 1 (original diffusion model with untransformed branch lengths). The PGLS was also applied using the *ape* package.

2.2.2 Size-scaling of growth rate and species thermal tolerance curves

Using the compilation of growth responses to temperature provided by Thomas et al. (2012), the thermal tolerance curve of each species was fit. We followed the same procedure as Thomas et al. (2012) and applied a maximum likelihood estimation (MLE) using the *bbmle* package in *R* (R Development Core Team, 2008). Using the thermal tolerance curve of each species, the optimum temperature was selected as the temperature at which growth rate is maximum.

These thermal tolerance curves provide estimates, for each species, of the growth rate at different temperatures. We calculated the size scaling of growth rate at 1 degree intervals from 2 to 33°C using for each species the predicted growth rate from the thermal tolerance curve. Linear and quadratic regressions were then applied to the log-log relationship between growth rate and cell size at each temperature, both with and without phylogenetic correction.

2.2.3 Temperature normalization

For each species in López-Urrutia et al. (2006), growth rate was corrected for the effects of photosynthetic active radiation using the parameters given in Table 1 of López-Urrutia et al. (2006). As in Chen and Liu (2011), normalization for temperature was applied using the Van't Hoff-Arrhenius equation (Arrhenius, 1915) with the activation energy given by López-Urrutia et al. (2006). Corrected growth rates were averaged for each species to have one measurement for each rRNA sequence.

For Thomas et al. (2012) data, we used the maximal growth rates and optimum temperature of each species as obtained by the MLE fits. To correct the effect of temperature, we used the slope (S) from the relationship between log of maximum growth rate and optimum temperature , so that $\log_{10}(\mu) - \mathrm{SxT}$ is the temperature-corrected growth rate (T;°C).

2.3 Results

The optimum temperature for growth and cell volume are correlated (r^2=0.04, p<0.05) Figure 2.1A). Species with a cell volume lower than 1 μm^3 (i.e. picophytoplankton species) show maximum growth rates at temperatures higher than 22°C, while larger species have optimum temperatures for growth between 2 and 33°C. The small species in Thomas et al. (2012) dataset are adapted to warm conditions whereas large phytoplankton species are more diverse regarding their optimum temperatures for growth with species with optima along almost the full ocean thermal range (Figure 2.1A). Regardless of cell-size, the maximum growth rate of species which have a growth optimum in warm conditions is higher than that of species with an optimum in colder environments. There is an exponential relationship between maximum growth rate of each species and optimum temperature (Figure 2.1B, $\log_{10}(\mu)_{\max} = 0.013xT - 0.41$, r^2=0.07, p<0.01).

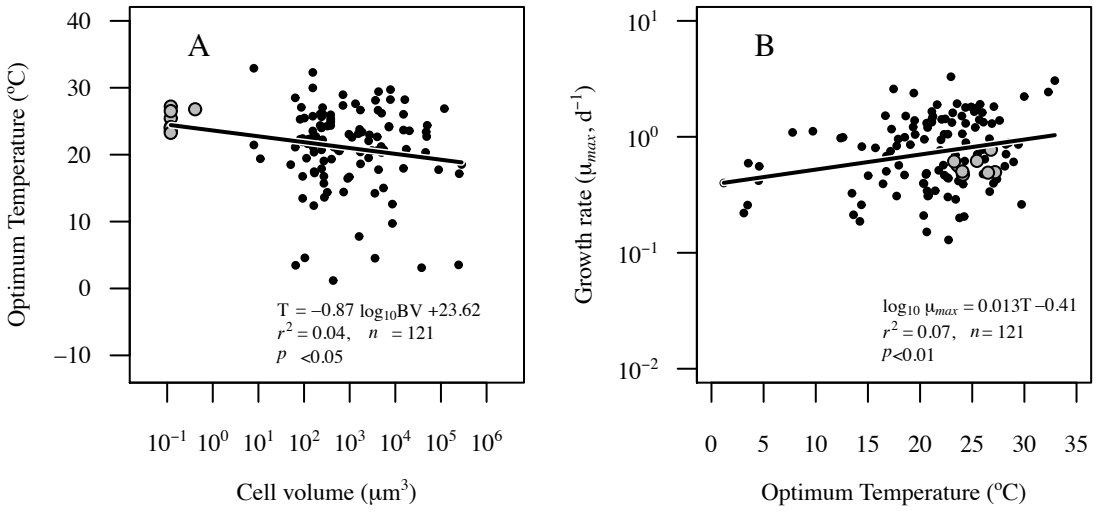

Figure 2.1: Relationship between species optimum temperature and **(A)** cell size and **(B)** maximum growth rate.

When we correct the maximum growth rates obtained from the thermal curve fit for the effects of temperature using the exponential coefficient in Figure 2.1B, there is a unimodal relationship between growth rate and cell volume. The quadratic term

in the relationship $\log_{10}(\mu)_{max} = \log_{10}BV + \log_{10}(BV)^2$ is significant (r^2=0.07, p<0.01, AIC= 48.57) and the quadratic model is a better predictor than the linear model (r^2=0.01, p=0.383, AIC= 54.08) (Figure 2.2A). This unimodal pattern is mainly due to the picophytoplankton species having lower than average growth rates.

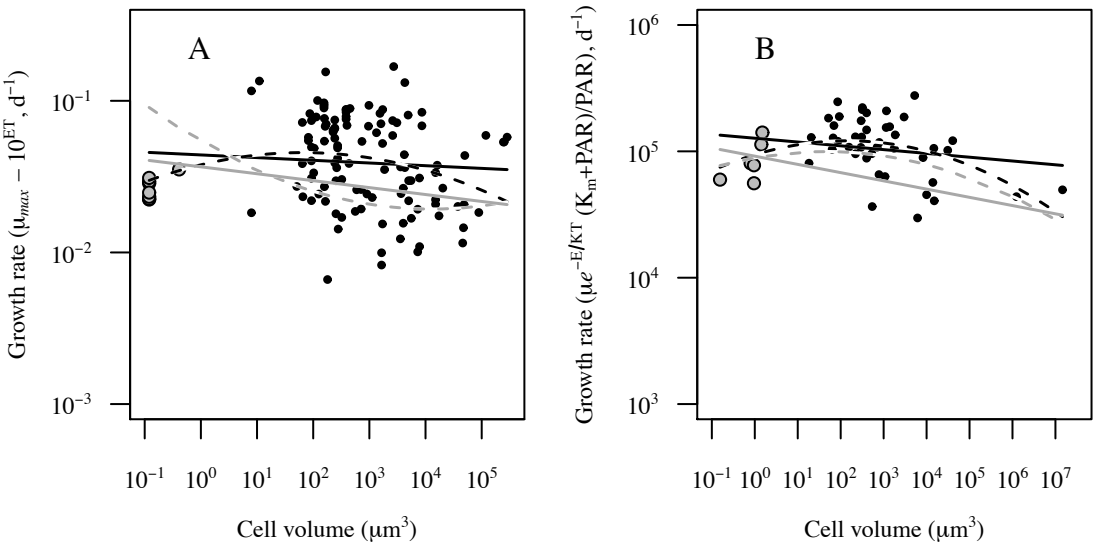

Figure 2.2: Size scaling of growth for: **(A)** Thomas et al. (2012) data. The black solid line corresponds to a linear fit ($\log_{10}(\mu) = -0.02\log_{10}(BV) - 0.36$; ANOVA: r^2 = 0.01, n = 121, p-value = 0.38). The black dashed line corresponds to a quadratic fit ($\log_{10}(\mu) = -0.02\,[\log_{10}(BV)]^2 + 0.09\,\log_{10}(BV) - 0.42$; ANOVA: r^2 = 0.07, n = 121, p-value < 0.01). The grey solid line corresponds to a linear PGLS fit ($\log_{10}(\mu) = -0.04\,\log_{10}(BV) - 0.43$, AIC = 21.09, p-value = 0.12, λ=0.96). The grey dashed line corresponds to a quadratic PGLS fit ($\log_{10}(\mu) = 0.02\,[\log_{10}(BV)]^2 - 0.21\,\log_{10}(BV) - 0.26$, AIC = 27.25, p-value = 0.16, λ=0.96). **(B)** López-Urrutia et al. (2006) data. Same color coding as in **(A)**, black solid line is the linear fit ($\log_{10}(\mu) = -0.03\,\log_{10}(BV) + 5.10$; ANOVA: $r^2 = 0.04$, $n = 49$, p-value = 0.17), black dashed line is quadratic fit ($\log_{10}(\mu) = -0.02\,[\log_{10}(BV)]^2 + 0.10\,\log_{10}(BV) + 4.97$; ANOVA: r^2 = 0.17, n = 49, p-value < 0.01), grey solid line is the linear PGLS fit ($\log_{10}(\mu) = -0.06\,\log_{10}(BV) + 4.96$, AIC = -4.54, p-value < 0.01, λ=0.92) and grey dashed line is the quadratic PGLS fit ($\log_{10}(\mu) = -0.02\,[\log_{10}(BV)]^2 + 0.06\,\log_{10}(BV) + 4.95$, AIC = 1.39, p-value =0.06 ,λ=0.91).

A similar pattern is evident in the dataset given by López-Urrutia et al. (2006) as analysed by Chen and Liu (2011) (Figure 2.2B). Although Chen and Liu (2011) used cell carbon as an estimate of cell size, the same pattern is obtained using cell volume. After normalization for temperature and photosynthetically active radiation, a quadratic model explains a higher amount of variance than a linear one (Figure 2.2B. Quadratic model:r^2=0.2, p<0.01, AIC=-9.65; linear model: r^2=0.004, p=0.173, AIC= -2.23). Again, the unimodal pattern is mainly determined by the picophytoplankton growth rates, what suggests a phylogenetic origin for the curvature.

We replicated these analyses applying a PGLS regression to both datasets. The quadratic term is no longer significant in any of them (λ=0.91, p=0.06, AIC= 1.39 for López-Urrutia et al. (2006); λ=0.96, p=0.157, AIC= 27.24 for Thomas et al. (2012)). The phylogenetic analyses yielded the lowest AIC values for the linear fits (λ=0.92, p<0.05, AIC= -4.54 for López-Urrutia et al. (2006); λ=0.956, p=0.123, AIC= 21.09 for Thomas et al. (2012)). Although for the López-Urrutia et al. (2006) dataset the PGLS linear fit was significant, the relationship between temperature corrected growth rate and cell size was not significant for Thomas et al. (2012) data. In addition, λ values were close to 1 for all analyses revealing a strong phylogenetic signal in the data. This implies that differences in the species growth rate are correlated to the phylogenetic distance amongst species. These results suggest that the observed curvature in the size scaling of growth rate is a consequence of the shared evolutionary history.

Up to this point, we have evaluated the effect of phylogeny on the allometric scaling on the basis of temperature-corrected growth rates. This is the common practice when data are compiled for different species measured at different temperatures. The alternative way to analyse the size scaling of growth is to measure the growth rates of a set of species at the same temperature (i.e. Marañón et al. 2013). With the growth vs temperature growth curves we can simulate such experiments at different temperatures. For each temperature, we estimate the growth rate of each species and use that data to analyse the size scaling. For example, Figure 2.3A represents the growth estimates at 30°C. If we calculate with the data for all species (grey circles) the size scaling, the quadratic term is

not significant (Quadratic model: r^2=0.03, p=0.18, AIC= 160.51; linear model: r^2=0.001, p=0.78, AIC= 160.36). Similarly, at 10°C we can plot the predicted growth rates for each species (Figure 2.3B) but here the quadratic term is significant and better predictor than the linear one (Quadratic model: r^2=0.21, p<0.001, AIC= 142.40 ; linear model: r^2=0.016, p=0.22, AIC= 161.94).

We can repeat this process at 1°C intervals from 2 to 33°C and calculate the significance of the quadratic term (column ″p-value″ in Figure 2.3C) for each temperature. The unimodal growth rate scaling does not occur at the extremes of the thermal range. At the highest temperatures, the growth rates of picophytoplankton are not significantly lower than those of nano and microphytoplankton. At the lowest temperatures, the growth rates of picophytoplankton and nanophytoplankton are lower than those of the larger phytoplankton, the quadratic term is not significant but there is a positive allometric scaling. At temperatures from 5 to 25 °C the unimodal scaling of phytoplankton growth rate is significant and contributes to explain a significant amount of the variance (right panel in Figure 2.3C). When a PGLS is applied to the size scaling of growth rate at each temperature, and hence the shared evolutionary history of species is taken into account, the curvature is no longer significant at any temperature, supporting the hypothesis of its evolutionary origin. The colour matrix plot in Figure 2.3C summarizes these results. For each temperature degree, we split the cell size range into 7 different classes and calculated the average growth rate for each cell size bin (see Figures 2.3A & 2.3B for examples). We observe a clear pattern where as we move toward higher temperatures the curvilinear scaling disappears. This pattern is the result of picophytoplankton adaptation to high temperatures. The unimodality on the relationship between cell size and growth rate depends strongly on temperature and it is not significant from ~25°C upwards, i.e., where picophytoplankton grows at their optimum temperatures.

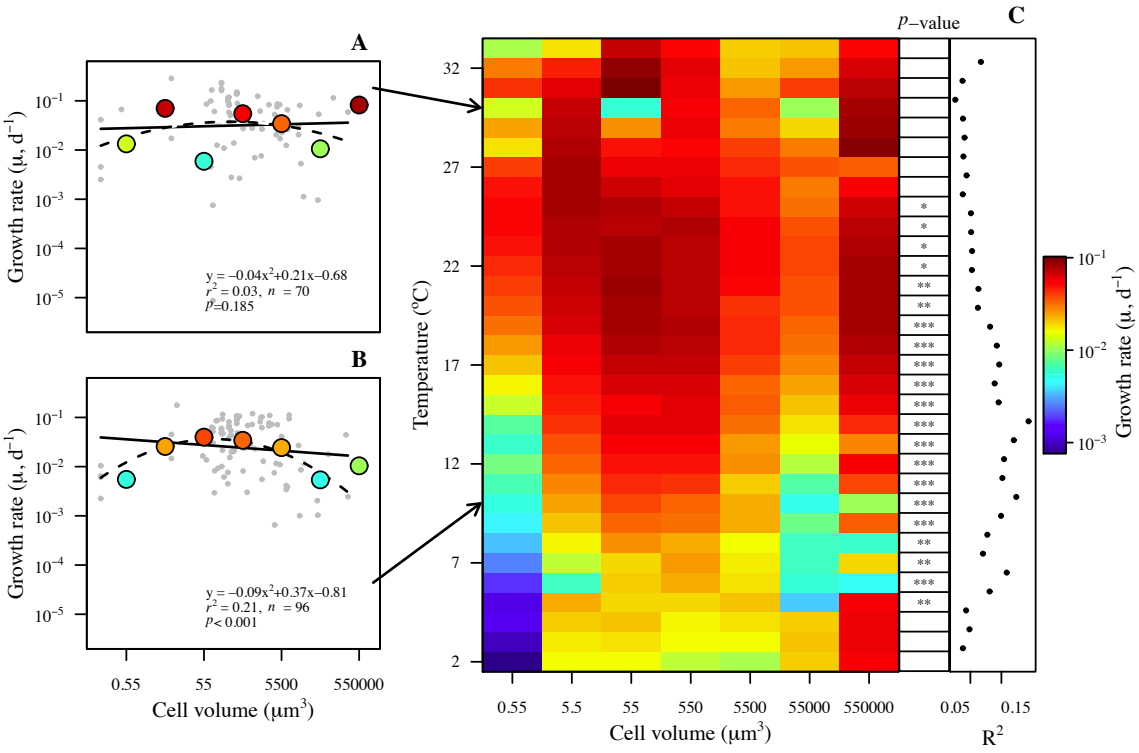

Figure 2.3: Effect of temperature on the size scaling of growth rate. Panels on the left show the size scaling of growth (log10 transformed) for predicted growth rates at **(A)** 10° and **(B)** 30°. Grey dots show all data points whereas colors dots show the corresponding averaged growth rates for each size bin as used in the colour matrix plot **(C)** . The black solid line corresponds to a linear fit. The black dashed line corresponds to a quadratic fit. Linear fit in **(A)**: $\log_{10}(\mu) = -0.07\log_{10}(\mathrm{BV}) - 0.47$; ANOVA: r^2 = 0.02, n = 143, p-value = 0.11. Linear fit in **(B)**: $\log_{10}(\mu) = -0.02\log_{10}(\mathrm{BV}) - 0.46$; ANOVA: r^2 = 0.0006, n = 109, p-value = 0.8. Quadratic fits are shown in the panels. **(C)** The colour matrix shows for each temperature from 2 to 33°C (y axis) the averaged growth rate at each cell size bin (x axis). The *p-value* column shows the degree of significance of the quadratic fit for the log10-log10 relationship between growth rate and cell size using all data points (no data binning). When the quadratic term is not significant, i.e. p-value>0.05 the box appears empty. (*) indicates p-value<0.05, (**) indicates p-value<0.01 and (***) p-value<0.001. The right panel shows the ratio between the r-squared of the quadratic term and the r-squared of the linear term for the different fits at each temperature, i.e., the proportional increase in explained variance of the quadratic fit in relation to the linear fit.

2.4 Discussion

The role of the evolutionary history of species on the study of the allometric scaling of marine phytoplankton has been hardly considered explicitly. We have evaluated the causes of the unimodal relationship between mass-specific growth rate and cell size (Chen and Liu, 2011; Marañón et al., 2013) using two different datasets. We have used Phylogenetic General Least Square (PGLS) regression (Felsenstein, 1985) to understand the evolutionary effects on the linear and quadratic fits. Our results show that, in both datasets, the quadratic/unimodal relationship is not significant after the phylogenetic correlation in the data is taken into account.

The curvature in the scaling relationship between mass-specific growth rate and cell size is mainly due to prokaryotic picophytoplankton. When we compare the growth rate of phytoplankton species at their thermal optimum (Figures 2.2A & S2.1), picophytoplankton have lower growth rates than larger phytoplankton but when phylogenetic correction is used, these lower growth rates are not significant. Chen and Liu (2011) suggested that the unimodal pattern may be the result of evolutionary adaptation of picophytoplankton to nutrient availability in oligotrophic environments. This was pointed out originally by Raven (1998), who suggested that the reduction in size in picophytoplankton increases the availability of resources at low nutrient levels but at the cost of a reduction in the proportion of scalable components devoted to cell growth. In addition, marine picocyanobacteria such as *Prochlorococcus* or *Synechococcus* form a phylogenetic branch separated not only from larger phytoplankton taxa but also from larger species within the cyanobacteria group (Figures S2.2 & S2.3). Specially, *Prochlorococcus* has suffered an extensive genome streamlining that has affected most lineages at different proportions (Palenik, 1994; Penno et al., 2006; Rocap et al., 2002; Urbach et al., 1998). Hence, the high variability of growth rates exhibited within the *Prochlorococcus* group (Figure 2.1B) seems to correspond to different levels of genome streamlining rather to be a consequence of its tiny cell size (Partensky and Garczarek, 2010). Recent studies suggest that both genome and cell size are mutually correlated (Ting et al., 2007) and therefore they have decreased concurrently during evolution (Partensky and Garczarek, 2010).

These conundrum between phylogeny, size and growth rate is evidenced by the strong phylogenetic signal in our data ($\lambda > 0.9$). The growth rate and size estimates for the different species are not independent but closely related species have growth rates and sizes more similar than species selected at random. The independence of data is one of the assumptions of conventional methods for data analysis and its violation might have various consequences, from biases in the regression coefficients to severe underestimation of uncertainties related to these values. Hence, if instead of using a phylogenetic correction as we do, all observations were treated as independent (Finkel, 2001; Litchman et al., 2007; Tang, 1995), a biased association may be observed between growth rate and cell size. But phylogenetic regressions have also been criticized mainly for two reasons: first because these methods attribute to ecology the remaining variation in character after phylogenetic correction, given thus priority to the latter over ecology when, actually, they are not mutually exclusive because of the phylogenetic niche conservatism (Freckleton et al., 2002; Grime and Hodgson, 1987; Harvey and Pagel, 1991; Westoby et al., 1995). And second, because they imply the validity of a ″Brownian motion″ to explain the constant rate of variability through the different branches of the phylogeny, which is not always appropriate. But when a strong phylogenetic signal is apparent, as is the case here, we argue that accounting for the shared evolutionary history of species is essential to avoid biased conclusions due to the non-independence in the data (Bruggeman, 2011; Martins and Garland, 1991). In the literature cases where the curvature in metabolic scaling has been found to be relevant (e.g. Kolokotrones et al. 2010), the quadratic term was found significant after phylogenetic correction, what warrants an interpretation of the curvature independent of the evolutionary history of species.

The relevance of the inclusion of picophytoplankton is evident in previous studies which only considered larger species and reported linear exponents (Banse, 1982; Finkel, 2001; Litchman et al., 2007; López-Urrutia et al., 2006; Sommer, 1989; Tang, 1995). It has been shown that the value of the linear exponent depends on the size range considered (see Figure 2 in Chen and Liu 2011). For instance, the difference in the slope obtained in Figure 2.1B of 0.03 and the -1/4 exponent observed by López-Urrutia et al. (2006) is that the latter study only considered

data where both phytoplankton volume and growth rate were measured in the same experiment. For Figure 2.1B we have also used volume estimates measured for the same species in other studies, what extends the size range to picophytoplankton and substantially reduces the size scaling slope. This low slope is apparent using either cell volume (Figure 2.1B) or carbon biomass (see Figure 1B in Chen and Liu (2011)). Therefore, the size-scaling of marine phytoplankton departs significantly from the predicted -1/4 power rule (Marañón et al., 2007) and mass-specific growth rate scales independent of body volume when a large range size is considered Marañón et al. (2013).

These conundrum between phylogeny, size and growth rate is further puzzled when we also consider that temperature affects both growth rates and phytoplankton cell size and complicated by the evolutionary adaptation of picophytoplankton to warm environments. To correct for the effects of temperature on growth rate when data are compiled for species growing at different temperatures, an exponential relationship between temperature and growth is used to standardize the growth rates of all species to the same temperature. But because both cell volume (Figure 2.1A) and growth rate (Figure 2.1B) are correlated with temperature it is hard to ascertain that the assumed exponent for the temperature correction is not biased by the fact that picophytoplankton species (theoretically with lower growth rates) are predominantly present at the highest temperatures. The estimated exponent for the optimum growth rates (Figure 2.1B) is lower than the value reported by Eppley (1972) (0.013 vs 0.0275). The choice of the thermal dependence exponent might introduce some bias in the size scaling analysis (Sal and Lopez-Urrutia, 2011). *A priori*, this caveat might be avoided measuring the growth rate of all species under study at the same temperature. But, paradoxically, our results show that the size scaling of phytoplankton growth rates is largely dependent on the temperature at which growth rates are measured. For instance, the non-phylogenetically corrected unimodal scaling of phytoplankton growth rate is significant from 5 to 25 °C, but not at higher or colder temperatures. Hence, our results support the unimodality at 18ºC reported by Marañón et al. (2013) but we add the perspective that, if growth rates were measured at different temperatures the size scaling might have differed.

This is the result of picophytoplankton adaptation to warm conditions while larger species have a more diverse thermal preference and may have optimum temperatures along the full ocean thermal range (Figure 2.1B). At warm temperatures, the picophytoplankton species in Thomas et al. (2012) compilation are all at their thermal optimum. But nano and micro-phytoplankton data consists of both species that have their optimum at high temperatures and species that have their optimum at temperate conditions but that nevertheless are able to growth at higher temperature. The inclusion of data of species out of their thermal optimum results in a different pattern in Figure 2.3A than in Figure S2.1 where only species that have their thermal optimum at high temperatures are considered. The optimum temperature of the species seems to be the result of evolutionary adaptation to the environmental conditions they experience locally Thomas et al. (2012). As picophytoplankton, specially *Prochlorococcus* strains, is usually most abundant in the warm oligotrophic waters (Flombaum et al., 2013), it is expected to have optimum growth at high temperatures.

Our temperature simulation experiment, combines the estimation of thermal reaction norms to predict the growth rate of each species at different temperatures and the analysis of size scaling at each temperature. Ideally, these results should be confirmed experimentally by making a full experimental design where both temperature responses and size-scaling experiments are performed in parallel. But the number of treatments in such a factorial design would make the study almost impractical. Community wide attempts (Boyd et al., 2013) might be the solution to fully test our hypothesis. Although the collation of data in Thomas et al. (2012) that we used to estimate the thermal reaction curves comes from a wide range of experimental protocols, a recent comparison with the dataset from such a community-wide study (Boyd et al., 2013) found slight differences on the maximum growth rate of species, but optimum temperatures and thermal reaction norms were similar across studies.

Although our results reveal that the unimodal scaling depends on temperature, the role of phylogeny seems to be much more important. Even at low temperatures, where picophytoplankton shows very low growth rates, a curvature appears to be non-significant after phylogenetic correction. In summary, our results state

that the allometric slope of phytoplankton growth rates are variable and do not consistently support a specific theoretical value when a large range of cell sizes are included. The strong phylogenetic signal exhibited in our data reveals that phylogeny should be borne in mind in allometric studies, since variability on the species growth rates seems to be consequence of a common evolutionary history rather than uniquely an effect of their size. This supports Raven's (1998) hypothesis that picophytoplankton have lower growth rates in an effort to increase the efficiency for the resources acquisition at low nutrient levels. Adaptations such as the latter, have been a common feature along the evolutionary history of organisms. In addition, this unimodal scaling of phytoplankton growth due to the different growth rate scaling of prokaryotic picophytoplankton is in accordance with the shift in metabolic scaling from prokaryotes to eukaryotes as a result of the dramatic changes in structure and function experienced across this major evolutionary transition (DeLong et al., 2010).

2.5 Supplementary table and figures

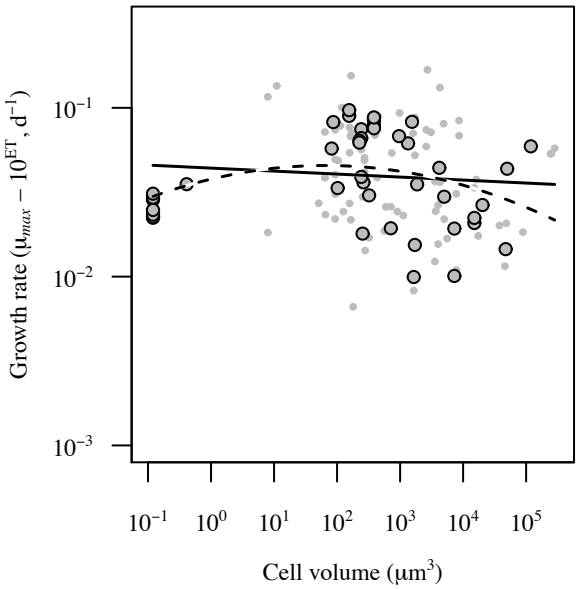

Figure S2.1: Size scaling of growth rate for those species with optimum temperatures between 23 and 28° in Thomas et al. (2012) data (big grey dots). The black solid line corresponds to a linear fit ($\log_{10}(\mu) = -0.005 \log_{10}(\mathrm{BV}) - 0.43$; ANOVA: r^2 = 0.001, n = 43, p-value = 0.82). The black dashed line correspond to a quadratic fit ($\log_{10}(\mu) = -0.04\,[\log_{10}(\mathrm{BV})]^2 + 0.14 \log_{10}(\mathrm{BV}) - 0.40$; ANOVA: $r^2 = 0.22$, $n = 43$, p-value < 0.005). Small grey dots on the background show the whole dataset.

2. Thermal adaptation, phylogeny and the unimodal size scaling of marine phytoplankton growth

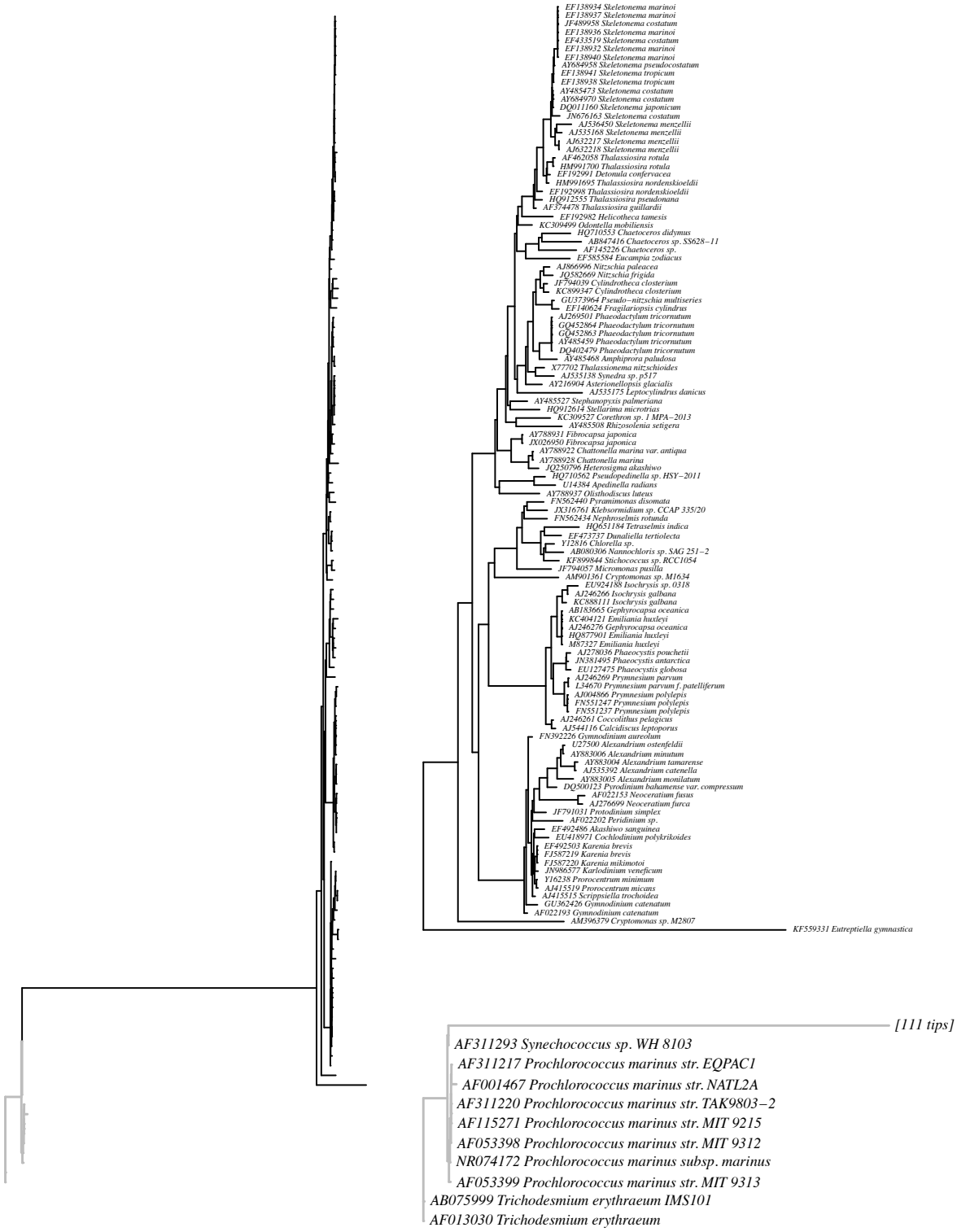

Figure S2.2: Phylogenetic tree for Thomas et al. (2012) data. Grey edges show the picophytoplankton branches.

Figure S2.3: Phylogenetic tree for López-Urrutia et al. (2006) data. Grey edges show the picophytoplankton branches.

Table S2.1. Cell size references for the species used in the study.

Species Name	Source
Akashiwo sanguinea	Olenina et al. (2006)
Alexandrium catenella	http://species-identification.org
Alexandrium fundyense	http://species-identification.org
Alexandrium minutum	Marañón et al. (2013)
Alexandrium monilatum	http://species-identification.org
Alexandrium ostenfeldii	Olenina et al. (2006)
Alexandrium tamarense	Marañón et al. (2013)
Amphiprora sp.	Olenina et al. (2006)
Apedinella radians	Olenina et al. (2006)
Asterionellopsis glacialis	Olenina et al. (2006)
Calcidiscus leptoporus	Marañón et al. (2013)
Chaetoceros didymus	Olenina et al. (2006)
Chaetoceros lorenzianus Bermuda	Olenina et al. (2006)
Chaetoceros pseudocurvisetus	Leblanc et al. (2012)
Chaetoceros sp.	http://www.eos.ubc.ca/research/phytoplankton
Chattonella marina	Band-Schmidt et al. (2012)
Chattonella marina var. antiqua	Band-Schmidt et al. (2012)
Chlamydomonas	Olenina et al. (2006)
Chlorella sp.	http://diatom.ansp.org/taxaservice/ShowList.aspx
Chrysochromulina polylepis	Olenina et al. (2006)
Coccolithus pelagicus ssp. Braarudii	http://nannotax.org
Cochlodinium polykrikoides	http://species-identification.org
Conticribra guillardii	Olenina et al. (2006)
Corethron pennatum	Timmermans et al. (2004)
Cryptomonas sp.	Olenina et al. (2006)
Cylindrotheca closterium	Olenina et al. (2006)
Dactyliosolen fragilissimus	Olenina et al. (2006)
Detonula confervacea	Olenina et al. (2006)
Dunaliella tertiolecta	http://www.algaebase.org
Emiliania huxleyi	Marañón et al. (2013)
Eucampia zodiacus	Olenina et al. (2006)
Eutreptiella gymnastica	Olenina et al. (2006)
Fibrocapsa japonica	http://nordicmicroalgae.org
Fragilariopsis cylindrus	http://nordicmicroalgae.org
Fragilariopsis kerguelensis	Timmermans (2010)

Gephyrocapsa oceanica	Marañón et al. (2013)
Gephyrocapsa oceanica var. typica	Marañón et al. (2013)
Gymnodinium aureolum	http://nordicmicroalgae.org
Gymnodinium catenatum	http://species-identification.org
Gymnodinium corollarium	http://nordicmicroalgae.org
Gymnodinium (probably G. simplex)	http://nordicmicroalgae.org
Helicotheca tamesis	http://nordicmicroalgae.org
Heterocapsa rotundata	http://nordicmicroalgae.org
Heteromastix pyriformis	http://www.serc.si.edu/labs/phytoplankton/guide/index.aspx
Heterosigma akashiwo	Olenina et al. (2006)
Isochrysis galbana	Marañón et al. (2013)
Isochrysis sp.	Liu and Lin (2001)
Karenia brevis	http://www.sms.si.edu/irlspec
Karenia mikimotoi	http://nordicmicroalgae.org
Karlodinium veneficum	Galimany et al. (2007)
Klebsormidium	Škaloud (2006)
Leptocylindrus danicus	http://nordicmicroalgae.org
Micromonas pusilla	http://nordicmicroalgae.org
Nannochloris (possibly Stichococcus) sp.	https://ncma.bigelow.org
Neoceratium furca	http://nordicmicroalgae.org
Neoceratium fusus	http://nordicmicroalgae.org
Neoceratium lineatum	http://nordicmicroalgae.org
Neoceratium tripos	http://nordicmicroalgae.org
Nitzschia frigida	Olenina et al. (2006)
Nitzschia paleacea	Olenina et al. (2006)
Odontella mobiliensis	Olenina et al. (2006)
Olisthodiscus luteus	Leadbeater (1969)
Peridinium sp.	http://diatom.ansp.org/taxaservice/ShowList.aspx
Phaeocystis antarctica	Zingone (1999)
Phaeocystis globosa	Olenina et al. (2006)
Phaeocystis pouchetii	Olenina et al. (2006)
Phaeodactylum tricornutum	Marañón et al. (2013)
Prochlorococcus marinus	Marañón et al. (2013)
Prorocentrum gracile	Marañón et al. (2013)
Prorocentrum micans	Olenina et al. (2006)
Prorocentrum minimum	Olenina et al. (2006)
Prymnesium parvum f. patelliferum	Green et al. (1982)
Prymnesium parvum	Green et al. (1982)
Pseudo-nitzschia multiseries	http://diatom.ansp.org/taxaservice/ShowList.aspx
Pseudopedinella pyriformis	http://www.smhi.se
Pyramimonas disomata	http://www.smhi.se
Pyrodinium bahamense var. compressum	http://species-identification.org
Rhizosolenia setigera	Olenina et al. (2006)

Scrippsiella trochoidea	Olenina et al. (2006)
Skeletonema ardens	https://ncma.bigelow.org
Skeletonema costatum	Marañón et al. (2013)
Skeletonema japonicum	https://ncma.bigelow.org/
Skeletonema marinoi dohrnii complex	https://ncma.bigelow.org
Skeletonema menzelii	https://ncma.bigelow.org
Skeletonema pseudocostatum	https://ncma.bigelow.org
Skeletonema tropicum	https://ncma.bigelow.org/
Stellarima microtrias	http://www.smhi.se
Stephanopyxis palmeriana	http://www.serc.si.edu/labs/phytoplankton/guide/index.aspx
Stichococcus (possibly S. cylindricus)	https://ncma.bigelow.org
Synechococcus	Marañón et al. (2013)
Synedra sp.	http://diatom.ansp.org/taxaservice/ShowList.aspx
Tetraselmis sp.	http://diatom.ansp.org/taxaservice/ShowList.aspx
Thalassionema nitzschioides	http://nordicmicroalgae.org
Thalassiosira nordenskioeldii	http://nordicmicroalgae.org
Thalassiosira pseudonana	http://nordicmicroalgae.org
Thalassiosira rotula	Marañón et al. (2013)
Trichodesmium erythraeum	Gárate-Lizárraga (2012)

CHAPTER

3

Multiple drivers of the latitudinal diversity gradient in marine phytoplankton

3.1 Introduction

The increase in species richness towards the equator results in a latitudinal diversity gradient (LDG) that has puzzled marine and terrestial ecologist for the last two centuries (Bates, 1862; Colwell and Hurtt, 1994; Humboldt and Bonpland, 1807; Pianka, 1966; Rohde, 1992; Stevens, 1989; Wallace, 1854). For marine taxa, Tittensor et al. (2010) found that species richness peaked across broad mid-latitudinal bands in an extensive compilation of oceanic data. Several modelling studies have attempted to reproduce this pattern for marine phytoplankton and have formulated different hypotheses to explain the LDG. Two major factors have been suggested as the drivers for the LDG: resource competition and temperature gradients. Although the effects of these drivers are not mutually exclusive most studies claim that it is either one of these factors what controls the LDG. For example, Barton et al. (2010*a*) used a global ocean circulation and ecosystem model to suggest that the higher diversity at low latitudes is due to the relatively steady environmental conditions in this area, which enable the prolonged coexistence of species with similar fitness. They conjectured that there is a balance between the removal of species through resources competition (Tilman, 1982) and the replacement of some of them by oceanic currents. Amongst the models that suggest that it is the temperature gradient what controls the LDG, Brayard et al. (2005) were the first to find evidence of a potential role of a *mid-domain effect* (MDE) that emerges as consequence of the combination between geometric constraints and sea surface temperature. Beaugrand et al. (2013) used a bioclimatic global model to suggest that the LDG is the result of a mid-domain effect (Colwell and Lees, 2000) in the thermal niche space. In short, the *thermal mid-domain effect* (TMDE) states that if each species is characterized by a thermal niche range and these niches are distributed at random along a temperature gradient, there is an increasing overlap of species ranges toward the centre of the temperature gradient or domain. This TMDE hypothesis therefore predicts higher species richness at mid-temperatures as an stochastic realization of a null model.

Although, at first glance, such a null model seems to be in stark contrast with the resource competition hypothesis by Barton et al. (2010*a*), there is no reason

why these two mechanism could not operate simultaneously. In fact, although Beaugrand et al.'s (2013) bioclimatic model does not allow for species coexistence, Barton et al. (2010*a*) used a global ecosystem model where species distribution are constrained, in addition to resource competition, grazing or mortality, by a randomly selected thermal niche. Barton et al. (2010*a*) considered the possible existence of a MDE in their model output but in the geographical domain instead of in the thermal domain, as Beaugrand et al. (2013) suggested. They found that species niche breadth do not decrease with latitude, and conclude that a MDE can not explain the latitudinal pattern. Hence, our first aim is to evaluate the extent of this thermal mid-domain theory as main driver of the LDG. We use the same 3D global ecosystem model configuration in Barton et al. (2010*a*) but modifying the parameterization of resource competition ability and temperature sensitivity to study their effects either combined or individually. Our final goal is to elucidate what are the main mechanisms that drive the patters of diversity of oceanic phytoplankton.

3.2 Material and Methods

We use a marine ecosystem model that couples a lower trophic foodweb model of planktonic organisms (phytoplankton and zooplankton) to a global ocean model of physical processes (advection and diffusion) (Dutkiewicz et al., 2009; Follows et al., 2007). The three dimensional (3D) global ocean model is based on a coarse resolution (1° x 1° horizontally, 24 levels vertically) of the MIT general circulation model (MITgcm) constrained to be consistent with large-scale hydrogeography and altimetry (Wunch and Heimbach, 2007). The model includes four limiting dissolved inorganic nutrients in several forms: phosphorous (P) as phosphate; nitrogen (N) as nitrate and ammonium; iron (Fe) as bioavailable soluble Fe^{2+}; silicon (Si) as silicic acid. The model was initialized with 78 phytoplankton species belonging to two size-classes and four major phytoplankton functional groups: analogs of *Prochlorococcus*, pico-eukariotes, non-diatom eukariotes, and diatoms. Functional grouping was based on nutrient requirement. All groups use phosphate, ammonium and iron. Diatoms are the only group requiring silica. *Prochlorococcus*

analogs are here limited to ammonium as their sole source of nitrogen. The pico-eukariotes, non-diatom eukariotes, and diatoms are assumed to take up ammonium preferentially over nitrate (Vallina and Le Quéré, 2011). The model also resolves two predator size classes that feed preferentially (although not exclusively) on small and large phytoplankton, respectively.

Physiological growth rates are a function of dissolved inorganic nutrients (DIN), photosynthetic active radiation (PAR), and sea surface temperature (SST). Nutrient co-limitation is computed with Liebig's law of the minimum (DeBaar, 1994). Phytoplankton losses are due to vertical sinking, background and grazing mortality, and physical dilution by dispersion. Physiological characteristics are assigned at random to the 78 phytoplankton species. Competitive interactions among organisms and environmental filtering will shape the local self-assembly of the phytoplankton community, ultimately leading to geographically distinct ecosystems. The community structure and diversity are thus emergent properties by ecological selection processes.

In this work, we performed several simulations to study the effect of nutrients and temperature, either combined or in isolation. For each configuration the model was run 10 times with physiological parameters selected at random. Each model run was integrated for 10 years after which each species either goes extinct or undergoes a repetitive seasonal cycle. Phytoplankton biomass distribution for each species was obtained as monthly outputs from the last year of simulation. The global maps of species diversity were obtained for the surface layer (0 m) and for the whole vertically integrated euphotic zone (0 - 260 m). Phytoplankton diversity was computed as the number of species whose biomass exceeds 0.1% of the total biomass locally. The global maps show the annual mean of monthly diversity at each location.

3.2.1 Model simulations

3.2.1.1 Simulation 1: DIN + SST + PAR niches (full model)

We replicated Barton et al.'s (2010*a*) model configuration in this first simulation. Phytoplankton growth rate is limited by nutrients, temperature and solar radiation (Figures 3.1A-C). The physiological characteristics of the species were assigned stochastically. Temperature optima values do not depend on phytoplankton size class but large phytoplankton species have higher solar radiation optima values than small phytoplankton (see Figure 3.1C). Phytoplankton species will tend to distribute according to their temperature and solar radiation optima within a tolerance range, which allows geographical segregation and thus global coexistence (Barton et al., 2010*a*). The two traits that define nutrient uptake capabilities (i.e. intrinsic maximum growth and half-saturation constant) depend on cell size in a way that can sometimes lead to an allometric competitive trade-off among species. The maximum growth rates are fixed for each phytoplankton size-class while the half-saturation constants for nutrient uptake are randomly selected from a distribution whose lower and upper values do not overlap. Large phytoplankton have a higher intrinsic maximum growth rate than small phytoplankton but they draw parameter values from a distribution with higher half-saturation constants (Follows et al., 2007). Therefore, some large species will be better competitors at high nutrient concentrations while some small species will be better competitors at low nutrient concentrations, which allows non-equilibrium coexistence. The rest of the species will never be a viable competitor for any nutrient concentrations and thus will be competitively excluded. See Barton et al. (2010*a*) Supplementary Material for further details on the model setup.

3.2.1.2 Simulation 2: DIN niches only

In order to test whether the diversity gradient can be driven by resource competition alone we removed SST and PAR niches. Specifically we removed temperature limitation and gave the same PAR saturation and inhibition constants to all phytoplankton. We also removed any size-based differences in grazing or background mortality and vertical sinking. This means that all species are able

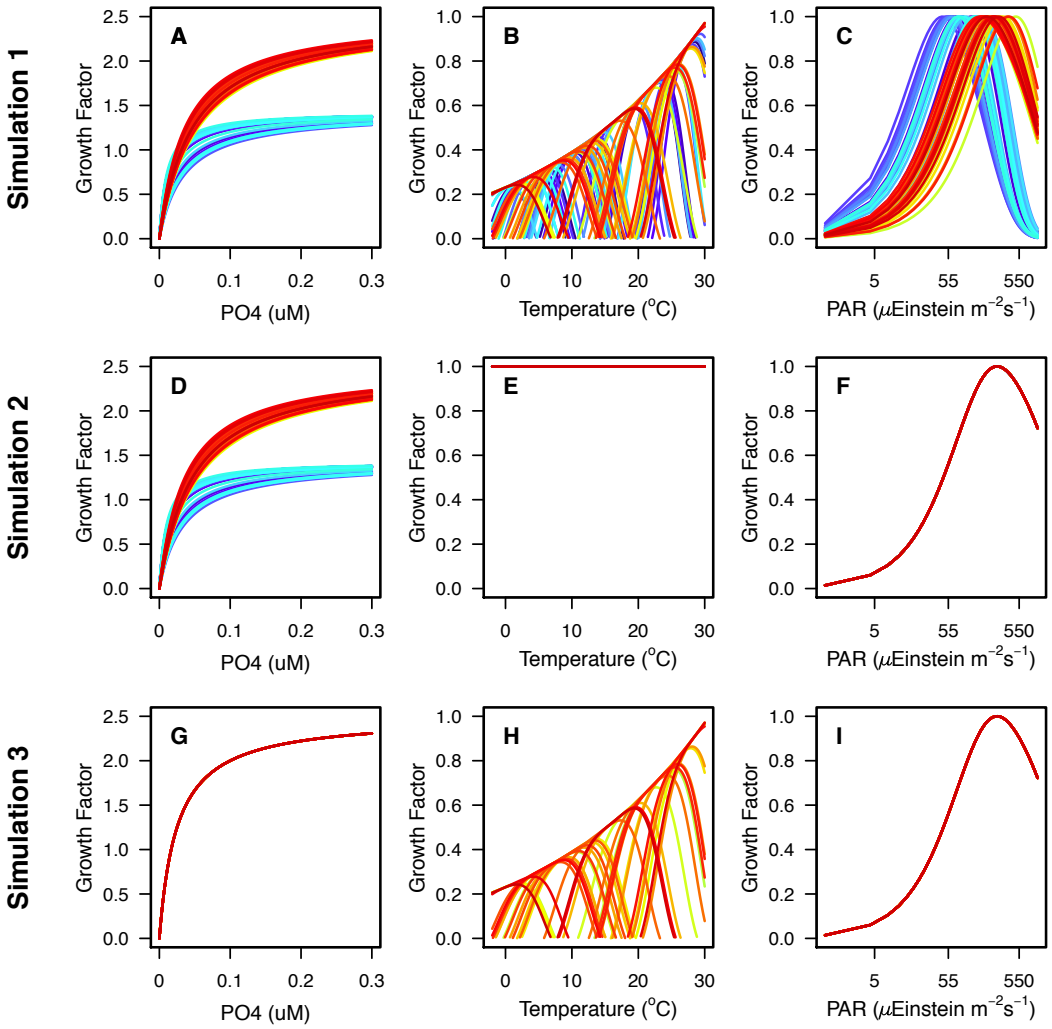

Figure 3.1: Summary of the parameterizations used in each simulation. Each coloured curve shows the response for one species. Red scale colors indicate r strategy phytoplankton types with high maximum growth rates and high half-saturation constant. Blue scale colors indicate k strategy phytoplankton types with low half-saturation constants and low maximum growth rates.

to grow over the whole temperature range (Figure 3.1E), have exactly the same light harvesting capabilities (Figure 3.1F) and suffer the same relative mortality loses. Therefore, phytoplankton species will only differ in their ability to acquire nutrients (Figure 3.1D).

3.2.1.3 **Simulation 3: SST niches only**

To evaluate the effect of temperature on the LDG, we simulated a scenario where the species growth only differs in their thermal niches (Figure 3.1H). Here, all phytoplankton species persisting at the last year of simulation share the same nutrient and PAR limitation functions, as well as the same relative mortality loses (i.e. grazing, background and sinking). For this model setup there is no allometric competitive trade-off between phytoplankton size-classes; i.e. large phytoplankton are better competitors than small phytoplankton for the whole range of nutrient concentrations (see Figure 3.1G) and thus all small phytoplankton species will be competitively excluded. Therefore, all phytoplankton species will distribute according to their thermal tolerance range exclusively.

3.3 Results

3.3.1 Simulation 1:DIN + SST + PAR niches (full model)

Simulation 1 reproduces the results of Barton et al. (2010*a*). Minor differences are due to random selection of physiological parameters. As previously reported, species richness increases towards the equator and it is maximum at several diversity "hotspots" (see Figure 3.2). This has been attributed to strong physical mixing of species with different physiological traits (i.e. SST and PAR optima, DIN uptake strategy) but similar overall local ecological fitness (Barton et al., 2010*a*). However, it is yet unclear whether biophysical constrains (i.e. SST and PAR niches) or functional grouping with competitive trade-offs (i.e. DIN niches) are the dominant drivers of the simulated latitudinal pattern of phytoplankton diversity.

3.3.2 Simulation 2: DIN niches only

Simulation 2 shows that a LDG emerges even in the absence of SST and PAR niches (see Figures 3.3A-B). This suggests that the resource competition among phytoplankton functional groups combined with the allometric competitive trade-off between phytoplankton size-classes (plus ocean mixing) leads to species

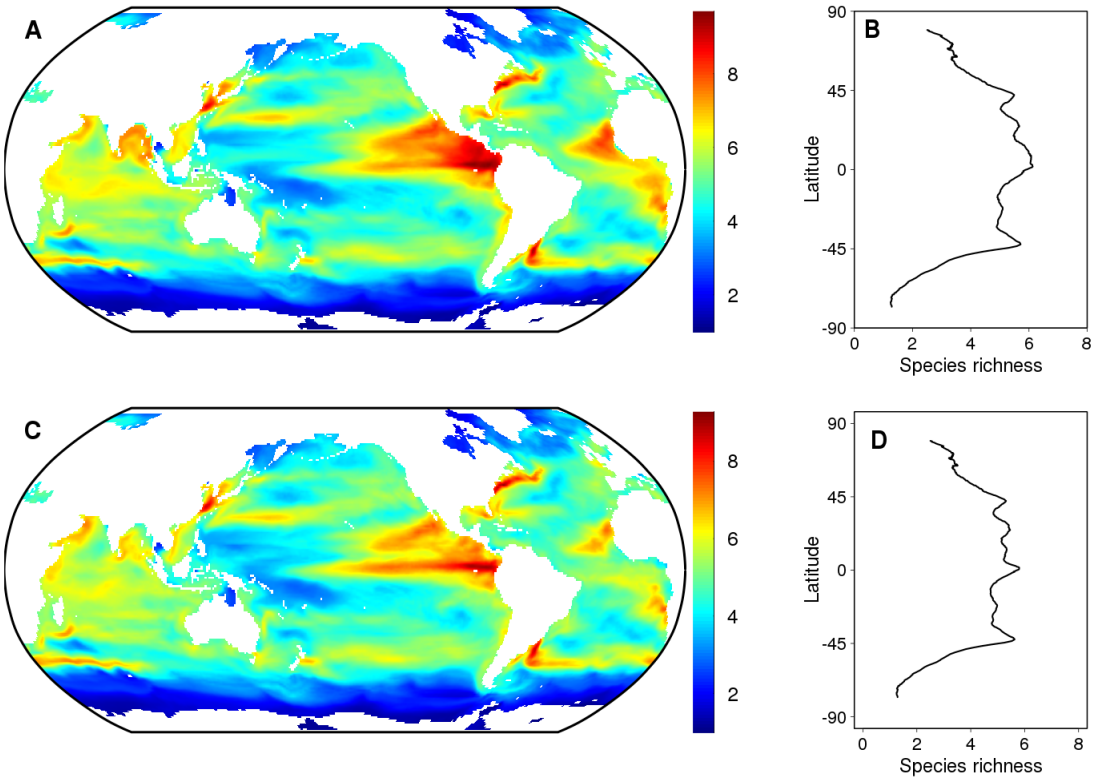

Figure 3.2: *Simulation 1:DIN + SST + PAR niches (full model)* outputs. Global diversity distribution of marine phytoplankton **(A)** integrated within the mixed layer (260m) and **(C)** only at surface and averaged annually across 10 runs. Species richness is defined as the number of species whose biomass exceeds 0.1% of the total for each point of the ocean for each time unit. **(B & D)** Mean latitudinal marine phytoplankton diversity gradient for panels A and C, respectively.

coexistence. That is, physical dispersion allows the locally transient non-equilibrium coexistence of at least one dominant species per functional group.

The latitudinal pattern of species diversity is weaker at surface than the vertically-integrated one for both Simulation 1 and Simulation 2 (see Figures 3.2 & 3.3). This suggests that vertical integration is capturing environmental heterogeneity that leads to vertical segregation of phytoplankton species according to their optimal niches. Therefore, vertically integrated diversity does not necessarily reflect species coexisting locally but species that may be present at

different depths of the same geographic location and therefore do not really interact or they do so weakly.

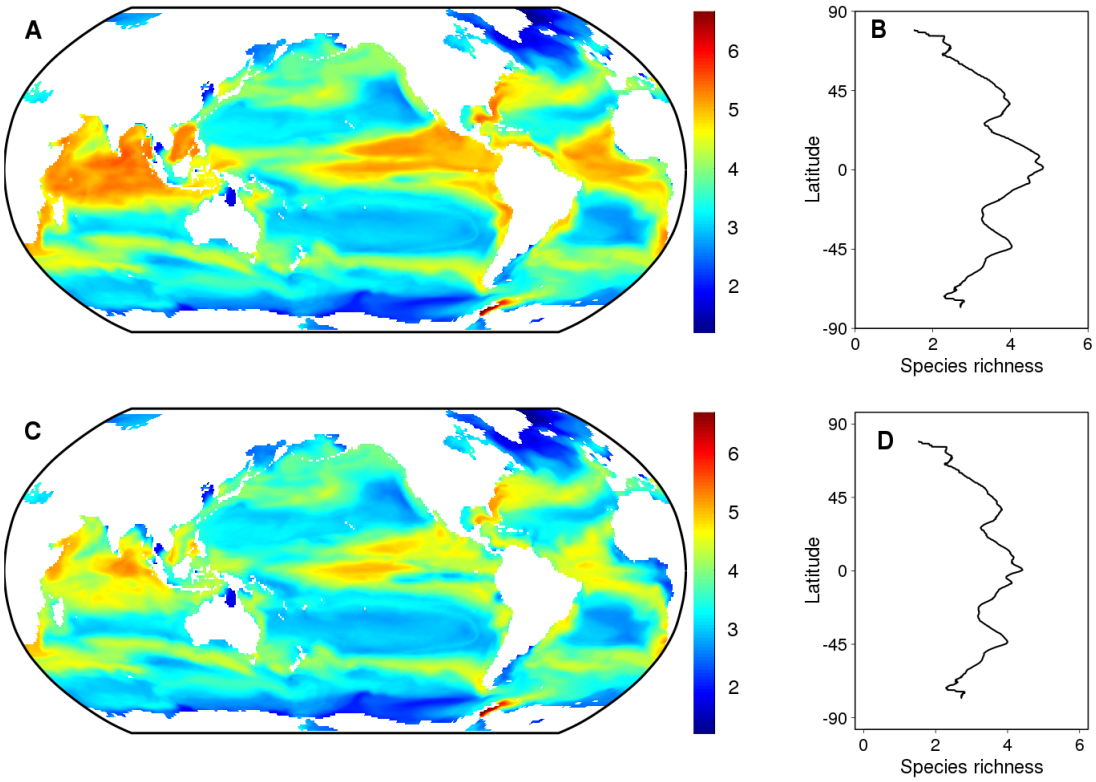

Figure 3.3: *Simulation 2: DIN niches only* outputs. Global diversity distribution of marine phytoplankton **(A)** integrated within the mixed layer (260m) and **(C)** only at surface and averaged annually across 10 runs. Species richness is defined as the number of species whose biomass exceeds 0.1% of the total for each point of the ocean for each time unit. **(B & D)** Mean latitudinal marine phytoplankton diversity gradient for panels A and C, respectively.

3.3.3 Simulation 3: SST niches only

In simulation 3, species distribute exclusively according to their thermal niches since all species have the same nutrient and light limitations. Hence, this simulation approaches a bioclimatic model where a thermal mid-domain effect develops. Species richness rises at the tropics and drops off at the equator (Figures 3.4B-D) (Beaugrand et al., 2013). Our simulations are slightly more realistic than

a pure bioclimatic model because they include nutrient and PAR limitations; i.e. temperature tolerance alone is a necessary but not sufficient condition for species occupancy of thermal niches. As occurs in simulations 1 & 2, the surface pattern is slightly weaker than the vertically integrated diversity because this metric is capturing the larger environmental variability of SST with depth at lower latitudes relative to higher latitudes that generally are more vertically homogeneous. Nevertheless the minimum diversity is clearly at the poles for both surface-only and vertically integrated diversity, which suggests a significant role of a thermal MDE on species richness.

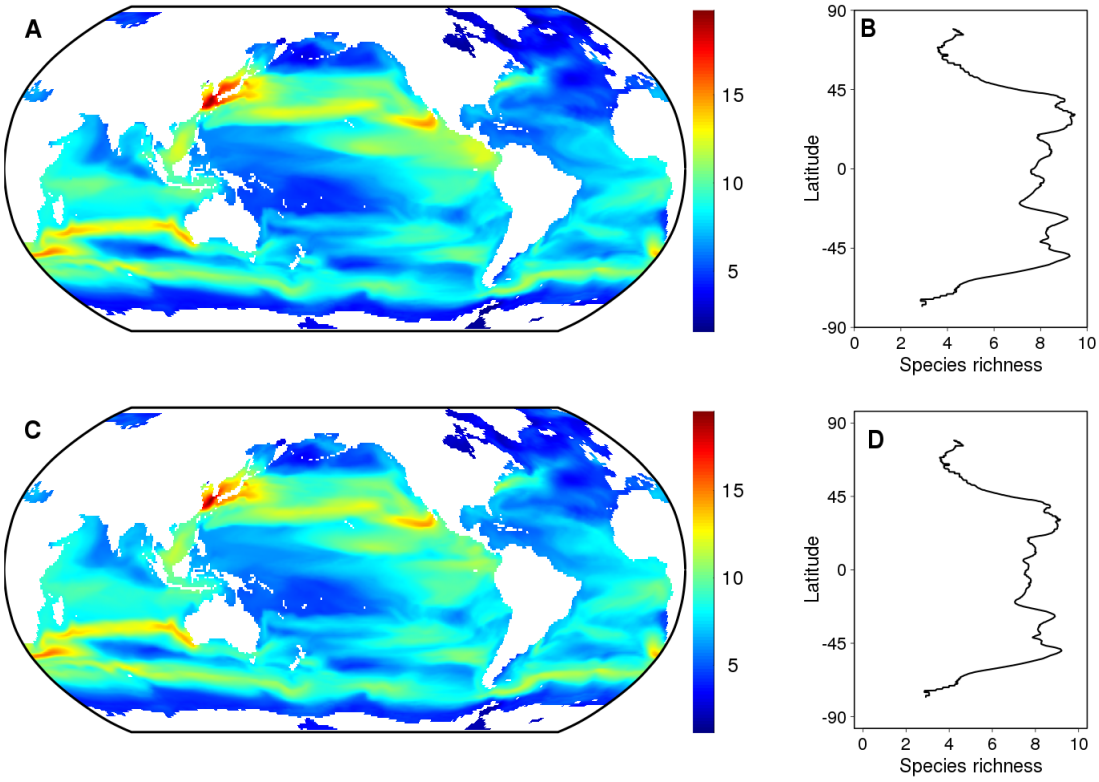

Figure 3.4: *Simulation 3: SST niches only* outputs. Global diversity distribution of marine phytoplankton **(A)** integrated within the mixed layer (260m) and **(C)** only at surface and averaged annually across 10 runs. Species richness is defined as the number of species whose biomass exceeds 0.1% of the total for each point of the ocean for each time unit. **(B & D)** Mean latitudinal marine phytoplankton diversity gradient for panels A and C, respectively.

3.4 Discussion

Our results suggest that the latitudinal pattern of diversity is the result of several effects. The vertical integration of species occurrence distorts the LDG, magnifying the pattern. Stronger vertical gradients of resources, SST and PAR at the inter-tropical area allow more environmental niches and hence more species that seem to coexist at the same location. However these species are not coexisting locally in the strict sense because they are vertical segregated and therefore they have weak or even absent competitive interactions. Therefore we suggest some caution when interpreting diversity patterns using vertically integrated values as "coexisting" species and we favor the more robust and also simpler approach of using surface-only diversity which ensures that the species are locally interacting. Nevertheless the pattern of a increased diversity towards the equator leading to a latitudinal diversity gradient can be observed for both vertically-integrated and surface-only species richness, although it is slightly weaker for the former due to the reasons outlined above.

To explain the emergence of such latitudinal diversity gradients, most models focus on one factor, either resource competition (Barton et al., 2010*a*) or temperature (Beaugrand et al., 2013; Brayard et al., 2005) and neglect other factors that may also interact with them, as happens in the field. But our results show that is actually the combination of several factors what drives the emergence of the LDG. *A priori*, local diversity is sustained by a dynamic balance between the local extinction of species through competition plus environmental filtering and the replenishment with allochthonous species by ocean physics (Barton et al., 2010*b*) (Figure 3.3). However our results suggest that a major driver of this non-equilibrium coexistence is the functional grouping with competitive trade-offs imposed in the model (i.e. DIN niches) (see Figure 3.5).

In the model definition, gleaner species are k-strategy phytoplankton types that dominate from mid to low latitudes, i.e. the more oligotrophic regions in the ocean (Figure 3.5A). Opportunist species such as the diatom analogs, are r-strategy phytoplankton who benefit from high nutrient availability and thus dominate the high latitudes and also in the upwelling systems, from where they can be carried

to the open ocean by lateral dispersal (Figure 3.5B). This is the reason of the overlapping between the two growth strategies at mid-latitudes (Figure 3.5C) and a latitudinal pattern results solely as a consequence of this parameterization of two main functional groups in the model, as has been previously suggested (Barton et al., 2010*b*; Dutkiewicz et al., 2009; Huisman, 2010).

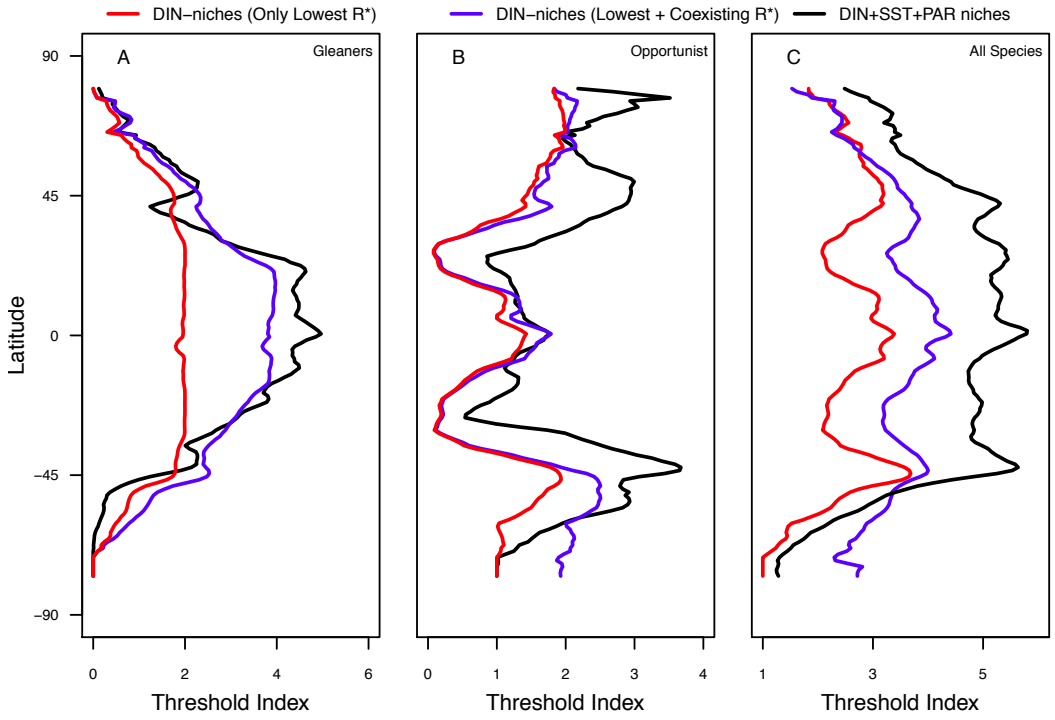

Figure 3.5: Mean latitudinal average for the surface outputs of simulations 1 & 2 considering **(A)** only gleaner species, **(B)** only opportunists or **(C)** both. Red lines show the latitudinal average of the winner species for each functional group. Blue lines consider those coexisting species with similar environmental fitness or R*. Black line is the equivalent to the blue one but for simulation 1.

In a steady-state model, only the species with the best competitive ability is expected to survive, i.e. the species which has the lowest R*. The R* is defined as the lowest environmental nutrient concentration at which growth and mortality are in balance. If there are multiple limiting resources and several functional groups,

where each is best competitor for a different nutrient, one species per functional group would survive (Barton et al., 2010*a*). In our model, if we assume that only those species which are best competitors should survive, this would lead to a maximum survival of 2 gleaners and 2 opportunistic species (red lines in Figure 3.5). These species would be the gleaner and opportunistic species with the lowest R* and, in addition, the gleaner which can not utilize nitrate (the ″*Prochlorococcus* analogs″) and the opportunistic type that use silica (the ″diatom analogs″) with the lowest R* (Dutkiewicz et al., 2009). The zonally-averaged diversity of these 4 dominant species shows an increase towards the equator (red line in Figure 3.5C). A latitudinally variable diversity of opportunists (3.5B) is overimposed to a latitudinal diversity gradient of specialists which dominate only at low-mid latitudes (3.5A), where environmental conditions are less variable. There are though numerous evidences that support the emergence of opportunists over a background of specialist in oligotrophic areas either exploiting sporadic pulses of nutrients (Chavez et al., 1990; Fryxell and Kaczmarska, 1994; Iriarte and Fryxell, 1995; Kaczmarska and Fryxell, 1994) or thanks to transient decoupling between cell growth and mortality by grazers (Cullen, 1991; Frost, 1991).

However, this zonally-averaged pattern (reconstructed on the basis of the species that should theoretically dominate in a steady-state model) differs from that in the DIN-niches only simulation (blue line in Figure 3.5C). This difference is specially relevant for gleaners in the tropical and subtropical areas (Figure 3.5A) where, as consequence of the non-steady state conditions in the model, species that have similarly low R* can coexist (Barton et al., 2010*a*). This is in accordance with recent field evidence suggesting that genomic diversity within coexisting members of *Prochlorococcus* species leads to small fitness differentials and niche differentiation, resulting in an increase in diversity (Kashtan et al., 2014).

This ecological distribution between gleaners and opportunists together with the coexistence of species with similarly low R* determine to a great extent the general pattern of the LDG (black line in Figure 3.5C), as suggested by Barton et al. (2010*a*). But in addition to these factors, our results suggest that temperature also plays an important role in the emergence of a latitudinal diversity distribution. Many other authors have found evidences for a link between temperature and

diversity (Fuhrman et al., 2008; Rombouts et al., 2009; Tittensor et al., 2010). However, most of these works are based on the metabolic theory of ecology (Brown et al., 2004). This theory states that metabolic rates increase with temperature leading to higher speciation and thus higher diversity (Allen and Gillooly, 2006; Rohde, 1992). Although this theory cannot explain our results because our model does not have mutations, other theories like the mid-domain effect (MDE) are well captured by our modelling approach. The MDE states that species ranges randomly distributed between two geographical boundaries tend to overlap at the midpoint as consequence of a geometric effect (Colwell and Lees, 2000). Furthermore, in addition to its geographical effect, the mid-domain effect also occurs within the thermal domain (Brayard et al., 2005). Barton et al. (2010*a*) discarded the MDE in the geographical domain as an important driver of the latitudinal diversity gradient. However, here we show that the MDE in the thermal domain can be a significant contributor to the general pattern (see Figure 3.4). Species whose temperature optimum is in the middle of the domain, have a thermal range that falls within the oceanic temperature range. On the other hand, species whose optimum temperature is closer to the thermal boundaries (equatorial and polar regions) have a thermal range where one of the edges is outside the ocean thermal range. For these species, the breadth of the thermal niche will thus be narrower. Consequently, there will be more niches overlapping at mid temperatures, allowing more species to coexist and increasing diversity at mid-latitudes (see Figure 3.5).

This relationship between the breadth of the niche and temperature has been shown in recent findings based on empirical data (Irwin et al., 2012). Narrower niches occur at extreme temperatures. In addition, diatoms are more likely to be found at lower temperatures and dinoflagellates at warmer ones, while at the interface, they overlap leading a thermal mid-domain effect. Thomas et al. (2012) also found a strong link between latitude and optimum temperature for strains belonging to the major phytoplankton groups.

The observed pattern in the SST-niches only simulation (Figure 3.4) is similar to what purely bioclimatic models have shown (Beaugrand et al., 2013; Brayard et al., 2005), even although our model includes the limitation of resources such as nutrients or PAR. In addition, this pattern where diversity is high at the equator

but is highest at tropical-latitudes has been reported in studies regarding the effect of temperature on species richness. Tittensor et al. (2010) show that oceanic groups on average, show an asymptotic relationship of diversity with the sea surface temperature (SST), with some taxa showing a decline of diversity at temperatures higher than 20°C, as occurs for planktonic foraminifera (Tittensor et al., 2010; Yasuhara et al., 2012).

In summary, we have found that the LDG emerges from the combination of: a) the subdivision of phytoplankton in functional groups with different nutrient uptake strategies and requirements that lead to competitive trade-offs; b) the large scale dispersion and mixing of phytoplankton species by oceanic currents; c) the coexistence of species with similar environmental fitness and d) temperature through a mid-domain effect. Therefore, even in a simplified representation of nature as in the ecological model presented here, there is not a single exclusive factor responsible for the LDG in marine phytoplankton but several factors act simultaneously. This would be further complicated in nature, where additional factors such as mutations, adaptation to solar radiation, grazing or sinking rates which affect the growth of species might enhance or modify the LDG.

CHAPTER

4

Marine microplankton diversity database

Sal S., Lopez-Urrutia A., Irigoien X., Harbour D.S., & Harris R.P.
Published as a Data Paper in Ecology 94:1658, (2013)
http://dx.doi.org/10.1890/13-0236.1

4.1 Introduction

The high diversity of phytoplankton has fascinated ecologists since the early works of Hutchinson (1961). Many theories have been developed to explain the factors regulating marine phytoplankton diversity patterns. Some suggest that species coexistence is enhanced at equilibrium conditions when competition for resources such as nutrients or light is high (Barton et al., 2010*a*). However, some authors showed that diversity can even increase when fluctuations take place (Connell 1978; Sommer 1985; Floder and Sommer 1999; Huisman 2010). Other theories relate phytoplankton diversity to energy availability as photosynthetically active radiation (PAR) or temperature (Wright, 1983). Phytoplankton diversity is also correlated to standing stock biomass, with higher diversity found at intermediate productivity levels (Irigoien et al., 2004; Stomp et al., 2011).

However analyzing the relative importance of these theories in natural systems is very difficult: experimental work is very complex at such broad scales. To test these theories there is a need for global databases with sufficient gradients in the proposed explanatory variables. Such diversity datasets with extensive geographical coverage exist for terrestrial plants. For example, *The Alwyn H. Gentry Forest Transect Data Set* (Gentry, 1988; Phillips and Miller, 2002) has been successfully used to test several macroecological theories (Clinebell et al., 1995; Enquist and Niklas, 2001; Simova et al., 2011). For marine ecosystems, such global databases are starting to be compiled. Most of these datasets are focused on the compilation of distribution maps like the *NMFS-COPEPOD: the global plankton database* (O'Brien, 2007) for marine copepods or the *World Modern Foraminifera Database* (Hayward et al., 2011), as part of the World Register of Marine Species (WoRMS). For marine phytoplankton, the *World Ocean Atlas of Plankton Functional Types* is being created from the compilation of datasets for different functional types. Some examples are the databases for picophytoplankton (Buitenhuis et al., 2012) or for diatoms (Leblanc et al., 2012). Although these databases are fairly complete including abundance, biovolume and carbon biomass, they lack environmental data. Furthermore, they are not suitable for diversity calculations. To provide a reliable measure of species diversity, the taxonomic

identification should be carried out by the same taxonomist over the whole dataset, or at best some standardization protocols need to be applied.

Identification of phytoplankton to the species level is often quite challenging, even for taxonomic experts. Consequently, many large phytoplankton databases are not internally consistent, because changes in personnel handling the taxonomic analyses have led to changes in species identification. In fact, this problem can be so severe that in several studies the observed changes in phytoplankton community structure have been attributed to changes in personnel or laboratory (Wiltshire and Durselen 2004; Peperzak 2010; Straile et al. 2013), rather than to environmental variation. Such major inconsistencies were avoided here.

In this work we compiled a dataset of marine microplankton species abundances (cells mL^{-1}), together with estimates of biomass and cell biovolume. These data were collected at 788 stations on a number of oceanographic cruises between 1992 and 2002. The compilation covers a wide range of marine ecosystems, ranging from coastal to open ocean. Environmental information has also been compiled for different oceanographic parameters (chlorophyll, temperature, PAR, nutrients, mixed layer depth) for each station. These data allow the study area to be characterized and can be used in studies on the environmental and biological controls of marine biodiversity. Most importantly, all species identification were made by the same taxonomist (Derek S. Harbour), which provides greater strength to the collection and ensures that estimates of species diversity are reliable. To our knowledge, this dataset is unique in marine phytoplankton diversity studies. We know of no other study which compiles abundance, biomass and biovolume for such a great number of species which have been identified by the same taxonomist and which also includes environmental data.

To date, some data included in this work have been used previously to identify global patterns of marine phytoplankton biodiversity (Irigoien et al., 2004) and also in studies relating species richness or phytoplankton abundance to cell size (Cermeño et al., 2006). In addition, parts of this global dataset have been used to study temporal variability (Rodríguez et al., 2000), seasonal succession (Marañón et al., 1996) or species distribution (Tyrrell et al., 2003). It is important to remark

that species names have not been standardized until now, this means that the same species could be named differently in each subset of the global database. This has hindered the use of the database for studies involving distribution patterns at the species level. The main feature of this new compilation is the inclusion of environmental data, which were scarce previously. This database aims to complete these studies and to enhance the development of new ones. In this way we hope it will contribute to a better understanding of the processes of diversification in the ocean. Understanding and assessing diversity will be essential to understand and predict the impact of environmental forcing on this major compartment (Simon et al., 2009).

4.2 Dataset Descriptors

Dataset title: Database of abundance for 736 microplankton taxa across 788 stations with corresponding environmental variables.

Principal investigators: Sofía Sal, Ángel López-Urrutia, Xabier Irigoien, Derek S. Harbour and Roger P. Harris

Key words: phytoplankton; microplankton; diversity; abundance; temperature; nutrients; chlorophyll; photosynthetically active radiation.

Objectives: The main objective of this work is to compile a dataset of marine microplankton species abundances which have been identified by the same taxonomist. We provide abundances (cells mL^{-1}) data, together with estimates of biomass, cell biovolume and environmental data (chlorophyll, temperature, nutrients, PAR, mixed layer depth) for each site.

Originators: Data contained in this database were originally collected by Dr. Xabier Irigoien and Dr. Roger P. Harris. Derek S. Harbour. was responsible for all sample analysis.

Period of Study: October 1992 to May 2002.

Source(s) of funding: Data compilation was supported by project METabolic OCean Analysis (METOCA) funded by Spanish National Investigation + Deve-

lopment + Innovation (I+D+I) Plan. S.S. was funded by a Formación de Personal Universitario (FPU) grant from the Spanish Ministry of Education. AMT sample collection and analysis was supported by the UK Natural Environment Research Council through the Atlantic Meridional Transect consortium (this is contribution number 233 of the AMT programme). The L4 programme is funded under the UK NERC Oceans 2025 programme as part of Theme 10, Sustained Observations.

4.3 Material and Methods

4.3.1 Study region

Data were compiled for 788 stations during different oceanographic cruises in temperate, polar and subtropical regions. Stations sampled cover a wide range of marine ecosystems, ranging from coastal to open ocean. North Atlantic Ocean samples include the Irminger Sea, Norwegian Sea, North Sea, and Iceland Basin. Samples were also collected on cruises along the South Atlantic Ocean (mainly Atlantic Meridional Transect cruises), Benguela current, Indian Ocean, and West Coast of the North Pacific Ocean. One of the experiments, ″Bergen″, took place in open-air mesocosms at the Espegrend Marine Biological Station (University of Bergen).

4.3.2 Experimental or sampling design.

Data were obtained from many experiments and observations made in the oceanographic cruises listed above. Species taxonomic identification and cell counts were all made by Derek S. Harbour. See Research Methods below.

4.3.3 Sampling methods

Microplankton abundance

Data analysed were collected from 1992 to 2002 at 788 sites. See Figure 4.1 and Table 4.1 for a detailed site description. Seawater samples were collected from

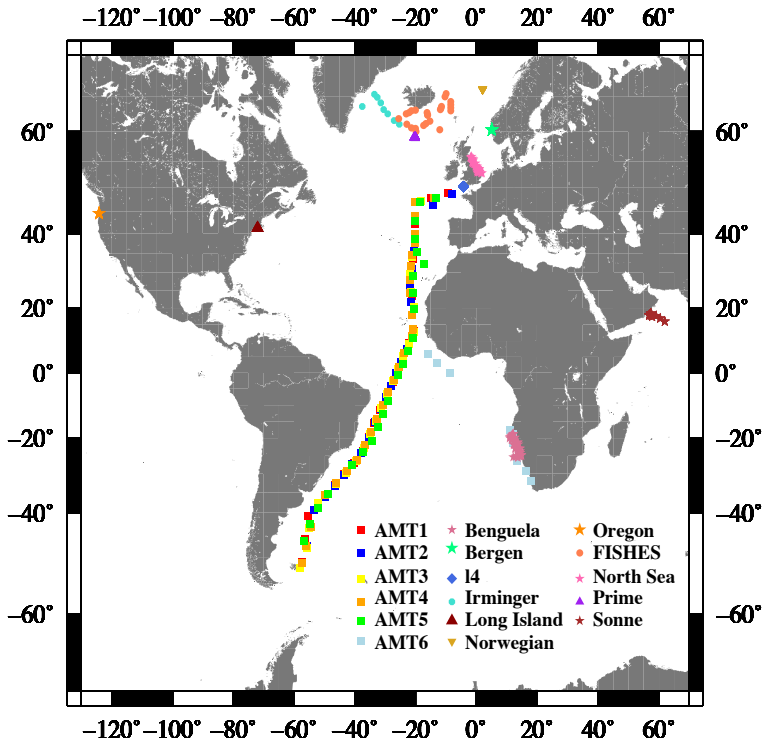

Figure 4.1: Map showing the different stations sampled in the study. Each symbol and color represents a cruise.

different depths (most of them in surface waters) from CTD Niskin bottles. For later microplankton cell counts, it is very important to handle seawater with care, as some organisms are very sensitive to turbulence (Gifford and Caron, 2000). Water samples were taken from the Niskin bottle and immediately preserved with 1-5 % acid-Lugol′s iodine solution (Throndsen, 1978). Samples were labelled and stored in cold, dark conditions during transportation to the laboratory.

Nutrients

We only have *in-situ* nutrients data for AMT cruises. Samples were taken from the underway pumping system between stations, from vertical profiles at each station,

or both. However, we only included samples obtained during the daily CTD casts coincident with the microplankton sampling. Water samples from the CTD/Rosette system (SeaBird) were sub-sampled into clean Nalgene bottles. Sample analysis was completed within 3 h of sampling, so no samples were stored.

Other variables

For Chlorophyll, between 200 and 300 ml of sea water from each depth in the water column were sequentially filtered through 0.2 μm, 2 μm and 20 μm polycarbonate filters. Chl-a was extracted from filters in 90% acetone at 20°C 12 to 24 hours. Samples were measured on a Turner 10-AU fluorometer calibrated with pure Chl-a.

Temperature and PAR were obtained either from CTD data or underway records from the ship. For those stations where it was impossible to obtain data, these were retrieved from satellite data.

4.3.4 Analysis

Microplankton abundance

Microplankton identification and cell counts was carried out by Derek S. Harbour at the Plymouth Marine Laboratory using inverted microscopy following the Utermöhl technique (Utermöhl, 1958). The ″Water quality - Guidance standard for routine microscopic surveys of phytoplankton using Utermöhl technique″ (BS EN 15204:2006) was followed:

Microplankton samples, preserved in Lugol′s iodine and formalin, were settled in sedimentation chambers while acclimatised to room temperature, to ensure a random distribution of cells. After this, sample bottles were rotated to help re-suspension and separation. Sub-samples with volumes between 10 and 256 mL were later transferred to plankton settling chambers. A variable area of the chamber bottom was counted under the microscope. The size of that area varies with species and abundance and under some circumstances different species were counted in different settled volumes to obtain consistency and reproducibility in

the counts. At least 100 cells of each of the more abundant species were counted. Settlement duration varied between 4h cm^{-1} for Lugol ′s iodine and 16 h cm^{-1} for formaldehyde samples.

Once the settling process finished, cells were identified, where possible, to species/genus level and assigned to different functional groups: Flagellates, Heterotrophic flagellates, Diatoms, Coccolithophores, Dinoflagellates, Heterotrophic dinoflagellates, and Ciliates. It should be noted that heterotrophic refers to organisms that do not contain pigments.

Abundance data for each species at each station was calculated in cells per ml. Dimensions of individual species were measured in μm units using digital measurements and calibrated against an ocular micrometer. Using the corresponding geometric shapes, these measurements were converted to volume using the Kovala and Larrance (1966) methodology. Once this was done, cell volumes were converted to carbon (pg $cell^{-1}$) using the formulae of Menden-Deuer and Lessard (2000).

Since all the plankton counts were obtained by light inverted microscopy they do not include pico-cyanobacteria, like *Prochlorococcus* and *Synechococcus*. The database adequately samples the microplankton size range and part of the nanoplankton abundance, small eukaryotes are also too small to be identified to the species level by light-microscopy. The Utermöhl technique is restricted to cells larger than 10 μm (within the nanoplankton size range). Smaller cells do not settle quantitatively even after Lugol′s iodine addition and cells are too small to classify to the species level.

Nutrients

To analyse nutrients, a Technicon AAII (four-five channel depending on the cruise) segmented-flow auto-analyser was used. Protocols used were different for each nutrient: phosphate and silicate were analysed as described by Kirkwood (1989). Nitrate and nitrite was analysed using a modified version of Grasshoff′s method (Grasshoff, 1976), as described by Brewer and Riley (1965). These were measured

as nitrate plus nitrite, since the nitrate was determined as nitrite using a copper-cadmium reduction column to reduce it to nitrite. We later calculated nitrate as the difference between the nitrite measure and the nitrite plus nitrate measure. Ammonium was measured only in cruise AMT 6. The chemical methodology used was the described by (Mantoura and Woodward, 1983). All results are presented as mmol m^{-3} (μmol L^{-1}) of the elements nitrogen, phosphorus and silica.

Environmental data

When in-situ environmental data were not available they were extracted from satellite data or global distribution maps. For Chl, Surface PAR and Diffuse attenuation coefficient at 490 nm (Kd490), we used SeaWIFS L3 datasets with 9km (1 pixel=9km) spatial resolution. We used SeaDAS (SeaWiFS Data Analysis System) to locate the closest pixel to the sampled location in the satellite image (radius of 0). Because sometimes this exact pixel contained a missing value we used the data of adjacent pixels using different search radius (from high to low accuracy), starting at 1 (radius of 1 pixel). When satellite data for the same day was not available we used the satellite image for the corresponding month and, ultimately, the monthly climatological data from the Ocean Color site (`http://oceandata.sci.gsfc.nasa.gov/SeaWiFS/Mapped/`).

For each variable a vector attached indicates the data quality flag (QF), starting at 0 when data is in-situ, and decreasing in precision going from data extracted from daily maps to data extracted from monthly climatologies.

QF are: 0 (real data), 1 (daily satellite data (DS), radius=0), 2 (DS, radius=1), 3 (DS, radius=3), 4 (DS, radius=5), 5 (DS, radius=10), 6 (DS, radius=20), 7 (monthly satellite data (MS), radius=0), 8 (MS, radius=1), 9 (MS, radius=3), 10 (MS, radius=5), 11 (MS, radius=10),12 (MS, radius=20), 13 (monthly climatology satellite data (CS), radius=0), 14 (CS, radius=1), 15 (CS, radius=3), 16 (CS, radius=5), 17 (CS, radius=10).

PAR at the sampled depth (PARz) was calculated using the Surface PAR and the Kd490. Mixed layer depth (MLD) data were extracted from the Ocean Productivity site (`http://orca.science.oregonstate.edu/1080.by.`

2160. monthly. hdf. mld. merge. php). Data are stored in maps on a monthly basis at 1080 by 2160 resolution. We used SeaDAS to extract the whole image for each month. Then we located the MLD value for each coordinate value. For those points where there were not data, we calculated an annual climatology based on the monthly dataset: We first interpolated maps to a lower resolution (360 by 180) and then calculated the mean for each month.

QF are defined as follows: 0 (in-situ data), 1 (monthly satellite data (MS)), 2 (monthly climatology satellite data (CS)). The use of a search radius is not needed because images are the output of a model and do not have missing values.

To obtain an estimate of temperature for samples collected at depths below the MLD and for nutrients, we compiled data from the annual climatologies from the World Ocean Atlas 09 (WOA09) database at one degree resolution and 10 depth levels (0, 10, 20, 30, 50, 75, 100, 125, 150, 200 meters) (http:// www. nodc. noaa. gov/ OC5/ WOA09/ woa09data. html). We extracted the value in the range of one degree around the specified coordinate.

QF are defined as follows: 0 (in-situ data), 1 (WOA data).

When the sample was collected at a depth shallower than the MLD, temperature was obtained from the Sea Surface Temperature (SST) data from the AVHRR satellite. We compiled daily datasets with 4km (1 pixel=4km) resolution from the NOAA site (ftp:// podaac-ftp. jpl. nasa. gov/ allData/ avhrr/ L3/ pathfinder_ v5/ daily/ night/ 04km/).

QF are defined as follows: 2 (daily satellite data (DS), radius=0), 3 (DS, radius=1), 4 (DS,radius=3).

Figure 4.2 shows the relationship between the in-situ data and estimated data for the different variables. Although for most of them, satellite can be a good estimation source, this does not occur for Chl and Silicate, where the correlation coefficient is too low.

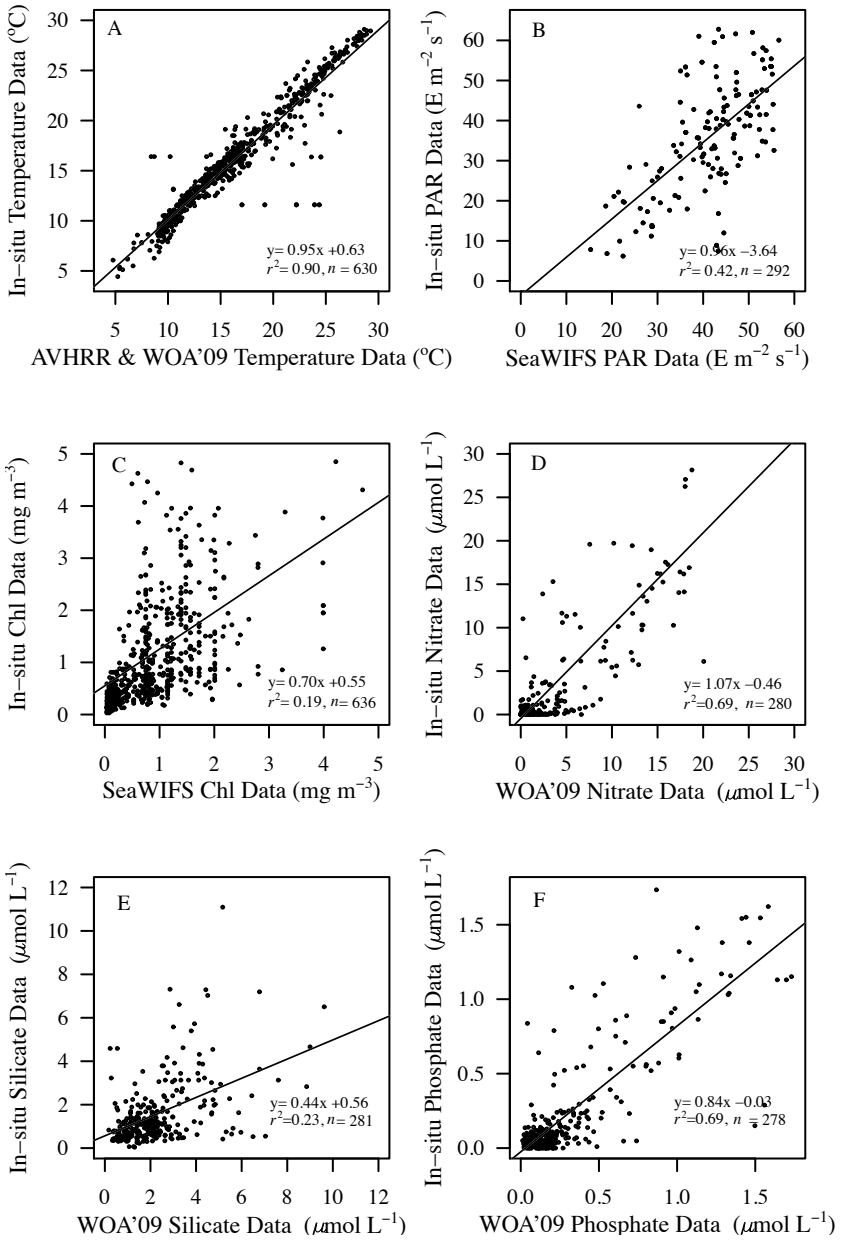

Figure 4.2: Relationship between in-situ data and estimated data for all variables: **(A)** Temperature, **(B)** PAR, **(C)** Chlorophyll, **(D)** Nitrate, **(E)** Silicate and **(F)** Phosphate. In each case, plotted points show only stations in which in-situ data is available.

4.3.5 Taxonomy and systematics

Taxonomic names were checked against the World Register of Marine Species (WoRMS). Names not matched within WoRMS were checked against various other taxonomic references (e.g., ITIS, algaebase). A column with author comments is attached for those species which were not matched to any taxonomic references.

4.4 Dataset status and accessibility

Latest update: 2013

Metadata status: Metadata are complete for this period and are stored with the data

Storage location and medium: The Ecological Society of America's Ecological Archives. Ecological Archives E094-149-D1. (http:// www. esapubs. org/ archive/ ecol/ E094/ 149/)

Contact persons:

Xabier Irigoien, Red Sea Research Center, 4700 King Abdullah University of Science and Technology, Thuwal 23955-6900,Kingdom of Saudi Arabia.

Roger P. Harris, Plymouth Marine Laboratory, Prospect Place, Plymouth, Devon PL1 3DH, United Kingdom.

Derek S. Harbour, Plymouth Marine Laboratory, Prospect Place, Plymouth, Devon PL1 3DH, United Kingdom.

Ángel López-Urrutia, Center oceanographic of Gijón, Spanish Institute of Oceanography, Avda Principe de Asturias 70bis, 33212, Gijón, Asturias, Spain.

Sofía Sal, Center oceanographic of Gijón, Spanish Institute of Oceanography, Avda Principe de Asturias 70bis, 33212, Gijón, Asturias, Spain.

4.5 Data Structural Descriptors

4.5.1 Dataset File

Identity: Dataset is downloadable as a single archive, PhytoDataBase.zip (215.5 KB), which contains the following *.csv data files:

- Table 1: Stations and cast description, including date, location and data for oceanographic variables such as nutrients or temperature.
- Table 2: Species identification for the whole dataset, including phylogenetic classification, author comments and carbon and biovolume for each species. Each row corresponds to each column in Table 4.3.
- Table 3: Abundance for each species (by columns) at each station (by rows). Species carbon content can vary from one station to another, for those cases the species is repeated each column representing a different carbon content as specified in Table 4.2. For this reason we have more columns than species total number.

Size:

- Table 1: 237.5 KB, 1043 rows and 30 columns.
- Table 2: 222.6 KB, 1335 rows and 14 columns.
- Table 3: 2.8 MB, 1043 rows and 1335 columns.

Format and storage mode:

CSV text, comma delimited. Special characters/fields: All missing values are denoted as ″NA″.

4.5.2 Variable definitions:

4. Marine microplankton diversity database

Column name	Variable definition	Units	Storage type	Range numeric values	Missing value codes
SampleID	Sample identification code	text	string	N/A	NA
Cruise	Cruise name	text	string	N/A	NA
Date	Date	date	string	N/A	NA
Original SampleNo	Original cruise sample nº	count	integer	1 to 14084	NA
Original StationNo	Original cruise station nº	count	integer	1 to 35575	NA
Depth	Depth	meters	integer	1 to 160	NA
Lat	Latitude	degrees	integer	-51.9314 to 66.0000	NA
Lon	Longitude	degrees	integer	-124.167 to 62.000	NA
Daylength	Daylength	hours	integer	8.0366 to 22.2324	NA
Chl	Chlorophyll concentration	mg m^3	integer	0.03 to 27.4966	NA
QFChl	Chlorophyll quality flag	count	integer	0 to 17	NA
Temperature	Temperature	celsius	integer	2.7 to 29.117	NA
QFTemp	Temperature quality flag	count	integer	0 to 4	NA
SurfacePAR	Surface photosynthetically active radiation	mol photons m^{-2} d^{-1}	integer	3.664 to 64.0054	NA
QFPAR	Surface photosynthetically active radiation quality flag	count	integer	0 to 14	NA
Kd490	Diffuse attenuation coefficient at 490 nm	m^{-1}	integer	0.0224 to 6.2144	NA
QFKd490	Diffuse attenuation coefficient quality flag	count	integer	1 to 17	NA
PARz	Depth photosynthetically active radiation	mol photons m^{-2} day^{-1}	integer	0 to 52.2669	NA
Nitrate	Nitrate concentration	μmol L^{-1}	integer	0 to 37.7919	NA
QFNO3	Nitrate quality flag	count	integer	0 to 1	NA
Nitrite	Nitrite concentration	μmol L^{-1}	integer	0 to 0.72	NA
QFNO2	Nitrite quality flag	count	integer	0	NA
Ammonium	Ammonium concentration	μmol L^{-1}	integer	0.62 to 3.13	NA
QFNH4	Ammonium quality flag	count	integer	0	NA
Phosphate	Phosphate concentration	μmol L^{-1}	integer	0 to 2.1075	NA
QFPO4	Phosphate quality flag	count	integer	0 to 1	NA
Silicate	Silicate concentration	μmol L^{-1}	integer	0.04 to 22.5392	NA
QFSil	Silicate quality flag	count	integer	0 to 1	NA
MLD	Mixed layer depth	m	integer	10.7578 to 400	NA
QFMLD	Mixed layer depth quality flag	count	integer	1 to 2	NA

Table 4.1: Description of contents in the Table 1 of the database

Column name	Variable definition	Units	Storage type	Range numeric values	Missing value codes
Group	Functional group	text	string	N/A	NA
Kingdom	Taxonomic kingdom	text	string	N/A	NA
Phylum	Taxonomic phylum	text	string	N/A	NA
Class	Taxonomic class	text	string	N/A	NA
Order	Taxonomic order	text	string	N/A	NA
Family	Taxonomic family	text	string	N/A	NA
Genus	Taxonomic genus	text	string	N/A	NA
Species	Taxonomic species	text	string	N/A	NA
Forma	Taxonomic forma	text	string	N/A	NA
Author Comments	Author specific comments about name, size or forma. Most times when the species is difficult to identify	text text text	string string string	N/A N/A N/A	NA NA NA
Author	Taxonomist name	text	string	N/A	NA
SpeciesID	Identification code for unique species	count	integer	1 to 736	NA
Carbon	Carbon content	pg cell^{-1}	integer	0.0 to 143194.7	NA
Biovolume	Cell volume	μm^3 cell^{-1}	integer	0 to 17671459	NA

Table 4.2: Description of contents in the Table 2 of the database

Column name	Variable definition	Units	Storage type	Range numeric values	Missing value codes
N/A	Sample identification code	text	string	N/A	NA
Species name	Species abundance	cell ml^{-1}	integer	0.0 to 59763.5	NA

Table 4.3: Description of contents in the Table 3 of the database

CHAPTER

5

The combined effects of thermal mid-domain and growth-temperature response curves on the latitudinal diversity gradient in marine phytoplankton

5.1 Introduction

Species richness usually decreases from the equator to the poles describing one of the most studied patterns in the global distribution of biodiversity, the latitudinal diversity gradient (LDG) (Gaston, 2000; Pianka, 1966; Rohde, 1992). Numerous evidences for a LDG have been found in nature. Some examples include all major groups of terrestial (Currie, 1991), freshwater (Oberdorff et al., 1995) and marine taxa, including specific taxonomic groups like bacteria (Fuhrman et al., 2008), planktonic foraminifera (Rutherford et al., 1999), copepods (Rombouts et al., 2009) and marine ciliates such as tintinnids (Dolan et al., 2006). For marine phytoplankton few studies have evaluated the latitudinal diversity gradient. Global models (Barton et al., 2010*a*; Prowe et al., 2012; Sal et al., in prep.; Thomas et al., 2012) and satellite data estimates (De Monte et al., 2013) have succeeded to find an increase of diversity from the poles to the equator. Global compilations of oceanic data (Tittensor et al., 2010) reveal clear latitudinal gradients although some empirical studies have failed to detect a LDG in marine phytoplankton (Cermeño et al., 2008).

Although more than 25 different hypothesis for mechanisms generating this pattern have been proposed (Gaston, 2000), and many of them are non-exclusive (Sal et al., in prep.), two hypotheses have been widely supported in recent years relating the emergence of the LDG to temperature. On one hand, many authors (Fuhrman et al., 2008; Rombouts et al., 2009; Tittensor et al., 2010; Yasuhara et al., 2012) support a metabolic based hypothesis where temperature enhances diversity by speeding up the biochemical reactions controlling speciation rates (Allen and Gillooly, 2006; Rohde, 1992). The other mechanism is based on a null model which excludes any direct environmental or evolutionary influence on species richness and suggests that a mid-domain peak in diversity emerges as result of a random distribution of species ranges between two geographical boundaries (Colwell and Hurtt, 1994). This phenomenon was first identified by Colwell and Lees (2000) as a *mid-domain effect* (MDE). However, some authors have supported the existence of a *thermal mid-domain effect* (TMDE) where the mid-domain takes place in the thermal niche space (Beaugrand et al., 2013; Brayard et al., 2005; Sal et al., in

prep.) rather than in a geographical space (Colwell and Lees, 2000). The metabolic and TMDE hypotheses differ on the shape of the predicted response of species richness to temperature. TMDE predicts a unimodal symmetrical distribution of diversity, while the metabolic based hypothesis predicts an exponential increase in diversity with temperature.

The TMDE hypothesis is based on the temperature range over which species can grow regardless of the shape of the thermal niche within those boundaries. The definition of such ranges is tightly related to the characterization of the thermal niche of species on the basis of growth response curves to temperature. These are usually unimodal and negative skewed curves where the maximum growth rate is achieved at the optimum temperature (Eppley, 1972). Thomas et al. (2012) developed an statistical approach to estimate the growth-temperature curves for a set of phytoplankton species, and evaluated the response of species richness to changes in temperature on the basis of the thermal range for each species. These growth-temperature curves characterize the *fundamental niche* sensu Hutchinson (1957) as the theoretical environmental space where a species could live indefinitely only according to how the species respond to the environment. However, when species interact in the natural environment the fundamental niche becomes reduced to a subset of it known as *realized niche* (Hutchinson, 1957).

In this work we present a new hypothesis to predict the distribution of species richness, hereinafter referred as the thermal niche effect (TNE), based on the combination of both metabolic and TMDE theories. Instead of using just the thermal range, as in the TMDE, we use the thermal niche as a way to account for the different probability of survival of the species within its thermal range. We suggest that the response of species richness to temperature results as a combination of the overlap of niches predicted by the TMDE and the exponential increase of growth rate with temperature. Hence TNE predicts a response of species richness to temperature which is halfway between a unimodal (as TMDE predicts) and an exponential (as MTE predicts) response. To characterize the ecological niches of species and validate our theory, we take advantage of a global database for marine

phytoplankton diversity (Sal et al., 2013). This dataset provides environmental and species abundance data which allows to assess the LDG at global scales.

5.2 Material and Methods

5.2.1 Empirical data

We used the *Marine microplankton diversity dataset* (Sal et al., 2013) on the abundance of an extensive number of marine phytoplankton species. Samples were taken along different cruises between 1992 and 2002 covering a wide range of ecosystems from subpolar to equatorial regions. This dataset also contains temperature data for each sample, either measured in-situ or estimated from satellite. Recorded temperatures range from 2.7 to 29.1°C. Likewise, the dataset covers a broad range of productivity from oligotrophic to eutrophic areas. As diversity has been shown to describe an unimodal relationship with productivity (Irigoien et al., 2004), and since our study is focused in depicting the effects of temperature independently to those based on productivity, we restricted the database to those samples belonging to mesotrophic regions (7 to 90 mgC m^{-3}), where the number of species is not expected to change as function of phytoplankton biomass. By selecting these mesotrophic regions we also discard the possibility of undersampling effects in oligotrophic areas (Cermeño et al., 2013). Hence, the dataset was finally reduced to 603 phytoplankton species in 595 different samples. However, the same analyses shown here were replicated using the whole dataset and the results are provided as supplementary information.

These data allowed us to validate the species richness distribution with temperature but also to assess if a latitudinal diversity gradient is observed in the Sal et al.'s (2013) database. We divided latitude into 5° bins and used a boxplot to characterize the number of species at each latitude.

The species thermal range was defined as the difference between the minimum and maximum temperature where the abundance of each species was greater than 0. We used these data to evaluate the random distribution of thermal ranges along the measured thermal domain and reproduce the TMDE. To further

analyse the relationship between temperature and species presence, we attempted to characterize the realized niche of each species. We first divided temperature into 12 bins. For each temperature bin, we calculated the percentage of samples where each species was present as an index of probability of species presence. This index of probability of species presence usually resembles a growth response curve with an optimum temperature where the probability of presence is highest and a unimodal and skewed pattern.

5.2.2 Niche modelling

To fit the curve of probability of presence for each species and characterize each thermal niche we applied a generalized linear model (GLM). The use of more sophisticated niche modelling algorithms such as MaxEnt (Phillips et al., 2006) is not appropriate here since sample distribution within our database is not homogeneous along the temperature gradient.

For each species we fitted a binomial response curve with logistic link using the glm function in *R* (R Development Core Team, 2008). First and second-order polynomials (linear and quadratic terms) were fit for each species in the GLM. An Akaike information criterion (AIC) (Akaike, 1974) was used to select the best fit for each case. To avoid bias due to undersampling in some temperature bins we removed those bins with less than 15 samples. In addition, we only considered the curve of those species that were found in at least 3 temperature bins to ensure a reliable fit and excluded those curves showing a minimum within the observed thermal range. So finally we accounted for a total of 304 species in our analyses. This reduction in the number of species studied was only considered for the fitted curves, i.e. for the observed data all species were taken into account, what ensures that the patterns observed are not biased by this reduction.

Besides Sal et al.'s (2013) database, we used the data compiled by Thomas et al. (2012) for a total of 194 phytoplankton isolate/strains in order to reproduce the fundamental niche of species and evaluate whether the difference between fundamental and realized niches influences the resulting pattern. To fit the growth vs temperature curves we followed the same statistical analysis as Thomas et al.

(2012) and applied a maximum likelihood estimation (MLE), using the *bbmle* package in *R* (R Development Core Team, 2008).

5.3 Results

When species richness data are divided in latitudinal bins a diversity gradient can be perceived (Figure 5.1A). Regardless of some differences between both hemispheres, diversity increases from high to mid latitudes reaching maximum species richness in the tropical areas. Then, there is a decline in species richness across the equator but this decline is less pronounced than the poleward decrease.

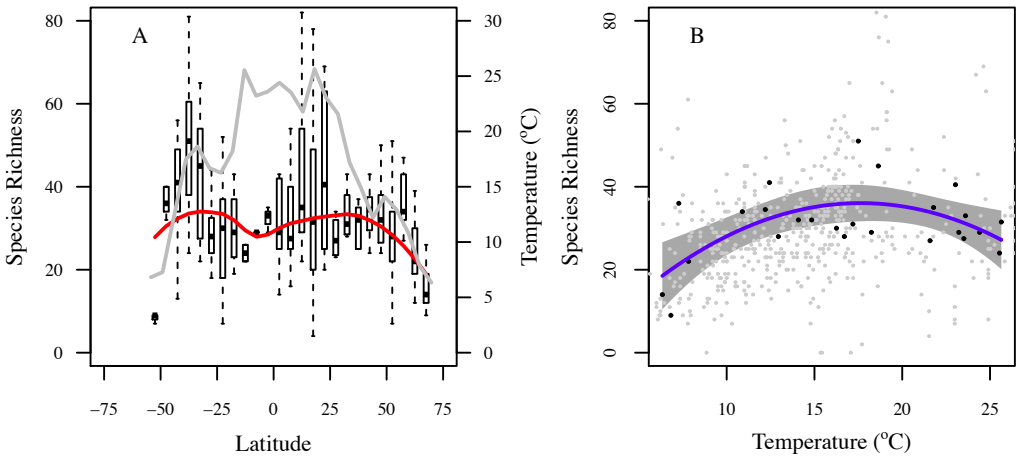

Figure 5.1: **(A)** Species richness distribution along the latitudinal gradient. The box plot shows the number of species found in Sal et al.'s (2013) database within each 5 degrees bins of latitude. Red line shows the predicted average number of species in each interval (Linear loess fit: n=25, span=0.75, Residual Standard Error: 7.892). Grey line shows the observed mean temperature for each latitude interval. **(B)** Species richness relationship with temperature. Grey dots show the observed number of species whose abundance is higher than 0 at each temperature. Black dots show the average number of species at each temperature in panel (A). Blue line shows the quadratic fit for black dots ($y = -0.14x^2 + 4.85x - 6.7$, r^2=0.37, p<0.01, AIC=174.67).

When this latitudinal pattern is viewed as a thermal gradient the result is a curvilinear relationship between species richness and temperature (Figure 5.1B). Richness increases from cold to temperate waters and saturates at around 20°C

(corresponding to the subtropical increase in richness), then there is a plateau at higher temperatures. Both the quadratic and linear fits of the relationship between species richness and temperature are significant but the quadratic fit was selected as the most parsimonious by the Akaike criterion (r^2=0.37, p<0.01, AIC=174.67 for the quadratic vs. r^2=0.08, p<0.001, AIC=182.041 for the linear fit) (Figure 5.1B).

For each of the 603 species compiled, we plotted its thermal range as a horizontal line centred at the midpoint (Figure 5.2A). This basically reproduces the pattern expected in a MDE (Colwell and Lees, 2000) but in a thermal domain. There is a clear trend where species with wider thermal ranges have their midpoints at the middle of the temperature domain and species with midpoints near a boundary necessarily have small ranges (Figure 5.2B). The species with narrow ranges can appear in any part of the domain as expected in a full stochastic model such as the MDE (Rober et al., 2004). Hence, using empirical data we obtain a random distribution of thermal ranges where a clear TMDE is observed. More species are present at the middle of the domain and the number of species decreases at almost the same rate as we move towards lower and higher temperatures (Figure 5.2C).

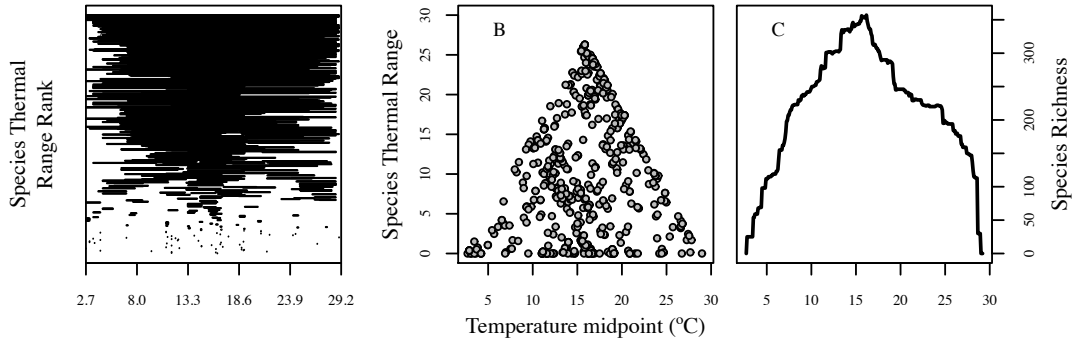

Figure 5.2: Thermal mid-domain for observed marine phytoplankton abundance data. **(A)** Phytoplankton species ranked by thermal range. Each bar shows the species niche breadth from narrower (at the bottom) to wider (at the top) centred on their mid-temperature. **(B)** For each bar in (A) the temperature range size is plotted against its thermal range midpoint. **(C)** Species richness along the thermal domain calculated as the number of species whose range overlap at each temperature (TMDE).

The predicted thermal niches from the GLM fits are shown in the Figure 5.3A as

the percentage of samples where a species is present at each temperature (a species was considered as present when the probability is higher than 0.001). Along the thermal domain these curves overlap allowing for the coexistence of species.

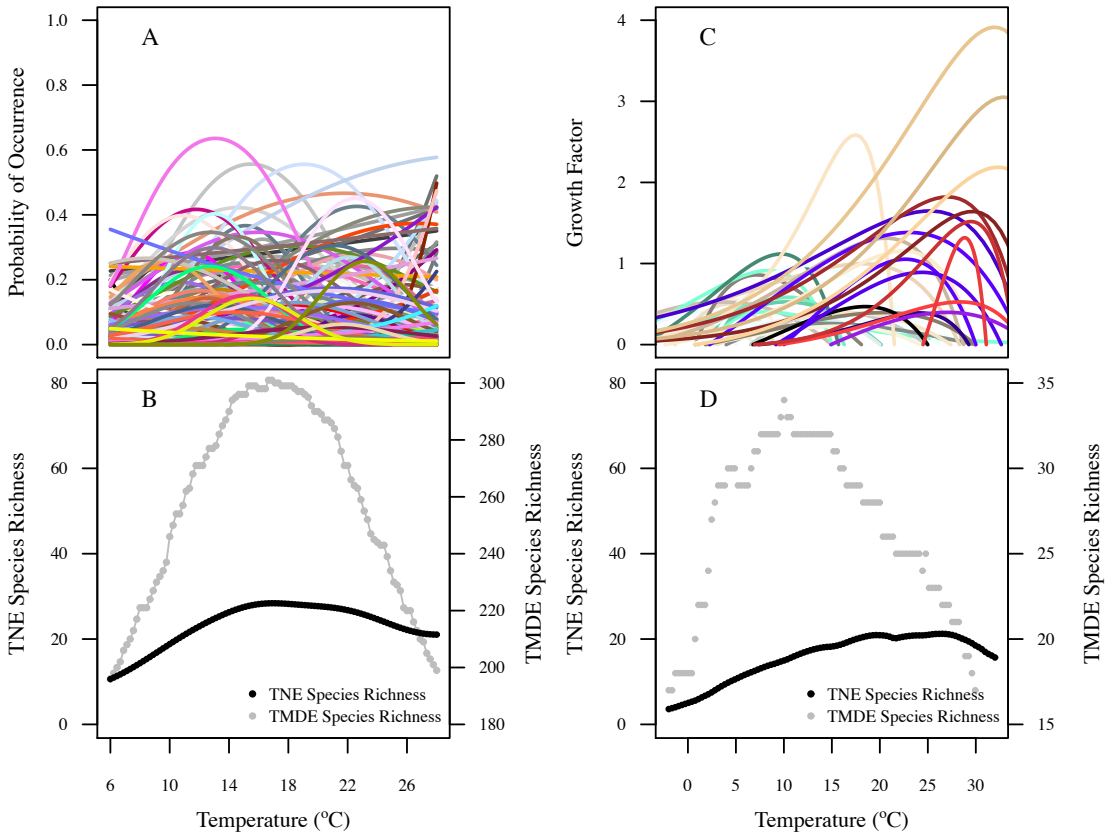

Figure 5.3: Results of GLM fit for Sal et al.'s (2013) database (left panels) and MLE fit for Thomas et al. (2012) data (right panels). In the upper panels each curve represents the thermal niche of each species.

Species richness can be calculated from these thermal niche curves in two different manners (Figure 5.3B). First we can calculate, for each temperature, the number of species present at each temperature. This is the equivalent to using the thermal range of the species and thus reveals the described TMDE where diversity increases at the middle of the thermal domain (i.e. similar to Figure 5.2C). In this TMDE a species has the same probability to be present in all parts of its

thermal domain. But the realized thermal niches show that usually species have a lower probability to be present at the extremes of their thermal range. We should account for this lower probability when the expected species richness distribution is calculated. Hence, an alternative way to estimate species richness from probability of occurrence data is to weight each species presence by the probability of that presence. So if at a given temperature there are *n* species all with low probability of occurrence, the expected species richness will be lower than at a temperature where there are *n* species all with high probability of occurrence. This results in the pattern predicted by the thermal niche effect theory (TNE) presented in Figure 5.3B which differs from the TMDE in that the decrease at higher temperatures is less pronounced than at lower temperatures. This less pronounced decrease at higher temperatures is because, on average, species that have their maximum probability of occurrence (MPO) at higher temperatures have a higher probability of occurrence, what is observed for both empirical and fitted data (Figure 5.4).

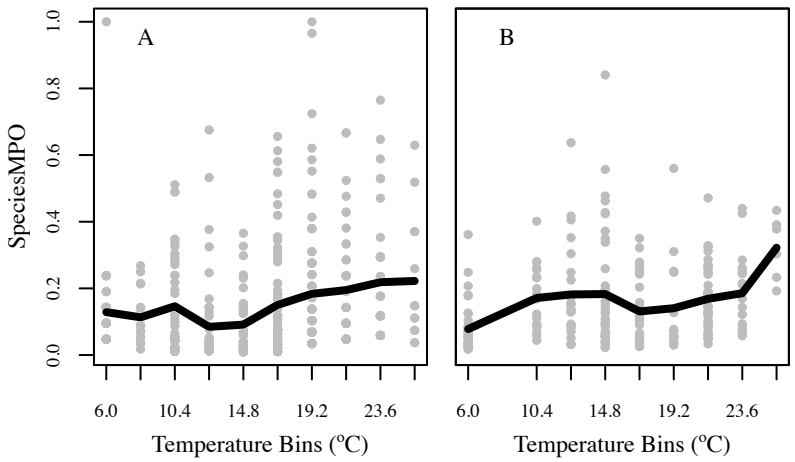

Figure 5.4: Relationship between the maximum probability of occurrence (MPO) and the temperature bin at which the MPO is reached for each species (grey dots). **(A)** Observed data for all 603species in the original dataset. **(B)** Results of GLM fit, i.e. predicted data. Black line shows the average MPO for each temperature bin.

This increase in MPO is expected from a fundamental niche perspective where maximum growth increases with temperature following Eppley's curve (Eppley,

1972). The MLE fit to the species growth data (Figure 5.3C) clearly evidences Eppley's curve. If we calculate species richness from these thermal growth curves as the number of species whose growth rate is greater than 0 at each temperature (Figure 5.3D), we reproduce again a TMDE with the highest number of species at the middle of the thermal domain and a symmetrical drop-off at the boundaries. Thomas et al. (2012) suggested that this increase of diversity at mid-latitudes is a result of sampling bias in their species compilation which included more species with a thermal optimum in temperate waters. To avoid this bias we randomly selected the same number of species with optimum at each temperature. Here the pattern predicted by TMDE is still apparent when we calculate species richness as the number of species with a growth rate greater than 0 at each temperature (Figure 5.3D). But, similarly to what occurs for presence data, a species does not grow at the same rate across its thermal niche. Consequently, the possibility of survival will be different at each temperature and it is expected that higher growth rates would result in higher probability of survival. Therefore we recalculated the species richness from these growth response curves weighting at each temperature the probability of presence of each species by its growth rate. This results in a diversity-temperature trend (Figure 5.3D) very similar to the presence data (Figure 5.3B). As predicted by TNE the slope of the species richness decline at lower temperatures is much steeper than at higher ones.

For those species that match between Thomas et al. (2012) compilation and ours, we compared the fundamental niche characterized by Thomas et al. (2012) and the realized niche found within our database (Figure 5.5). As expected, in most cases the realized niche appears reduced to a small space within the fundamental niche. However, some species were found at temperatures outside its thermal tolerance range, what might be the result of interactions such as dispersal or even to the fact of comparing different strains of a same species (Kashtan et al., 2014; Partensky and Garczarek, 2010). We also represent the probability of occurrence from which we fitted the thermal niche, which shows the high accuracy accomplished by the GLM approach.

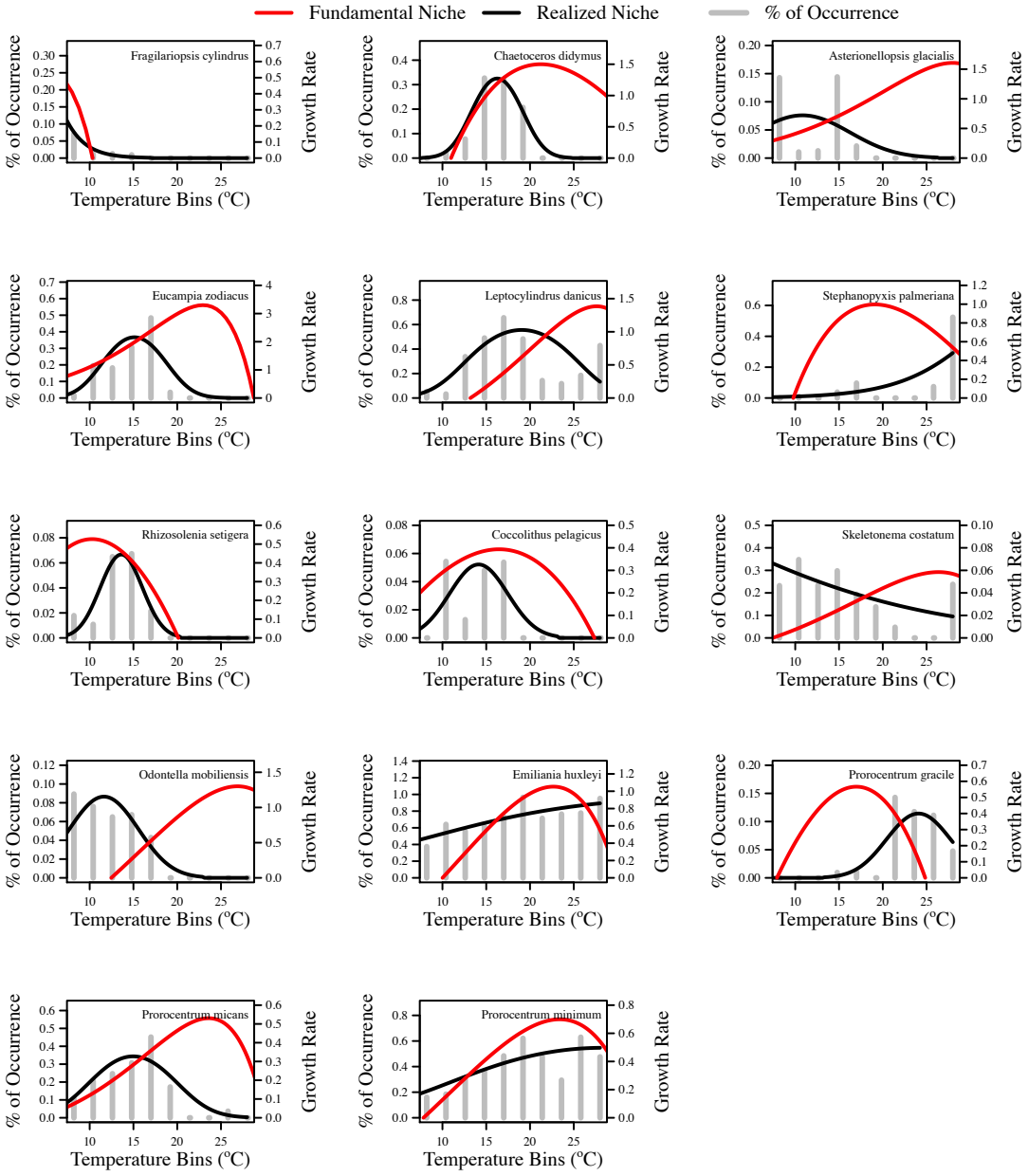

Figure 5.5: Comparison of *fundamental* and *realized niches* along the observed thermal domain for those species that match between our database and Thomas et al. (2012) data. The vertical grey bars show the observed probabilities of occurrence for each species in the Sal et al.'s (2013) database, which were used to fit the *realized niches* using a GLM fit. *Fundamental niches* correspond to the MLE fits for Thomas et al. (2012) data.

5.4 Discussion

Our results reveal that marine phytoplankton species richness increases with temperature up to ~20°C and that richness declines at the highest temperatures (Figure 5.1B). This pattern departs from the exponential increase predicted by MTE (Brown et al., 2004). Although when relationships between species richness and temperature have been encountered they have been usually attributed to MTE, many times this relationship is not exponential but asymptotic or lineal. This is the case of global compilations of oceanic data (Tittensor et al., 2010) but also for specific taxa such as marine bacteria (Fuhrman et al., 2008), copepods (Rombouts et al., 2009) or planktonic foraminifera (Tittensor et al., 2010; Yasuhara et al., 2012).

On the other hand, the thermal mid-domain theory (TMDE) predicts a hump-shaped relationship between temperature and species richness. It suggests that the ranges of species randomly distributed between two thermal boundaries tend to overlap at mid-temperatures, allowing the coexistence of a higher number of species in the middle of the thermal domain (Beaugrand et al., 2013; Brayard et al., 2005; Sal et al., in prep.). This overlap is observed in our empirical data analysis (Figure 5.2) and it is caused by 2 main constrains: on one hand wider niches have their midpoints at the middle of the thermal domain and, secondly, smaller thermal ranges occur in any part of the domain. As consequence, the number of overlapping niches is larger in the middle of the thermal domain (Figure 5.2C & Figure5.3B).

Nevertheless, this symmetrical pattern predicted by the TMDE is at odds with the observed relationship between species richness and temperature (Figures 5.1A & 5.1B), where the decline of species at the highest temperatures is less pronounced than at the coldest temperatures. We suggest that this difference between predicted and observed patterns is due to the assumption in TMDE that species have the same probability of survival within all their thermal range (Beaugrand et al., 2013). Our results reveal that this probability of survival, and hence of presence at a given temperature, is not uniform within the thermal range. Each species has a temperature within its thermal range where the probability of occurrence is highest, i.e. where it reaches its MPO. In addition, species that have their optimum at higher

temperatures usually have a higher MPO (Figure 5.4). This increase in MPO across species with increasing temperature (Figure 5.4) is probably a consequence of the increase in the maximum growth rate of species with increasing temperature (Eppley, 1972). The exponential increase of growth rates with temperature is apparent in the fundamental niches compiled by Thomas et al. (2012) (Figure 5.3C) and reflected in the realized niches (Figure 5.3 A) through an overall tendency to have a higher MPO at the highest temperatures (Figure 5.4). Our explanation for the relationship between temperature and species richness is a combination of a TMDE and a metabolic effect through the increase in growth rate with temperature as in Eppley's curve (Eppley, 1972).

Differences between both *fundamental* and *realized niches* for those species that match between Thomas et al.'s (2012) dataset and ours (Figure 5.5) show that for most cases the thermal space where a species occurs is restricted to a small part of the fundamental niche. This supports the theory of Hutchinson (1957), who attribute this fact to competitive exclusion. A few species are present outside of its physiological niche. Pulliam (2000) found that species might occur outside their fundamental niche as a consequence of dispersal. Indeed, dispersal is another effect that can contribute to the generation of a LDG (Barton et al., 2010*a*; Brayard et al., 2005; Sal et al., in prep.; Thomas et al., 2012). Hence, although temperature seems to play an essential role to explain the emergence of a LDG (Figure 5.1A) this does not rule out the possibility of other factors that contribute to the LDG. Species richness also describes a unimodal relationship with productivity (Irigoien et al., 2004; Smith, 2007). We restricted our database to mid-productivity levels to show that, independent of the productivity - diversity relationship, the TNE results in a LDG. In any case, when both temperature and productivity effects are considered using the whole dataset (Figure S5.1), the relationship between species richness and temperature remains very similar to that predicted by TNE.

Based on the TNE predictions to explain the relationship between species richness and temperature, we analysed the implications of this new hypothesis on the distribution of species richness over the oceans. Thomas et al. (2012) based their results on temperature predictions for historical (1991-2000) and future ther-

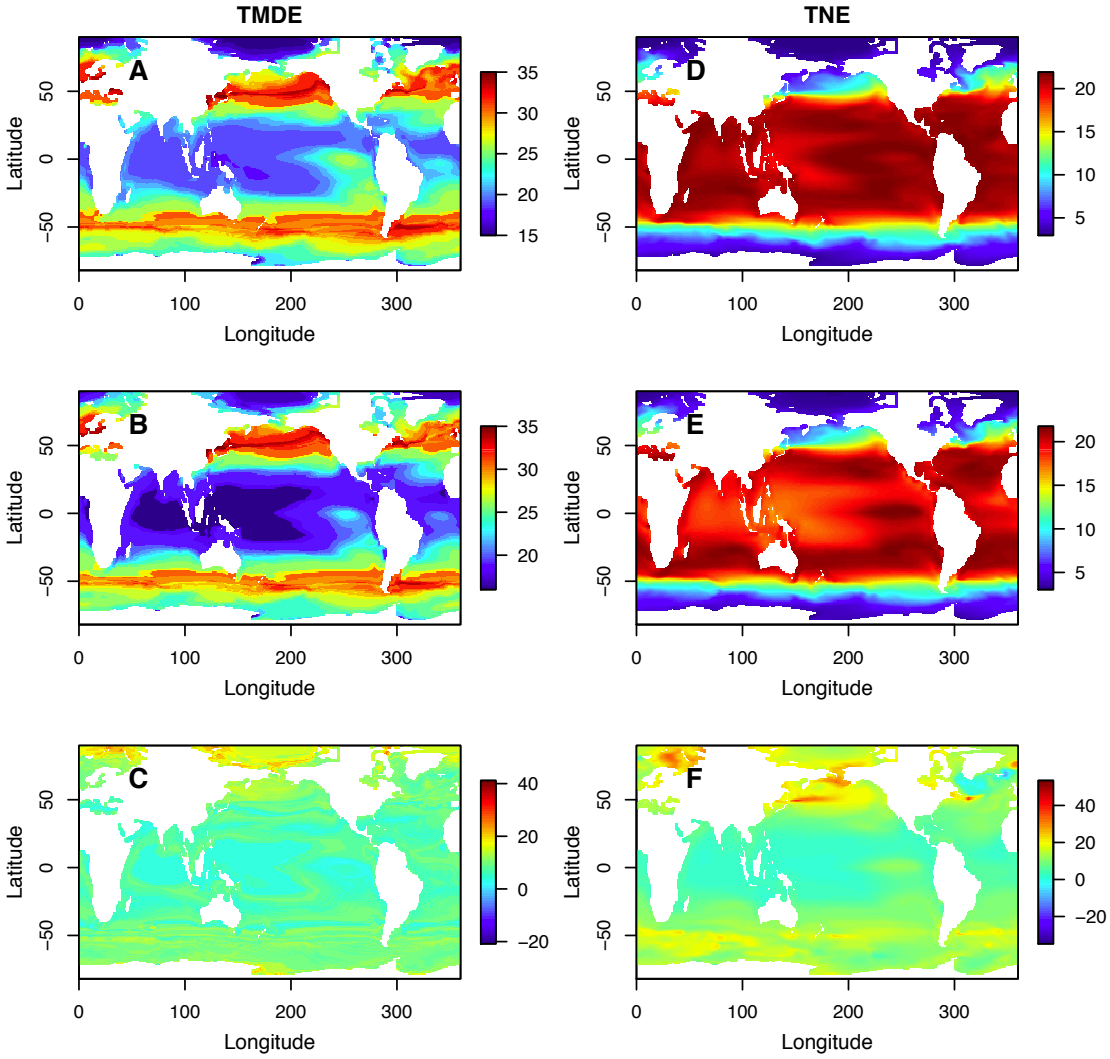

Figure 5.6: Species richness distribution under historical (1991-2000) and future (2091-2100) temperature regimes based in both hypotheses: TMDE (left panels) and TNE (right panels). **(A & D)** Historical species richness prediction. **(B & E)** Future species richness prediction. **(C & F)** Percentage of change in species richness between historical and future temperature regimes.

mal regimes (2091-2100). Combining these predictions with the thermal response curves compiled by Thomas et al. (2012), we estimated species distributions under both hypotheses: TMDE (similar to Thomas et al. (2012) but using the same number of species with optimum values at each temperature, as in Figure 5.3D

(Figures 5.6A-C) and TNE, where unlike the TMDE, the species presence is weighted by the possibility of survival at each temperature (Figures 5.6D-F).

The major difference between both hypotheses relies on the predictions for historical thermal regimes. Whereas the TNE is able to predict the slight decline of species that it has been shown to occur at the equator, Thomas et al. (2012) predict a symmetrical decline at both sides of the tropical areas that is at odds with the observed pattern (Figure 5.1A). However, the percentage of change in species richness when comparing historical and future regimes remains similar under both predictions. In fact, TNE and TMDE predictions agree in that tropical communities are the most vulnerable since a shift of species towards the poles is expected to occur for the last decade of this century under the predicted scenario of global warming.

5.5 Supplementary figure

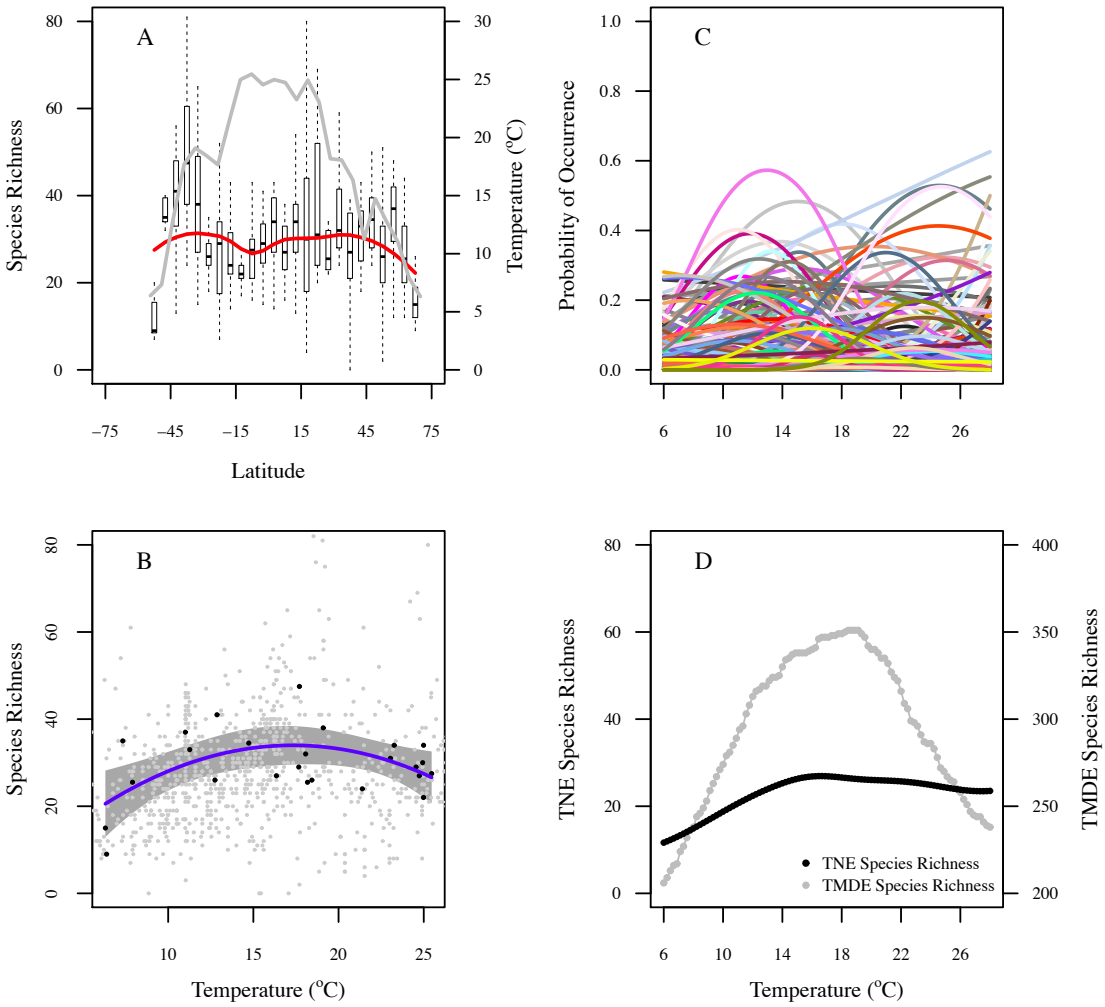

Figure S5.1: Results using the whole database in (Sal et al., 2013) where the productivity restriction is not applied. **(A)** Species richness distribution along the latitudinal gradient. The boxplot shows the number of species found within each 5 degrees bins of latitude. Red line shows the predicted average number of species within each interval (Linear loess fit: n=25, span=0.75, Residual Standard Error: 7.755). Grey line shows the observed mean temperature within each latitude interval. **(B)** Species richness distribution along the thermal domain. Grey dots show the number of species which total abundance is higher than 0 at each temperature. Black

dots show the average number of species at each temperature in panel (A). Blue line shows the quadratic fit for black dots ($y = -0.11x^2 + 3.84x + 0.73$, r^2=0.28, p<0.05, AIC=172.92). **(C & D)** Results of GLM fit. Each curve in **(C)** represents the thermal niche of each species as a probability of occurrence index (realized niche). **(D)** Phytoplankton species richness calculated as result of both: TMDE (number of species whose probability of occurrence is higher than 0 at each temperature) and TNE (sum of probabilities of presence at each temperature).

General Discussion

Throughout this thesis we have tried to disentangle and understand the factors that influence the growth and distribution of marine phytoplankton. The main problems to achieve this goal are on one hand that many of these factors are interrelated, what makes difficult to separate their effects. On the other hand, the scarcity or inconsistency within datasets may lead to confounding results. Combining empirical datasets with theoretical simulations and the use of global ecological models, we have been able to answer our main objectives and, hopefully, contributed to the understanding of the ecosystem functioning. There are however some points that it is worth to discuss in this last section.

The trade-off between intrinsic maximum growth and half-saturation constant

A relevant point in our results suggests that the allometric slopes of phytoplankton growth rates are variable and do not consistently support a specific theoretical value when a large range of cell size is included. When this includes picophytoplankton, we have found that the resulting unimodal relationship between growth rate and cell size is a consequence of the shared evolutionary history of species rather than a size effect.

This seems to be in contrast with the parameterization followed in *Darwin* model (Chapter 3). Here, phytoplankton species are grouped into two size-classes and the two traits that define nutrient uptake capabilities (i.e. intrinsic maximum growth and half-saturation constant) depend on cell size in a way that can sometimes

lead to an allometric competitive trade-off among species. The maximum growth rates are fixed for each phytoplankton size-class where large phytoplankton have a higher intrinsic maximum growth rate than small phytoplankton (Follows et al., 2007). But according to Chapter 2, there is no reason to impose that small species have lower growth rates than the larger ones and thus considering a trade-off such as this might not be a true representation of nature. Phytoplankton types in the model are initialized according to four functional groups: (1) diatom analogs, (2) other large phytoplankton, (3) other small phytoplankton, and (4) *Prochlorococcus* analogs (Follows et al., 2007). Although for instance *Prochlorococcus* have lower growth rates that some larger species, they may also have similar growth rates than some species of the largest groups such as diatoms (see Figure 2.2 in Chapter 2). Therefore, although this trade-off between cell size and growth rate could occur for some specific phytoplankton types, recent studies have shown that it should not be considered as a general fact as it is imposed in the model (Edwards et al., 2012; Fiksen et al., 2013).

Although we acknowledge this controversy, we justify the use of this parameterization to reproduce the results found by Barton et al. (2010*a*) and to be able to evaluate whether their results are not mutually exclusive with a *thermal mid-domain effect* for driving the latitudinal diversity gradient of marine phytoplankton. Our results in Chapter 3 reveal that a major driver of the non-equilibrium coexistence between species is indeed the functional grouping with competitive trade-offs imposed in the model (i.e. DIN niches) (Figure 3.5). In fact, besides dispersal effects, the resulting LDG in Simulation 2 (DIN niches only) is mainly driven by this allometric competitive trade-off while the TMDE leads to a LDG without accounting for this imposition. This might suggest that the role of temperature on the LDG could be greater than is usually thought, but further investigation would be needed to assert the extent of this suggestion.

The scope of the *thermal niche effect*

In an effort to evaluate the relevance of the TNE hypothesis to explain the species richness relationship with temperature (Chapter 5), we used the Simulation 1 in *Darwin* (Chapter 3). In the model, the thermal tolerance curves of species are

characterized following the exponential increase of growth rate with increasing temperature as described by Eppley (1972). In addition, for each phytoplankton species a temperature optimum is assigned at random. Following the initial setup conditions, we reproduced the species *fundamental niche*, which only accounts for the effect of temperature on the species growth rate. We also characterized the *realized niche* for the 78 species in the model using the surface outputs of Simulation 1 after 10 years integration. For both niche types, we calculated the species richness along the thermal domain according to both the TMDE and TNE hypotheses (Figures 6 A-B) in the same way as we did for the Figure 5.3 (see Results section in Chapter 5).

When comparing the resulting patterns with the observed relationship between species richness and temperature obtained in Simulation 1 (Figure 6C), the TNE pattern seems to be closer to the model outputs. Both reflect that the decline of species is much less pronounced at higher than at lower temperatures (Figure 6C), what was also observed in the empirical data (Figure 5.1B).

Unlike the TMDE hypothesis, the TNE accounts for the probability of presence/growth of each species at each temperature. As we explained in Chapter 5, when considering this effect to calculate the number of species present at each temperature, the effect of Eppley's curve is reflected across both *fundamental* and *realized* niches. This means that the exponential increase of maximum growth rate with increasing temperature seems to condition the maximum probability of presence of the species at each temperature. For instance, species with an optimum value at higher temperatures, have a greater maximum growth rate and thus a greater maximum probability of presence that species with lower optimums. As result, as temperature increases, the number of species at each temperature for both *fundamental* and *realized* niches increases. The combination of this effect with the the lower overlapping of niches at high temperatures, as suggested by the TMDE, results in the slight decline of the number of species under warm conditions. Although this was already shown in Chapter 5, the model allows the possibility of reproducing both *fundamental* and *realized* niches for the same species and thus give further support to our hypothesis.

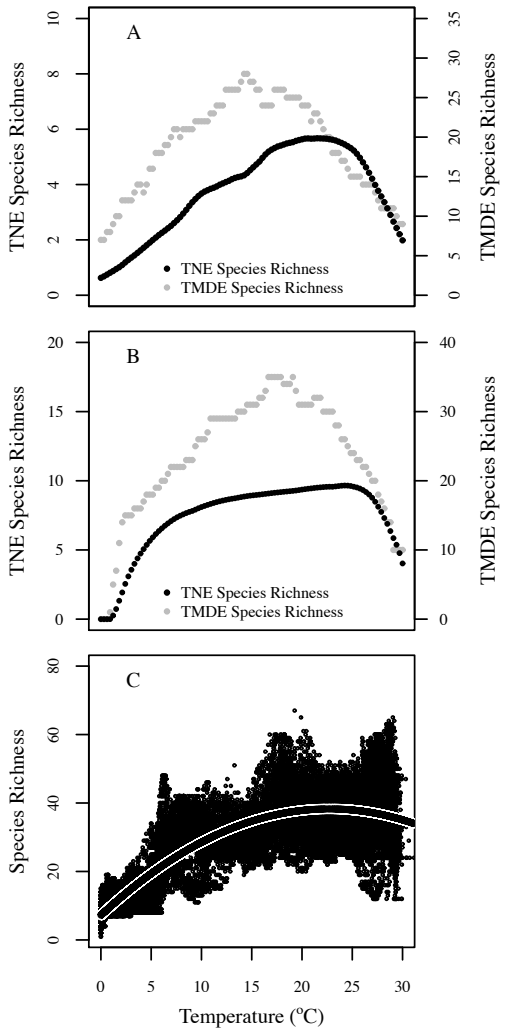

Figure 6: Species richness prediction based on **(A)** fundamental and **(B)** realized niches for TNE and TMDE hypotheses. **(C)** Observed species richness distribution along the thermal domain for the surface outputs of Simulation 1.

Conclusiones

1. Las pendientes alométricas de las tasas de crecimiento de fitoplancton son variables y no apoyan consistentemente un único valor teórico cuando se considera un espectro de tamaños grande, es decir que incluya desde pico hasta microfitoplancton.

2. La aparente relación unimodal entre la tasa de crecimiento específica y el tamaño celular del fitoplancton es el resultado de la historia evolutiva común de las especies, en concreto de la adaptación del picofitoplancton a ambientes oligotróficos, y por tanto la curvatura desaparece cuando dicho efecto es corregido. Esta especialización del picofitoplancton a zonas cálidas implica que la curvatura sea significativa o no en función de la temperatura a la que las tasas de crecimiento son medidas.

3. El cálculo del exponente a la hora de corregir la tasa de crecimiento por el efecto de la temperatura, puede estar influenciada por la correlación entre la temperatura y el tamaño. Para evitar sesgos en el estudio de las relaciones alométricas, dicha elección debe hacerse utilizando valores determinados teóricamente, o bien corroborados con trabajos experimentales, siempre y cuando el efecto de terceras variables, como el tamaño o los nutrientes, puedan ser controlados. Una alternativa a estas tradicionales correcciones es utilizar las curvas de tolerancia térmica para predecir la tasa de crecimiento de cada especie a diferentes temperaturas y analizar así el escalamiento a cada temperatura.

4. El uso de modelos globales permite no sólo reproducir el gradiente latitudinal de diversidad (GLD), sino poder estudiar en conjunto y por separado los factores que

contribuyen a su mantenimiento, y que con datos empíricos resulta casi imposible estimar. Así observamos que el GLD es el resultado de no uno sino varios factores: la exclusión competitiva entre especies especialistas y oportunistas, la coexistencia de especies con similares requerimientos en zonas de estabilidad ambiental (R* similar), la dispersión oceánica y la temperatura a través de un *thermal mid-domain effect* (TMDE). No descartamos sin embargo que otros factores como pueden ser la radiación solar o la predación puedan contribuir a su mantenimiento.

5. La base de datos de diversidad de microplancton recopilada en el capítulo 4 aporta datos ambientales y abundancia de especies, proporcionando oportunidades únicas para el estudio de la distribución de fitoplancton marino a escalas amplias. Además, es la única base de datos donde la identificación de las especies ha sido llevada a cabo por el mismo taxonomista. Junto con los datos de abundancia, biomasa y volumen, aporta datos ambientales para cada estación.

6. Dicha base de datos ha permitido demostrar con datos empíricos la existencia de un gradiente latitudinal de diversidad (GLD) para la comunidad completa de fitoplancton marino. Dicho patrón se distribuye latitudinalmente incrementando el número de especies desde los polos hacia el ecuador. Se trata de una distribución bimodal donde el mayor riqueza específica se sitúa en los trópicos.

7. El *thermal niche-effect* (TNE) parece explicar con mayor certeza la relación entre el número de especies y la temperatura, donde nuestra recopilación de datos empíricos sugiere que la riqueza específica aumenta con la temperatura hasta ~20° y disminuye lentamente hacia temperaturas más altas. Esta hipótesis resulta de la combinación de dos hipótesis: la predicción del TMDE que explica un mayor solapamiento de los nichos a temperaturas intermedias y por tanto una mayor coexistencia de especies que a temperaturas altas o bajas; y en segundo lugar, el aumento exponencial de la tasa máxima de crecimiento con la temperatura que predice la curva de Eppley.

8. El aumento exponencial de las tasas máximas de crecimiento con la temperatura observado en los nichos fundamentales de las especies parece verse reflejado también en los nichos realizados. Esto sugiere que las especies que tienen su

óptimo a temperaturas elevadas, tienen no sólo una tasa máxima de crecimiento mayor sino también una probabilidad máxima de ocurrencia mayor que especies con óptimos a temperaturas más bajas.

9. Las estimaciones de la distribución global del fitoplancton en el océano en función de la temperatura predichas por la hipótesis del TNE parecen reproducir mejor los patrones observados en datos empíricos. Por tanto, esta hipótesis permite mejorar las predicciones sobre cómo el calentamiento global podría afectar a estas distribuciones en el futuro. Nuestra hipótesis apoya recientes estudios que estiman que durante la última década de este siglo se podría producir un desplazamiento en los nichos de las especies hacia los polos.

10. Datos empíricos y modelizados muestran resultados similares, lo que determina la validez de la base de datos compilada en el capítulo 4, así como del modelo global *Darwin* empleado en el capítulo 3. Dichos resultados demuestran la importancia de testar resultados con ambos tipos de estudios para justificar cualquier hipótesis.

Agradecimientos

Es difícil resumir más de 4 años de trabajo en unas cuantas páginas, pero casi más difícil resulta agradecer en unas pocas líneas a todas las personas a las que me han acompañado estos años y han hecho posible que hoy pueda poner punto final a esta tesis.

Y de todas esas personas, el agradecimiento más grande va para mi director, *Ángel López-Urrutia*. Sin duda esta tesis te la debo a ti, desde el día en que se me ocurrió embarcarme en esta aventura (allá por el verano de 2007), hasta hoy. Gracias por las millones de horas dedicadas, en la silla de al lado o desde el otro lado del charco. Gracias por tus consejos, por tus ideas y por los millones de pruebas y alguna más! ;) Gracias por haberme enseñado taaaaaaaaaaaaaaanto, por tu increíble paciencia, por sacar lo mejor de mí.. y dar lo mejor de ti. Estoy segura que no podría haber dado con alguien mejor, así que de verdad, *Ángel*, GRACIAS.

Queridos amigos de la sala de becarios y alrededores, está clarísimo que sin compañeros como vosotros, una tesis sencillamente no se termina! Así que mil gracias a todos y cada uno de los que habéis pasado por aquí, a los que os fuisteis y a los que seguiréis: *Evii, Virgi, Martuki, Evita (y JF!), Nestor, Leti, Tamara, Lucie, Aurore, Sarina, Floren, Ale, Alex, Pili, Tere, Maite, Eneko, Lara, Ana Mari...* GRACIAS por los cafés mañaneros, las cerves de viernes, las cenas temáticas, las tardes de verano en la cuesta, los días de surf, las excursiones al japo y por supuesto los espichones!! Sois geniales!!

Gracias muy especiales a *Juan* y *Paqui* por todo lo anterior, pero además por vuestros consejos y comentarios a lo largo y ancho de la tesis (sobrevivir a *R* fue

más fácil juntos ☺). Gracias también por vuestra colaboración en el Capítulo 2, donde además tengo que dar unas gracias enormes a *Laura* por introducirme al mundo de la filogenia ;)

Y por supuesto GRACIAS al resto de compañeros del Centro Oceanográfico de Gijón. Con unos compartí más y con otros menos, pero siempre guardaré un gran recuerdo de mis años aquí: Itziar, Iñaki, Felipe, Dani, Luis Angel, Xelu, Gonzalo, Laura Díaz, Alma, Eva S., Eva A., Fernando, Nacho, Montse, Rafa, Quique, Renate, Mikel, César, Cristobo, Pilar, Carmen Cabeza, Carmen Castro, Venicio, Jose Mª, Paco, Ester, Rosa, Roberto, Helena, Jesús, Ángela y Pili.

Ya queda lejos, pero recuerdo con muchísimo cariño los 4 meses que pasé en Boston. Desde el primer día hasta el último fueron muchos los momentos vividos y por eso no puedo olvidarme de dar un GRACIAS inmenso a mis Bostonianos favoritos: a *Jesús* (*compiii!!*), a *Lore, Ali, Silvina, Maite, Pablo, Javi/s, Jaime, Nati, Bego, Inma, Eli, Sara, Salva, Ross, Nia*... A *Ser*, a ti las gracias van por partida doble, sin tu ayuda el Capítulo 3 no habría terminado nunca ;)

I would like to thank *David Siegel* for hosting me and for all his attention during my stay at the UCSB. It was a really great pleasure to work with you. I am also very grateful to *Mick Follows* and *Stephanie Dutckiewich* for hosting me at the MIT. Thank you so much for giving me the oportunity to collaborate in the *Darwin* project, which was key for Chapter 3. But specially thanks for your help and comments. I hope we can collaborate again in the future.

Thank you sooo much to *Christine*! It was great living with you during my 2 months in Santa Barbara. Many thanks to *Sarah, Bryan, Gavin* and all those great people with whom I shared those months in California!

Many thanks to *Xabier Irigoien, Roger Harris* and *Derek Harbour*, for your invaluable help in Chapter 4, for providing the data but also for your comments. It was a pleasure to work together.

Las campañas en el B.O.Hespérides y en el RV Sarmiento de Gamboa han sido de las mejores experiencias y los mejores recuerdos que me llevo de estos años. Y eso sin duda se lo debo a la increíble gente con la que conviví, y que acabaron por

ser grandes amigos. Muy especiales GRACIAS a *Zuky, Fran, Marcos, Jesús, Mar, Ame y María* (mis *Queridas mujeres:*). Muchísimas gracias a *Alonso, Lola, Elena, Vero, David, Eli, Iván, Toni, Alex, Eugenio, Javi, Edu, Paloma, Raquel, Jose, Rosa, Salva, Juan* y un larguísimo etcétera que comprende a las tripulaciones de ambos barcos durante la Intercalibración y el Leg 24ºN de Malaspina 2010.

Ya en el terreno más personal me gustaría agradecer a mis amigos de siempre por hacerme saber que seguía habiendo vida al otro lado de la tesis, por compartir taaantos momentos estos años, por estar ahí siempre (incluso a pesar de mis idas y venidas) y apoyarme en los buenos y en los malos momentos. Gracias a *Cris, Pauli, Urs* y al resto de mis *cartujas*: *Ana, Andrea, Fani, Mari, María, Marta, Paulina, Sil, Yai*. Graaacias a *Pau V, Richo, Pochi, Juan, Alfredo, Ani* y a todos esos que seguro se me quedan en el tintero.

Un GRACIAS enorme a toda mi gente de Cádiz (residentes y exiliados) por haber seguido estando tan cerca todos estos años. Vosotros sabéis lo importantes que habéis sido y sois... Así que gracias a *Chur, Ali, Dudu, Eri, Ángel, Inma* (gracias por esa pedazo de portada!). A *Edu y Emilio* por ese ASLO-Japón inolvidable! Gracias a mis *cariss* ☺: *Marina, Tanita y Sori*; a todos los *GPD's* y allegados: *María, Adolf, Moli, Fran* y a *Carlos*...

A mi *Paqui*, no sólo por todo lo referente a la tesis, sino por ser casi como una hermana (tú ya sabes el resto ☺).

GRACIAS a mi familia por todo su apoyo durante estos años.

Pero por encima de todo GRACIAS a mis padres. Todo lo que he conseguido os lo debo sin duda a vosotros. Gracias por vuestros consejos, por vuestro apoyo, por vuestra paciencia, por saber entenderme y por haber estado ahí *siempre e incondicionalmente*. Y *papá*... estoy segura de que haber acabado ligando mi vida al mar no ha sido casualidad, GRACIAS ☺

Agradecimientos

Esta tesis ha sido financiada por el Ministerio de Educación, a través de una beca de Formación de Personal Universitario (FPU). La mayor parte del trabajo realizado se llevó a cabo en el Centro Oceanográfico de Gijón, perteneciente al Instituto Español de Oceanografía - Ministerio de Economía y Competitividad. Además esta tesis se ha beneficiado de los proyectos CONSOLIDER Malaspina 2010 and METabolic OCean Analysis (METOCA) financiados por el Plan Nacional Español de Investigación+Desarrollo+Innovación (I+D+I) y por el Theme 6 of the EU Seventh Framework Program through the Marine Ecosystem Evolution in a Changing Environment (MEECE 212085).

References

Akaike, H. 1974. A new look at the statistical model identification. Automatic Control, IEEE Transactions on **19**: 716–723. 21, 75

Aksnes, D. L., and J. K. Egge. 1991. A theoretical-model for nutrient-uptake in phytoplankton. Marine Ecology-progress Series **70**: 65–72. 15

Allen, A. P., J. H. Brown, and J. F. Gillooly. 2002. Global biodiversity, biochemical kinetics, and the energetic-equivalence rule. Science **297**: 1545–1548. 3

Allen, A. P., and J. Gillooly. 2006. Assessing latitudinal gradients in speciation rates and biodiversity at the global scale. Ecology Letters **9**: 947–954. 52, 72

Allen, A. P., J. F. Gillooly, and J. H. Brown. 2005. Linking the global carbon cycle to individual metabolism. Functional Ecology **19**: 202–213. 12

Arrhenius, O. 1921. Species and area. Journal of Ecology **9**: 95–99. 3

Arrhenius, S. 1915. Quantitative laws in biological chemistry. London. 2, 12, 22

Banavar, J. R., M. E. Moses, J. H. Brown, J. Damuth, A. Rinaldo, R. M. Sibly, and A. Maritan. 2010. A general basis for quarter-power scaling in animals. Proceedings of the National Academy of Sciences of the United States of America **107**: 15816–15820. 16

Banse, K. 1976. Rates of growth, respiration and photosynthesis of unicellular algae as related to cell size. A review. Journal of Phycology **12**: 135–140. 18

REFERENCES

Banse, K. 1982. Cell volumes, maximal growth rates of unicellular algae and ciliates, and the role of ciliates in the marine pelagial. Limnology and Oceanography **27**: 1059–1071. 18, 29

Barton, A. D., S. Dutkiewicz, G. Flierl, J. Bragg, and M. J. Follows. 2010*a*. Patterns of Diversity in Marine Phytoplankton. Science **327**: 1509–1511. 40, 41, 43, 45, 49, 51, 52, 56, 72, 83, 90

Barton, A. D., S. Dutkiewicz, G. Flierl, J. Bragg, and M. J. Follows. 2010*b*. Response to Comment on "Patterns of Diversity in Marine Phytoplankton". Science **329**: 5991. 49, 50

Bates, H. W. 1862. Contributions To An Insect Fauna of the Amazon Valley (lepidoptera, Heliconidae). Transactions of the Linnean Society **23**: 495–566. 3, 40

Beaugrand, G., I. Rombouts, and R. R. Kirby. 2013. Towards an understanding of the pattern of biodiversity in the oceans. Global Ecology and Biogeography **22**: 440–449. 40, 41, 47, 49, 52, 72, 82

Behrenfeld, M. J., R. T. O'Malley, D. A. Siegel, C. R. McClain, J. L. Sarmiento, G. C. Feldman, A. J. Milligan, P. G. Falkowski, R. M. Letelier, and E. S. Boss. 2006. Climate-driven trends in contemporary ocean productivity. Nature **444**: 752–755. 1

Bissinger, J. E., D. J. S. Montagnes, J. Sharples, and D. Atkinson. 2008. Predicting marine phytoplankton maximum growth rates from temperature: Improving on the Eppley curve using quantile regression. Limnology and Oceanography **53**: 487–493. 12, 13

Björklund, M. 1994. The independent constrasts method in comparative biology. Cladistics **10**: 423–433. 19

Blackburn, T. M., and K. Gaston. 1998. Some methodological issues in macroecology. The American Naturalist **151**: 68–83. 19

Blasco, D., T. T. Packard, and P. C. Garfield. 1982. Size dependence of growth rate, respiratory electron transport system activity, and chemical composition in marine diatoms in the laboratory. Journal of Phycology **18**: 58–63. 18

Boyce, D. G., M. R. Lewis, and B. Worm. 2010. Global phytoplankton decline over the past century. Nature **466**: 591–596. 4

Boyd, P., T. Rynearson, E. Armstrong, K. Hayashi, F.-X. Fu, D. Hutchins, Z. Hu, R. Kudela, E. Litchman, M. Mulholland, U. Passow, R. Strzepek, E. Whittaker, E. Yu, and M. Thomas. 2013. Marine phytoplankton temperature versus growth responses from polar to tropical waters - outcome of a scientific community-wide study. PLoS ONE **8 (5)**: e63091. 31

Brayard, A., G. Escarguel, and H. Bucher. 2005. Latitudinal gradient of taxonomic richness: combined outcome of temperature and geographic mid-domains effects? Journal of Zoological Systematics and Evolutionary Research **43**: 178–188. 3, 40, 49, 52, 72, 82, 83

Brewer, P., and J. Riley. 1965. The automatic determination of nitrate in seawater. Deep Sea Research **12**: 765–72. 62

Brown, J. H., J. F. Gillooly, A. P. Allen, V. M. Savage, and G. B. West. 2004. Toward a metabolic theory of ecology. Ecology **85**: 1771–1789. 2, 10, 18, 52, 82

Bruggeman, J. 2011. A phylogenetic approach to the estimation of phytoplankton traits. Journal of Phycology **47**: 52–65. 19, 29

Bruggeman, J., J. Heringa, and B. Brandt. 2009. PhyloPars: estimation of unknown parameters using phylogeny. Nucleic Acids Research **37**: 179–184. 19

Buitenhuis, E. T., W. K. W. Li, D. Vaulot, M. W. Lomas, M. R. Landry, F. Partensky, D. M. Karl, O. Ulloa, L. Campbell, S. Jacquet, F. Lantoine, F. Chavez, D. Macias, M. Gosselin, and G. B. McManus. 2012. Picophytoplankton biomass distribution in the global ocean. Earth System Science Data **4**: 37–46. 5, 56

Capellini, I., C. Venditti, and R. Barton. 2010. Phylogeny and metabolic scaling in mammals. Ecology **91(9)**: 2783–2793. 19

Cermeño, P., and P. G. Falkowski. 2009. Controls on Diatom Biogeography in the Ocean. Science **325**: 1539–1541. 4

Cermeño, P., E. Marañón, D. Harbour, F. G. Figueiras, B. G. Crespo, M. Huete-Ortega, M. Varela, and R. P. Harris. 2008. Resource levels, allometric scaling of population abundance, and marine phytoplankton diversity. Limnology and Oceanography **53**: 312–318. 72

Cermeño, P., E. Marañón, D. Harbour, and R. P. Harris. 2006. Invariant scaling of phytoplankton abundance and cell size in contrasting marine environments. Ecology Letters **9**: 1210–1215. 57

Cermeño, P., T. Rodríguez-Ramos, M. Dornelas, F. Figueiras, E. Marañón, I. Teixeira, and S. Vallina. 2013. Species richness in marine phytoplankton communities is not correlated to ecosystem productivity. Marine Ecology Progress Series **488**: 1–9. 74

Chavez, F., K. Buck, and R. Barber. 1990. Phytoplankton taxa in relation to primary production in the Equatorial Pacific. Deep-Sea Research Part A-Oceanographic Research Papers **37(11)**: 1733–1752. 51

Chen, B., and H. Liu. 2011. Comment: Unimodal relationship between phytoplankton-mass-specific growth rate and size: A reply to the comment by Sal and Lopez-Urrutia (2011). Limnology and Oceanography **56**: 1956–1958. 9, 18, 21, 22, 25, 28, 29, 30

Chen, B. Z., and H. B. Liu. 2010. Relationships between phytoplankton growth and cell size in surface oceans: Interactive effects of temperature, nutrients, and grazing. Limnology and Oceanography **55**: 965–972. 10, 11, 12, 13, 18

Chisholm, S., 1992. Phytoplankton Size. Pages 213–237– *in* P. Falkowski, A. Woodhead, and K. Vivirito, editors. Environmental Science Research, volume 43. Springer US. 18

Clinebell, R. R., O. L. Phillips, A. H. Gentry, N. Stark, and H. Zuuring. 1995. Prediction of Neotropical Tree and Liana Species Richness From Soil and Climatic Data. Biodiversity and Conservation **4**: 56–90. 56

Colwell, R. K., and G. C. Hurtt. 1994. Nonbiological Gradients In Species Richness and A Spurious Rapoport Effect. American Naturalist **144**: 570–595. 3, 40, 72

Colwell, R. K., and D. C. Lees. 2000. The mid-domain effect: geometric constraints on the geography of species richness. Trends In Ecology & Evolution **15**: 70–76. 3, 40, 52, 72, 73, 77

Connell, J. H. 1978. Diversity In Tropical Rain Forests and Coral Reefs - High Diversity of Trees and Corals Is Maintained Only In A Non-equilibrium State. Science **199**: 1302–1310. 56

Connolly, J. A., M. J. Oliver, J. M. Beaulieu, C. A. Knight, L. Tomanek, and M. A. Moline. 2008. Correlated evolution of genome size and cell volume in diatoms (*Bacillariophyceae*). Journal of Phycology **44**: 124–131. 19

Cullen, J. 1991. Hypothesis to explain high-nutrient conditions in the sea. Lim **36**: 1578–1599. 51

Currie, D. J. 1991. Energy and Large-scale Patterns of Animal-species and Plant-species Richness. American Naturalist **137**: 27–49. 3, 72

De Monte, S., A. Soccodato, S. Alvain, and F. d'Ovidio. 2013. Can we detect oceanic biodiversity hotspots from space? The ISME journal **7**: 2054–2056. 72

DeBaar, H. 1994. von Liebig's law of the minimum and plankton ecology (1899-1991),. Progress In Oceanography **33(4)**: 347–386. 42

DeLong, J., J. Okie, M. Moses, R. Sibly, and J. H. Brown. 2010. Shifts in metabolic scaling, production, and efficiency across evolutionary transitions of life. Proceedings of the National Academy of Sciences **107(29)**: 12941–5. 32

Dolan, J., R. Lemée, S. Gasparini, and C. Mousseau, L.and Heyndrickx. 2006. Probing diversity in the plankton: using patterns in tintinnids. Developments in Hydrobiology **183**: 143–157. 72

Dutkiewicz, S., M. J. Follows, and J. G. Bragg. 2009. Modeling the coupling of ocean ecology and biogeochemistry. Global Biogeochemical Cycles **23**: GB4017. 41, 50, 51

Edgar, R. 2004. MUSCLE: multiple sequence alignment with high accuracy and high throughput. Nucleic Acids Research **32**: 1792–1797. 21

Edwards, K., M. Thomas, C. Klausmeier, and E. Litchman. 2012. Allometric scaling and taxonomic variation in nutrient utilization traits and maximum growth rate of phytoplankton. Limnology and Oceanography **57**: 554–556. 18, 90

Ehnes, B., B. Rall, and U. Brose. 2011. Phylogenetic grouping, curvature and metabolic scaling in terrestrial invertebrates. Ecology Letters **14**: 993–1000. 19

Enquist, B. J., E. P. Economo, T. E. Huxman, A. P. Allen, D. D. Ignace, and J. F. Gillooly. 2003. Scaling metabolism from organisms to ecosystems. Nature **423**: 639–642. 4

Enquist, B. J., and K. J. Niklas. 2001. Invariant scaling relations across tree-dominated communities. Nature **410**: 655–660. 56

Eppley, R. W. 1972. Temperature and phytoplankton growth in sea. Fishery Bulletin **70**: 1063–1085. 2, 12, 13, 15, 19, 30, 73, 79, 83, 91

Falkowski, P. G., R. T. Barber, and V. Smetacek. 1998. Biogeochemical controls and feedbacks on ocean primary production. Science **281**: 200–206. 3

Farquhar, G. D., S. V. Caemmerer, and J. A. Berry. 1980. A biochemical-model of photosynthetic CO_2 assimilation in eaves of C-3 species. Planta **149**: 78–90. 12

Felsenstein, J. 1985. Phylogenies and the comparative method. The American Naturalist **125**: 1–15. 19, 21, 28

Felsenstein, J. 2008. Comparative methods with sampling error and within-species variation: contrasts revisited and revised. The American Naturalist **171**: 713–725. 19

Field, C. B., M. J. Behrenfeld, J. T. Randerson, and P. Falkowski. 1998. Primary production of the biosphere: Integrating terrestrial and oceanic components. Science **281**: 237–240. 1

Fiksen, O., M. Follows, and D. L. Aksnes. 2013. Trait-based models of nutrient uptake in microbes extend the Michaelis-Menten framework. Limnology And Oceanography **58(1)**: 193–202. 90

Finkel, Z. V. 2001. Light absorption and size scaling of light-limited metabolism in marine diatoms. Limnology and Oceanography **46(1)**: 86–94. 29

Finkel, Z. V., J. Beardall, K. J. Flynn, A. Quigg, T. A. V. Rees, and J. A. Raven. 2010. Phytoplankton in a changing world: cell size and elemental stoichiometry. Journal of Plankton Research **32**: 119–137. 3

Floder, S., and U. Sommer. 1999. Diversity in planktonic communities: An experimental test of the intermediate disturbance hypothesis. Limnology and Oceanography **44**: 1114–1119. 56

Flombaum, P., J. Gallegos, R. Gordillo, J. Rincón, L. Zabala, N. Jiao, D. Karl, W. Li, M. Lomas, D. Veneziano, C. Vera, J. Vrugt, and A. Martiny. 2013. Present and future global distributions of the marine Cyanobacteria *Prochlorococcus* and *Synechococcus*. Proceedings Of The National Academy Of Sciences Of The United States Of America **110(24)**: 9824–9829. 31

Follows, M. J., S. Dutkiewicz, S. Grant, and S. W. Chisholm. 2007. Emergent biogeography of microbial communities in a model ocean. Science **315**: 1843–1846. 41, 43, 90

Freckleton, R., H. Harvey, and M. Pagel. 2002. Phylogenetic analysis and comparative data: a test and review of evidence. American Naturalist **160**: 712–726. 29

Frost, B. 1991. The role of grazing in nutrient-rich areas of the open sea. Limnology And Oceanography **36(8)**: 1616–1630. 51

Fryxell, G., and I. Kaczmarska. 1994. Specific variability in Fe-enriched cultures from the Equatorial Pacific. Journal of Plankton Research **16(7)**: 755–769. 51

Fuhrman, J. A., J. A. Steele, I. Hewson, M. S. Schwalbach, M. V. Brown, J. L. Green, and J. H. Brown. 2008. A latitudinal diversity gradient in planktonic marine bacteria. Proceedings of the National Academy of Sciences of the United States of America **105**: 7774–7778. 4, 52, 72, 82

Galimany, E., A. Place, M. Ramón, M. Jutson, and R. Pipe. 2007. The effects of feeding Karlodinium veneficum (PLY 103; *Gymnodinium veneficum Ballantine*) to the blue mussel *Mytilus edulis*. Harmful algae **7**: 91–98. 37

Gárate-Lizárraga, I. . M. n.-M. R. 2012. Blooms of *Trichodesmium erythraeum* and *T. thiebautii* (Cyanobacteria, Oscillatoriales) in the Bahía de la Paz, Gulf of California. CICIMAR Oceánides **27(1)**: 61–64. 38

Garland, T., P. Midford, and A. Ives. 1999. An introduction to phylogenetically-based statistical methods with a new method for confidence intervals on ancestral values. The American Zoologist **39**: 374–388. 19

Gaston, K. J. 2000. Global patterns in biodiversity. Nature **405**: 220–227. 3, 72

Gentry, A. 1988. Changes in plant community diversity and floristic composition on environmental and geographic gradients. Annals of the Missouri Botanical Garden **75**: 1–34. 5, 56

Gifford, D., and D. Caron. 2000. Sampling, preservation, enumeration and biomass of marine protozooplankton. In: Harris R.P. et al. (eds) ICES Zooplankton Methodology Manual. Academic Press, London pages 193–221. 60

Gillooly, J. F., J. H. Brown, G. B. West, V. M. Savage, and E. L. Charnov. 2001. Effects of size and temperature on metabolic rate. Science **293**: 2248–2251. 2

Gillooly, J. F., E. L. Charnov, G. B. West, V. M. Savage, and J. H. Brown. 2002. Effects of size and temperature on developmental time. Nature **417**: 70–73. 13

Gitay, H., A. Suárez, R. Watson, and D. Dokke, Gitay2002. Climate change and biodiversity. IPCC Technical Paper. Technical report, United Nations Environment Programme and World Meteorological Organization. 4

Glazier, D. 2005. Beyond the "3/4-power law": variation in the intra-and interspecific scaling of metabolic rate in animals. Biological Reviews **80**: 611–662. 19

Grasshoff, K. 1976. Methods of seawater analysis. Verlag Chemie, Weinheim and New York page 317pp. 62

Green, J., D. Hibberd, and R. Pienaar. 1982. The taxonomy of *Prymnesium* (Prymnesiophyceae) including a description of a new cosmopolitan species, *P. patellifera sp.* nov., and further observations on *P. pavum* N. Carter. British Phycological Journal **17**: 363–382. 37

Grime, J., and J. Hodgson. 1987. Botanical contributions to contemporary ecological theory. New Phytologist Supplement **106**: 283–295. 29

Guindon, S., and O. Gascuel. 2003. PhyML: 'A simple, fast and accurate algorithm to estimate large phylogenies by maximum likelihood'. Systematic Biology **52(5)**: 696–704. 21

Harvey, P., and M. Pagel. 1991. The comparative method in evolutionary biology. Oxford University Press. Oxford,UK. 29

Hays, G. C., A. J. Richardson, and C. Robinson. 2005. Climate change and marine plankton. Trends in Ecology & Evolution **20**: 337–344. 4

Hayward, B., T. Cedhagen, M. Kaminski, and O. Gross. 2011. World Modern Foraminifera database. Available online at http://www.marinespecies.org/foraminifera. pages Consulted on 2013–01–22. 56

Hemmingsen, A. M. 1960. Energy metabolism as related to body size and respiratory surfaces, and its evolution. Rep. Steno Mem. Hosp. **9**: 15–22. 18

Herndl, G. J., and T. Reinthaler. 2013. Microbial control of the dark end of the biological pump. Nature Geosci **6**: 718–724. 2

Housworth, E. A. 2004. The phylogenetic mixed model. The American Naturalist **163**: 84–96. 19

Huete-Ortega, M., P. Cermeño, A. Calvo-Díaz, and E. Marañón. 2012. Isometric size-scaling of metabolic rate and the size abundance distribution of phytoplankton. Proceedings of the Royal Society B-biological Sciences **279**: 1815–1823. 18

Huisman, J. 2010. Comment on "Patterns of Diversity in Marine Phytoplankton". Science **329**: 5991. 50, 56

Humboldt, A., and A. Bonpland. 1807. Essai sur la Géographie des Plantes Accompagné d′un Tableau Physique des Régions Équinoxiales. [Reprint 1977, Arno Press, New York]. 3, 40

Hutchinson, G. E. 1957. Population Studies - Animal Ecology and Demography - Concluding Remarks. Cold Spring Harbor Symposia On Quantitative Biology **22**: 415–427. 73, 83

Hutchinson, G. E. 1961. The Paradox of the Plankton. American Naturalist **95**: 137–145. 56

Iriarte, J., and G. Fryxell. 1995. Microphytoplankton at the Equatorial Pacific (140-degrees-W) during the JGOFS EQPAC time-series studies. March to April and October 1992. Deep-Sea Research Part II-Topical Studies in Oceanography **42**: 2–3. 51

Irigoien, X., J. Huisman, and R. P. Harris. 2004. Global biodiversity patterns of marine phytoplankton and zooplankton. Nature **429**: 863–867. 3, 4, 56, 57, 74, 83

Irwin, A. J., A. M. Nelles, and Z. V. Finkel. 2012. Phytoplankton niches estimated from field data. Limnology and Oceanography **57**: 787–797. 52

Ives, A. R., P. E. Midford, and T. Garland. 2007. Within-Species Variation and Measurement Error in Phylogenetic Comparative Methods. Systematic Biology **56**: 252–270. 19

Johnson, M. D., J. Volker, H. V. Moeller, E. Laws, K. J. Breslauer, and P. G. Falkowski. 2009. Universal constant for heat production in protists. Proceedings of the National Academy of Sciences of the United States of America **106**: 6696–6699. 15, 16

Kaczmarska, I., and G. A. Fryxell. 1994. The genus Nitzschia: Three new species from the equatorial Pacific Ocean. Diatom Research **9**: 87–98. 51

Kashtan, N., S. E. Roggensack, S. Rodrigue, J. W. Thompson, S. J. Biller, A. Coe, H. Ding, P. Marttinen, R. R. Malmstrom, R. Stocker, M. J. Follows, R. Stepanauskas, and S. W. Chisholm. 2014. Single-Cell Genomics Reveals Hundreds of Coexisting Subpopulations in Wild Prochlorococcus. Science **344**: 416–420. 51, 80

Kirkwood, D. 1989. Simultaneous determination of selected nutrients in seawater. ICES CM **C:29**. 62

Kiørboe, T. 1993. Turbulence, phytoplankton cell size, and the structure of pelagic food webs. Advances in Marine Biology **29**: 1–72. 2

Kleiber, M. 1947. Body size and metabolic rate. Physiol. Rev. **27**: 511–541. 18

Kolokotrones, T., V. Savage, E. J. Deeds, and W. Fontana. 2010. Curvature in metabolic scaling. Nature **464**: 753–756. 19, 21, 29

Kovala, P. E., and J. D. Larrance. 1966. Computation of phytoplankton cell numbers, cell volume, cell surface and plasma volumne per litre, from microscopical counts. Department of Oceanography. University of Washington. Special Report **38**. 62

Leadbeater, B. 1969. A fine structural study of *Olisthodiscus luteus* carter. Br. Phycol. **4(1)**: 3–17. 37

Leblanc, K., J. Arístegui, L. Armand, P. Assmy, B. Beker, A. Bode, E. Breton, V. Cornet, J. Gibson, M. Gosselin, E. Kopczynska, H. Marshall, J. Peloquin, S. Piontkovski, A. Poulton, B. Quéguiner, R. Schiebel, R. Shipe, J. Stefels, M. van Leeuwe, M. Varela, C. Widdicombe, and M. Yallop. 2012. A global diatom database - abundance, biovolume and biomass in the world ocean. Earth System Science Data **4**: 149–165. 5, 36, 56

Li, W. K. W. 2002. Macroecological patterns of phytoplankton in the northwestern North Atlantic Ocean. Nature **419**: 154–157. 3

Litchman, E., C. A. Klausmeier, O. M. Schofield, and P. G. Falkowski. 2007. The role of functional traits and trade-offs in structuring phytoplankton communities: scaling from cellular to ecosystem level. Ecology Letters **10**: 1170–1181. 18, 29

Liu, C., and L. Lin. 2001. Ultrastructural study and lipid formation of *Isochrysis sp.* CCMP1324. Bot. Bull. Acad. Sin. **42**: 207–214. 37

López-Urrutia, A., E. San Martin, R. P. Harris, and X. Irigoien. 2006. Scaling the metabolic balance of the oceans. Proceedings Of The National Academy Of Sciences Of The United States Of America **103**: 8739–8744. 4, 10, 12, 13, 15, 18, 21, 22, 24, 25, 29, 35

Mantoura, R. F. C., and E. M. S. Woodward. 1983. Optimization of the Indophenol Blue Method For the Automated-determination of Ammonia In Estuarine Waters. Estuarine Coastal and Shelf Science **17**: 219–224. 63

Marañón, E. 2008. Inter-specific scaling of phytoplankton production and cell size in the field. Journal Of Plankton Research **30**: 157–163. 15, 18

Marañón, E., P. Cermeño, D. López-Fernandez, T. Rodríguez-Ramos, S. Sobrino, M. Huete-Ortega, J. Blanco, and J. Rodríguez. 2013. Unimodal size scaling of phytoplankton growth and the size dependence of nutrient uptake and use. Ecology Letters **16**: 371–379. 18, 19, 25, 28, 30, 36, 37, 38

Marañón, E., P. Cermeño, J. Rodriguez, M. V. Zubkov, and R. P. Harris. 2007. Scaling of phytoplankton photosynthesis and cell size in the ocean. Limnology and Oceanography **52**: 2190–2198. 18, 30

Marañón, E., E. Fernández, R. Harris, and S. D. Harbour. 1996. Effects of the diatom-*Emiliania huxleyi* succession on photosynthesis, calcification and carbon metabolism by size-fractionated phytoplankton. Hydrobiologia **317**: 189–199. 57

Margalef, R. 1978. Life-forms of phytoplankton as survival alternatives in an unstable environment. Oceanol. **Acta 1**: 493–509. 3

Martins, E., and T. Garland. 1991. Phylogenetic analyses of the correlated evolution of continuous characters: a simulation study. Evolution **45**: 534–557. 29

McNab, B. 2008. An analysis of the factors that influence the level and scaling of mammalian BMR. Comparative Biochemistry and Physiology **Part A 151**: 5–28. 19

Mei, Z. P., Z. V. Finkel, and A. J. Irwin. 2009. Light and nutrient availability affect the size-scaling of growth in phytoplankton. Journal of Theoretical Biology **259**: 582–588. 16

Menden-Deuer, S., and E. J. Lessard. 2000. Carbon to volume relationships for dinoflagellates, diatoms, and other protist plankton. Limnology and Oceanography **45**: 569–579. 62

Mittelbach, G. G., C. Steiner, S. Scheiner, K. Gross, H. Reynolds, R. Waide, M. R. Willig, S. Dodson, and L. Gough. 2001. What is the observed relationship between species richness and productivity? Ecology **82**: 2381–2396. 3

Moisan, J. R., T. A. Moisan, and M. R. Abbott. 2002. Modelling the effect of temperature on the maximum growth rates of phytoplankton populations. Ecological Modelling **153**: PII S0304–3800(02)00008–X. 2

Monod, J. 1949. The Growth of Bacterial Cultures. Annual Review of Microbiology **3**: 371–394. 1

Morán, X., A. López-Urrutia, A. Calvo-Diaz, and W. K. W. Li. 2010. Increasing importance of small phytoplankton in a warmer ocean. Global Change Biology **16**: 1137–1144. 4

Niklas, K. J., and B. J. Enquist. 2001. Invariant scaling relationships for interspecific plant biomass production rates and body size. Proceedings of the Royal Society B-biological Sciences **98**: 2922–2927. 18

Oberdorff, T., J. F. Guegan, and B. Hugueny. 1995. Global scale patterns of fish species richness in rivers. Ecography **18**: 345–352. 72

O'Brien, T. 2007. COPEPOD: The Global Plankton Database. A review of the 2007 database contents and new quality control methodology. U.S. Dep. Commerce, NOAA Tech. Memo. NMFS-F/ST-34 page 28p. 56

Olenina, I., S. Hajdu, L. Edler, A. Andersson, N. Wasmund, S. Busch, J. Göbel, S. Gromisz, S. Huseby, M. Huttunen, A. Jaanus, P. Kokkonen, I. Ledaine, and E. Niemkiewicz. 2006. Biovolumes and size-classes of phytoplankton in the Baltic Sea. HELCOM Balt.Sea Environ. Proc. **106**: 144pp. 36, 37, 38

Pagel, M. 1999. Inferring the historical patterns of biological evolution. Nature **401**: 887–884. 21

Palenik, B. 1994. Cyanobacterial community structure as seen from RNA polymerase gene sequence analysis. Applied and Environmental Microbiology **60**: 3212–3219. 28

Paradis, E., J. Claude, and K. Strimmer. 2004. APE: analyses of phylogenetics and evolution in R language. Bioinformatics **20**: 289–290. 21

Partensky, F., and L. Garczarek. 2010. *Prochlorococcus*: Advantages and Limits of Minimalism. Annu. Rev. Marine. Sci. **2**: 305–331. 18, 28, 80

Passy, S. 2008. Continental diatom biodiversity in stream benthos declines as more nutrients become limiting. Proceedings of the National Academy of Sciences **105**: 28, 9663–9667. 4

Penno, S., D. Lindell, and A. Post. 2006. Diversity of *Synechococcus* and *Prochlorococcus* populations determined from DNA sequences of the N-regulatory gene ntcA. Environmental Microbiology **8**: 1200–1211. 28

Peperzak, L. 2010. An objective procedure to remove observer-bias from phytoplankton time-series. Journal of Sea Research **63**: 152–156. 57

Phillips, O., and J. Miller. 2002. Global Patterns of Plant Diversity: Alwyn H. Gentry Forest Transect Data Set. Monogr. Syst. Bot. Missouri Bot. Gard. **89**. 56

Phillips, S. J., R. P. Anderson, and R. E. Schapire. 2006. Maximum entropy modeling of species geographic distributions. Ecological Modelling **190**: 231–259. 75

Pianka, E. R. 1966. Latitudinal Gradients In Species Diversity - A Review of Concepts. The American Naturalist **100**: 33–46. 3, 40, 72

Prowe, A., M. Pahlow, S. Dutkiewicz, M. Follows, and A. Oschlies. 2012. Top-down control of marine phytoplankton diversity in a global ecosystem model. Progress in Oceanography **101**: 1–13. 72

Ptacnik, R., T. Andersen, P. Brettum, L. Lepisto, and E. Willen. 2010. Regional species pools control community saturation in lake phytoplankton. Proceedings of the Royal Society B **277**: 3755–3764. 4

Pulliam, H. 2000. On the relationship between niche and distribution. Ecology Letters **3**: 349–361. 83

R Development Core Team, 2008. R: A language and environment for statistical computing. R Foundation for Statistical Computing, Vienna, Austria. 21, 22, 75, 76

Ratkowsky, D. A., R. Lowry, T. McMeekin, A. Stokes, and R. Chandler. 1983. Model for bacterial culture growth rate throughout the entire biokinetic temperature range. Journal of bacteriology **154(3)**: 1222–1226. 2

Raven, J. A. 1998. The twelfth Tansley Lecture. Small is beautiful: the picophytoplankton. Functional Ecology **12**: 503–513. 10, 18, 28, 32

Raven, J. A., J. Beardall, A. W. D. Larkum, and P. Sánchez-Baracaldo. 2013. Interactions of photosynthesis with genome size and function. Philosophical Transactions of the Royal Society B: Biological Sciences **368**. 18

Reynolds, C. 1984. The Ecology of Freshwater. Cambridge: Cambridge University Press. 384 p. 3

Ricklefs, R., and J. Starck. 1996. Application of phylogenetically independent contrasts: a mixed progress report. Oikos **77**: 167–172. 19

Rober, K. C., C. Rahbek, and J. Nicholas. 2004. The Mid Domain Effect and Species Richness Patterns: What Have We Learned So Far? The American Naturalist **163**: E1–E23. 77

Rocap, G., D. Distel, J. Waterbury, and S. Chisholm. 2002. Resolution of *Prochlorococcus* and *Synechococcus* ecotypes by using 16S-23S ribosomal DNA internal transcribed spacer sequences. Applied and Environmental Microbiology **68**: 1180–1191. 28

Rodríguez, F., E. Fernández, R. N. Head, D. S. Harbour, G. Bratbak, M. Heldal, and R. P. Harris. 2000. Temporal variability of viruses, bacteria, phytoplankton and zooplankton in the western English Channel off Plymouth. Journal of the Marine Biological Association of the United Kingdom **80**: 575–586. 57

Rohde, K. 1992. Latitudinal Gradients In Species-diversity - the Search For the Primary Cause. Oikos **65**: 514–527. 3, 40, 52, 72

Rombouts, I., G. Beaugrand, F. Ibanez, S. Gasparini, S. Chiba, and L. Legendre. 2009. Global latitudinal variations in marine copepod diversity and environmental factors. Proceedings of the Royal Society B-biological Sciences **276**: 3053–3062. 4, 52, 72, 82

Rosenzweig, M. 1995. Species Diversity in Space and Time. Cambridge University Press. 3

Rutherford, S., S. D'Hondt, and W. Prell. 1999. Environmental controls on the geographic distribution of zooplankton diversity. Nature **400**: 749–753. 72

Sal, S., and A. Lopez-Urrutia. 2011. Comment: Temperature, nutrients, and the size-scaling of phytoplankton growth in the sea. Limnology and Oceanography **56**: 1952–1955. 30

Sal, S., A. Lopez-Urrutia, X. Irigoien, D. S. Harbour, and R. P. Harris. 2013. Marine microplankton diversity database. Ecology **94**: 1658. http://dx.doi.org/10.1890/13–0236.1. 74, 75, 76, 78, 81, 86

Sal, S., A. López-Urrutia, S. Vallina, S. Dutkiewicz, and M. Follows. in prep. Multiple drivers of the latitudinal diversity gradient in marine phytoplankton . 72, 82, 83

Sarmiento, J. L., R. Slater, R. Barber, L. Bopp, S. C. Doney, A. C. Hirst, J. Kleypas, R. Matear, U. Mikolajewicz, P. Monfray, V. Soldatov, S. A. Spall, and R. Stouffer. 2004. Response of ocean ecosystems to climate warming. Global Biogeochemical Cycles **18**: GB3003. 4

Simon, N., A.-L. Cras, E. Foulon, and R. Lemee. 2009. Diversity and evolution of marine phytoplankton. Comptes Rendus Biologies **332**: 159–170. 58

Simova, I., D. Storch, P. Keil, B. Boyle, O. L. Phillips, and B. J. Enquist. 2011. Global species-energy relationship in forest plots: role of abundance, temperature and species climatic tolerances. Global Ecology and Biogeography **20**: 842–856. 56

Smith, V. H. 2007. Microbial diversity-productivity relationships in aquatic ecosystems. FEMS Microbiology Ecology **62**: 181–186. 83

Sobek, S., L. J. Tranvik, and J. J. Cole. 2005. Temperature independence of carbon dioxide supersaturation in global lakes. Global Biogeochem. Cycles **19**: GB2003. 4

Sommer, U. 1985. Comparison Between Steady-state and Non-steady State Competition - Experiments With Natural Phytoplankton. Limnology and Oceanography **30**: 335–346. 56

Sommer, U. 1989. Maximal Growth-rates of Antarctic Phytoplankton - Only Weak Dependence On Cell-size. Limnology and Oceanography **34**: 1109–1112. 18, 29

Stevens, G. 1989. The latitudinal gradient in geographic range: how so many species coexist in the tropics. The American Naturalist **113**: 240–256. 3, 40

Stomp, M., J. Huisman, G. G. Mittelbach, E. Litchman, and C. A. Klausmeier. 2011. Large-scale biodiversity patterns in freshwater phytoplankton. Ecology **92**: 2096–2107. 56

Straile, D., M. C. Jochimsen, and R. Kümmerlin. 2013. The use of long-term monitoring data for studies of planktonic diversity: a cautionary tale from two Swiss lakes. Freshwater Biology **58(6)**: 1292–1301. 57

Strathmann, R. 1967. Estimating the organic carbon content of phytoplankton from cell volume or plasma volume. Limnology and Oceanography **12**: 411–418. 12

Tang, E. 1995. Why do dinoflagellates have lower growth rates? Journal Of Plankton Research **17**: 1325–1335. 29

Thomas, M. K., C. T. Kremer, C. A. Klausmeier, and E. Litchman. 2012. A Global Pattern of Thermal Adaptation in Marine Phytoplankton. Science **338**: 1085–1088. 4, 19, 20, 21, 22, 23, 24, 25, 31, 33, 34, 52, 72, 73, 75, 78, 80, 81, 83, 84, 85

Throndsen, J. 1978. Preservation and storage. In: Sournia A (ed) Phytoplankton manual. UNESCO Paris, pages 69–74. 60

Tilman, D. 1982. Resource Competition and Community Structure. Princeton University Press. 2, 3, 40

Timmermans, K. 2010. Variability in cell size, nutrient depletion, and growth rates of the Southern Ocean diatom *Fragilariopsis kerguelensis* (Bacillariophyceae) after prolonged iron limitation. Journal of Phycology **46**: 497–506. 36

Timmermans, K., B. van der Wagt, and H. de Baar. 2004. Growth rates, half-saturation constants, and silicate, nitrate, and phosphate depletion in relation to iron availability of four large, open-ocean diatoms from the Southern Ocean. Limnology and Oceanography **49(6)**: 2141–2151. 36

Ting, C., C. Hsieh, S. Sundararaman, C. Mannella, and M. Marko. 2007. Cryo-electron tomography reveals the comparative three-dimensional architecture of *Prochlorococcus*, a globally important marine cyanobacterium. Journal of Bacteriology **189(12)**: 4485–4493. 28

Tittensor, D. P., C. Mora, W. Jetz, H. K. Lotze, D. Ricard, E. Vanden Berghe, and B. Worm. 2010. Global patterns and predictors of marine biodiversity across taxa. Nature **466**: 1098–U107. 40, 52, 53, 72, 82

Turner, J. 2004. Explaining the global biodiversity gradient: energy, area, history and natural selection. Basic Appl. Ecol. **5**: 435–448. 3

Tyrrell, T., E. Maranon, A. J. Poulton, A. R. Bowie, D. S. Harbour, and E. M. S. Woodward. 2003. Large-scale latitudinal distribution of Trichodesmium spp. in the Atlantic Ocean. Journal of Plankton Research **25**: 405–416. 57

Urbach, E., D. Scanlan, D. Distel, J. Waterbury, and S. Chisholm. 1998. Rapid diversification of marine picophytoplankton with dissimilar light-harvesting structures inferred from sequences of *Prochlorococcus* and *Synechococcus* (Cyanobacteria). Journal of Molecular Evolution **46**: 188–201. 28

Utermöhl, H. 1958. Zur Vervolkommung der Quantitativen Phytoplankton-methodik. Mitt. Int. Ver. Limnol. **9**: 1–38. 61

Vallina, S., and C. Le Quéré. 2011. Stability of complex food webs: Resilience, resistance and the average interaction strength. Journal of Theoretical Biology **272(1)**: 160–173. 42

Škaloud, P. 2006. Variation and taxonomic significance of some morphological features in European strains of *Klebsormidium* (Klebsormidiophyceae, Streptophyta). Nova Hedwigia **83**: 3–4. 37

Wallace, A. R. 1854. XXIX. On the Habits of the Butterflies of the Amazon Valley. Transactions of the Royal Entomological Society of London **7**: 253–264. 3, 40

Wang, L., Q.-h. Cai, L. Tan, and L.-H. Kong. 2011. Longitudinal Differences of Phytoplankton Community during a Period of Small Water Level Fluctuations in a Subtropical Reservoir Bay (Xiangxi Bay, Three Gorges Reservoir, China). International Review of Hydrobiology **96**: 381–396. 4

West, G. B., J. H. Brown, and B. J. Enquist. 1999. The fourth dimension of life: Fractal geometry and allometric scaling of organisms. Science **284**: 1677–1679. 12, 16

Westoby, M., R. Leishman, and J. Lord. 1995. On misinterpreting the 'phylogenetic correction'. Journal of Ecology **83**: 531–534. 29

Wiltshire, K. H., and C. D. Durselen. 2004. Revision and quality analyses of the Helgoland Reede long-term phytoplankton data archive. Helgoland Marine Research **58**: 252–268. 57

Wright, D. H. 1983. Species-energy Theory - An Extension of Species-area Theory. Oikos **41**: 496–506. 3, 56

Wunch, C., and P. Heimbach. 2007. Practical global oceanic state estimation. Physica D: Nonlinear Phenomena **230(1-2)**: 197–208. 41

Yasuhara, M., G. Hunt, H. J. Dowsett, M. M. Robinson, and D. K. Stoll. 2012. Latitudinal species diversity gradient of marine zooplankton for the last three million years. Ecology Letters **15**: 1174–1179. 53, 72, 82

Zingone, A. 1999. Morphological and genetic characterization of *Phaeocystis cordata* and *P. Jahnii* (Prymnesiophyceae), two new species from the Mediterranean Sea. Journal of Phycology **35**: 1322–1337. 37